Using ESI-MS to Investigate the Organometallic Compound $Cp_2Ti(SC_6H_4CO_2)$ and Closely Related Compounds

A thesis submitted in partial fulfilment

of the requirements for the degree

of

Master of Science in Chemistry

at

The University of Waikato

by

Kai Song

THE UNIVERSITY OF
WAIKATO
Te Whare Wānanga o Waikato

2019

Abstract

This thesis reports investigations on the electrospray ionisation mass spectrometric (ESI-MS) behaviour of some metallocene complexes of titanium and molybdenum. The ESI-MS behaviour of titanocene dichloride (Cp_2TiCl_2) compound, which is has shown of interest as an anticancer agent was investigated. Cp_2TiCl_2 was dissolved in various solvents and spectra were recorded at various capillary exit voltages from 60 V to 250 V. Bis(ethylcyclopentadienyl) dichloridotitanium(IV) was also studied via ESI-MS. Results indicated clearly some main species like $[Cp_2TiH]^+$, $[Cp_2Ti(OCH_3)]^+$ and $[Cp_2Ti(OCH_3)_2+H]^+$ were observed. When the capillary exit voltage was greater than 150 V species containing two Ti centres like $[Cp_4Ti_2(OCH_3)_2Cl]^+$, $[Cp_4Ti_2(OCH_3)_3Cl+H]^+$ and $[(Cp_2Ti(OCH_3)_2+H^+)_2+Cl]^-$ disappeared and titanocene(III) species $[Cp_2Ti(CH_3OH)]^+$ was observed which indicated reduction of titanium(IV) during ESI-MS analysis. Larger ions which contain three or more Ti centres were not observed.

The main focus of this thesis was to investigate the chemistry and characterisation of the organometallic compound bis(cyclopentadienyl) thiosalicylatotitanium(IV) ($Cp_2Ti(tsal)$ tsal = $SC_6H_4CO_2$). A further experiment was done to run the spectrum of a mixed solution of Cp_2TiCl_2 and $Cp_2Ti(tsal)$ in CH_3OH to investigate the possibility of the tsal ligand bridging two Cp_2Ti centres. Characterisation of $Cp_2Ti(tsal)$ using ESI mass spectrometry in the presence of added alkali metal salts and the reactivity of $Cp_2Ti(tsal)$ towards soft electrophile was also studied.

At the same time, a new complex bis(ethylcyclopentadienyl) thiosalicylatotitanium(IV) ($(EtCp)_2Ti(tsal)$) was synthesised and studied by ESI-MS. Comparison of the ESI-MS spectra of $Cp_2Ti(tsal)$ with those of $(EtCp)_2Ti(tsal)$ was used to confirm the identity of some unknown species. This new complex was characterised by elemental analysis, melting point, nuclear magnetic resonance (NMR) and infra-red (IR) spectroscopy.

Finally the molybdocene dichloride (Cp_2MoCl_2) compound was studied by ESI-MS. The closely related compound bis(cyclopentadienyl) thiosalicylatomolybdenum(IV) ($Cp_2Mo(tsal)$) was synthesised and characterised by ESI-MS, melting point, NMR and IR spectroscopy. Less species can be observed

in the Mo system than in the Ti system. Most species in the Mo system contained a Cl ligand.

Acknowledgements

Firstly, I would like to thank my supervisor Professor Bill Henderson for giving me this opportunity and helping me with this experiment process. I appreciated his education for me on the ESI instruments and checking my paper over and over again.

I would like to acknowledge R.J. Hill Laboratories, and thank them for giving me the educational leave each week to finish my degree.

I would also like to thank Ryland Fortney-Zirker who helped me to explain the unknown ion observed during this research and enlightened me as to the superoxo complex $Cp_2TiO_2^+$.

A special thanks to Haiming Tang for helping me with NMR experiments and the use of NMR instruments.

Many thanks as well to Jenny Stockdill, the technical staff of Chemistry in Waikato University. She kindly helped me to find out some suppliers of chemicals used.

Thanks to Cheryl Ward, the university librarian who helped me fix the references.

Thanks to everyone in the lab C.3.04 for providing a positive learning environment.

Lastly, I would like to thank my parents, my wife Jennifer Zhang and friends for their support and encouragement throughout my degree.

Table of Contents

List of Figures

List of Tables

List of Schemes

Chapter 1

Introduction

1.1 Titanocene compounds

Since titanocene dichloride was first reported in 1954 [1], there has been growing interest in the development of the chemistry of titanocene compounds. This is because titanocene compounds can act as catalysts in organic synthesis and some of them even as antioxidative or antitumor agents [2]. Titanocene dichloride is a bright red solid with the formula $(\eta^5\text{-}C_5H_5)_2TiCl_2$ and abbreviated as Cp_2TiCl_2. (Figure 1.1). It is one of the most important titanocene compounds used in the world.

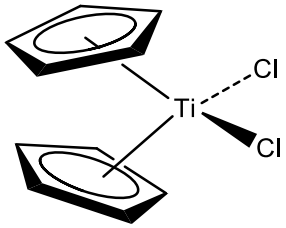

Figure 1.1: Chemical structure of titanocene dichloride

Cp_2TiCl_2 was first synthesised by Wilkinson and Birmingham by the reaction of titanium tetrachloride ($TiCl_4$) with sodium cyclopentadienide in dry tetrahydrofuran under an argon atmosphere [3]. It can be also prepared by reacting freshly distilled cyclopentadiene with $TiCl_4$ (Scheme 1.1) [4].

$$2NaC_5H_5 + TiCl_4 \longrightarrow (C_5H_5)_2TiCl_2 + 2NaCl$$

$$2C_5H_6 + TiCl_4 \longrightarrow (C_5H_5)_2TiCl_2 + 2HCl$$

Scheme 1.1: Two routes for the synthesis of Cp_2TiCl_2

This compound has been characterised by an X-ray structure determination which shows it has a quasi-tetrahedral structure with 2 chloride ligands and 2 cyclopentadienyl (Cp) ligands around the Ti metal centre. Two planar Cp ligands are in a bent sandwich configuration coordinated to the Ti [3]. The two Cp rings are inclined at an angle of 131º and the Cl-Ti-Cl angle is 94.5º. The Ti-Cl bond

distances is 2.36 Å and distance between the central of the Cp ring and Ti is 2.06 Å [5]. This kind of structure makes titanocene dichloride easily lose the chloride ligands and behave as a Cp_2Ti^{2+} source. Thus, it can undergo fast hydrolysis in water even through it has poor water solubility.

Cp_2TiCl_2 was the first non-platinum antitumor agent to be considered in clinical trials [1]. *In vivo*, Cp_2TiCl_2 shows a very pronounced growth inhibition on solid animal tumours and experimental ascites tumours. Its biological activity is superior to that achieved with equitoxic doses of cisplatin [6]. Cp_2TiCl_2 shows exceptional antitumor activity against lung, colon and breast cancers [7]. It has become the main representative of the early transition metal antitumor agents. Unfortunately, in phase II clinical trials in patients with breast cancer and metastatic renal cancer, the efficacy of Cp_2TiCl_2 was too low to pursue [8].

However, the remarkable activity of Cp_2TiCl_2 against cancer encouraged the development of other novel titanocene compounds with antitumor activity. Two famous series of drugs are Titanocene X ([1,2-di(cyclopentadienyl)-1,2-di-(4-*N*,*N*-dimethylaminophenyl)ethanediyl] titanium dichloride) and Titanocene Y (bis-[(*p*-methoxybenzyl)cyclopentadienyl] titanium(IV) dichloride) (Figure 1.2).

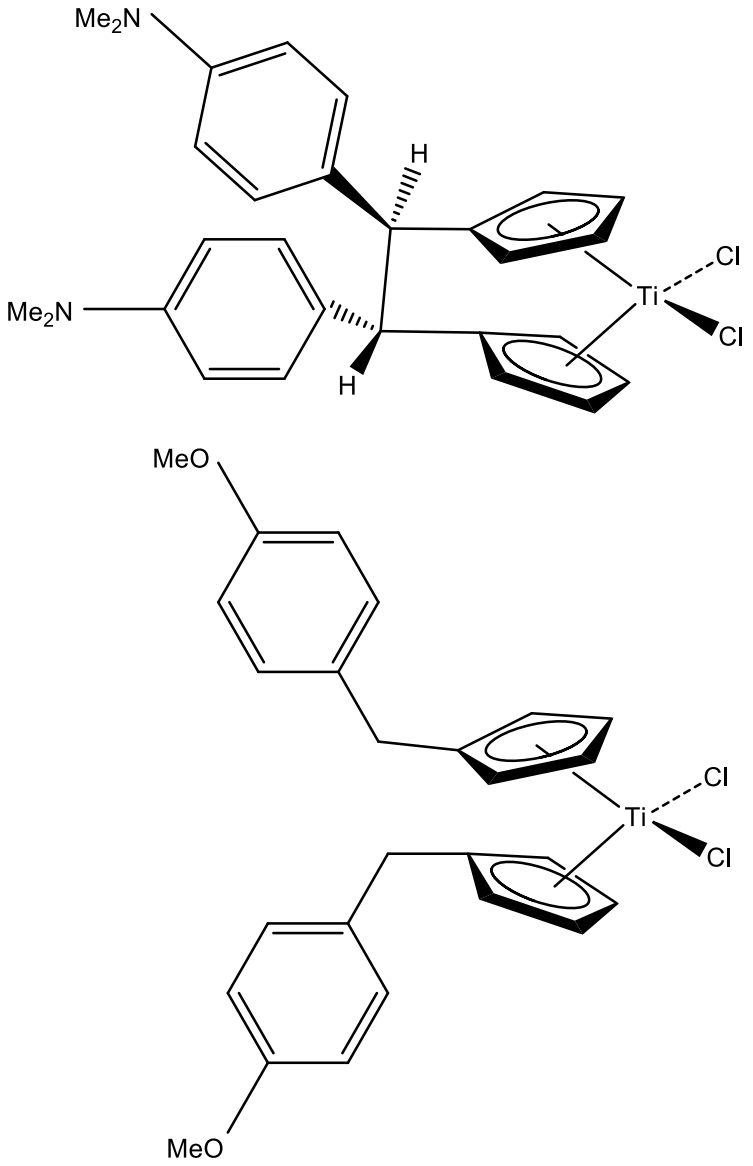

Figure 1.2: Chemical structures of Titanocene X (top) and Titanocene Y (bottom)

They displayed cytotoxic and antiproliferative effects in a variety of tumour cells and recent studies have shown that Titanocene Y had better effects against renal and uterine cancer cells than cisplatin [7]. In most cases, Titanocene Y has more potent cytotoxic activity than Titanocene X [8].

In recent years, many other titanocene compounds have been synthesised and tested as antitumor agents. Some examples are shown in Figure 1.3 [9].

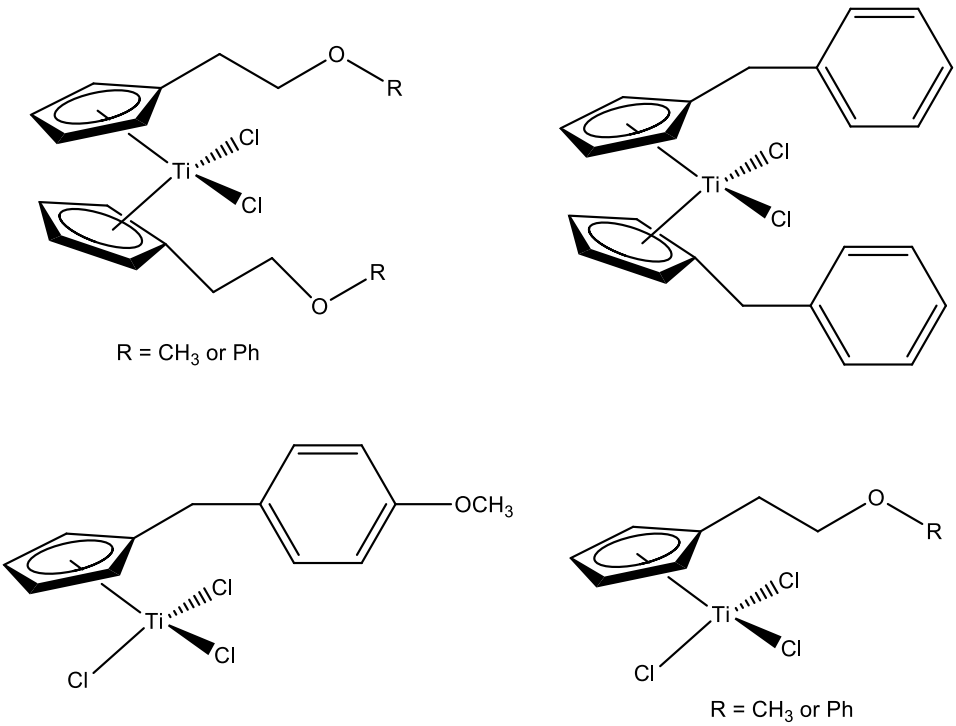

Figure 1.3: Some examples of titanocene compounds having antitumor activity

Due to the instability of Cp_2TiCl_2 in aqueous solution, most syntheses of titanocene compounds are conducted in the absence of water [10]. Most of the novel drugs are unbridged titanocene analogues, which increases the cytotoxicity [8]. These novel drugs all have the $TiCl_2$ moiety, which has the ability to be hydrolysed at physiological pH [7]. In a new generation of titanocene antitumor agents, the substituent methoxy-aryl of cyclopentadienes of Titanocene Y is replaced by ethenyl-methoxide or ethenyl-phenoxide [9]. This change increases the titanocene antitumor agent's stability and cytotoxic activity on breast cancer cells [9]. Some reports have shown that titanocene complexes having lipophilic groups have an improved antiproliferative effect on breast cancer cells [9]. Overall, the mechanism of action of titanocene compounds involves the Ti(IV) having very high affinity to serum protein transferrin (Tf). Two titaniums bound to transferrin (Ti_2-Tf) can be considered to specifically target cancer cells since most cancer cells are Tf receptors [11].

1.2 Thiosalicylate ligand and metal-thiosalicylate complexes

The thiosalicylate ligand, derived from thiosalicylic acid (Figure 1.4) by deprotonation of acidic hydrogens, is a hybrid ligand containing a combination of

hard oxygen donor atoms and a soft sulfur donor atom. This combination of donor atoms allows the thiosalicylate ligand to coordinate to various metal centres to form metal-thiosalicylate complexes [12]. The abbreviation tsal is used for the thiosalicylate ligand hereafter.

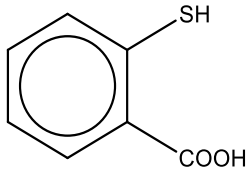

Figure 1.4: Chemical structure of thiosalicylic acid

Disregarding the protonation state of the thiosalicylate ligand, there are 22 various binding modes (Figure 1.5) for metal-thiosalicylate complexes [13].

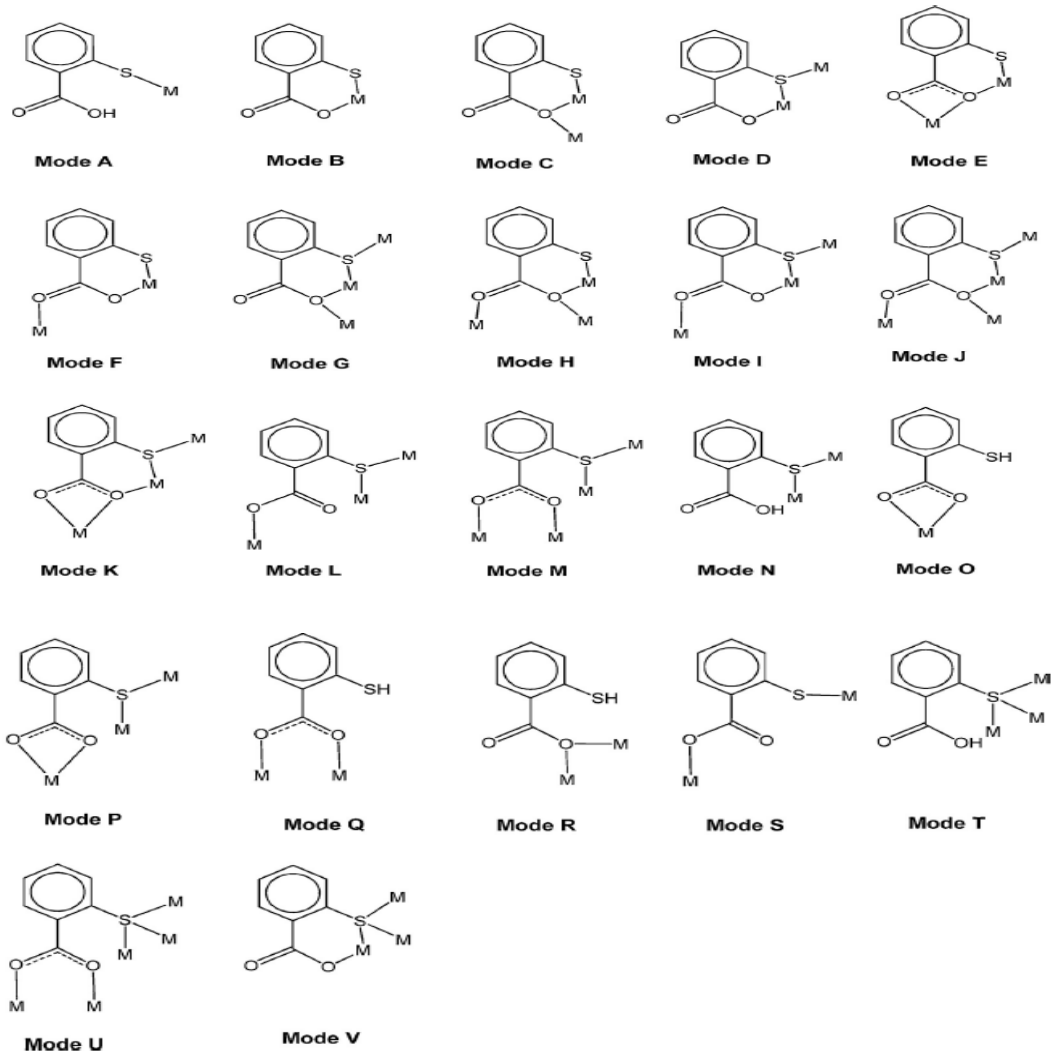

Figure 1.5: Summary of the binding modes in metal-thiosalicylate complexes

The coordination chemistry of the thiosalicylate ligand has been recently reviewed [13]. The next two sections summarise the coordination chemistry of thiosalicylate complexes, with an emphasis on those complexes that have been fully characterised.

1.2.1 Complexes of the thiosalicylate ligand with main-group elements

This section summarises the coordination chemistry of the thiosalicylate ligand with main-group elements. Due to the chemical hardness of the group 1 metals, alkali metal cations interact with tsal through the oxygen atoms [13]. A number of alkali metal-thiosalicylate complexes have been prepared and most of them are mixed-ligand complexes which contain cobalt or zinc etc. Examples include $(NEt_4)_3Na_3[\{Co(SC_6H_4COO)\}_2].6CH_3OH$, $(NEt_4)Na[Zn(SC_6H_4COO)_2].H_2O$ and $(NEt_4)_2Na[Co(SC_6H_4COO)_3].2H_2O$ [14].

In group 2, beryllium, calcium and strontium thiosalicylate complexes with other ancillary ligands have been prepared but poorly characterised. The best characterised is the barium thiosalicylate complex $[Ba(HSC_6H_4COO)_2(H_2O)_4]_n$ (Figure 1.6) [15].

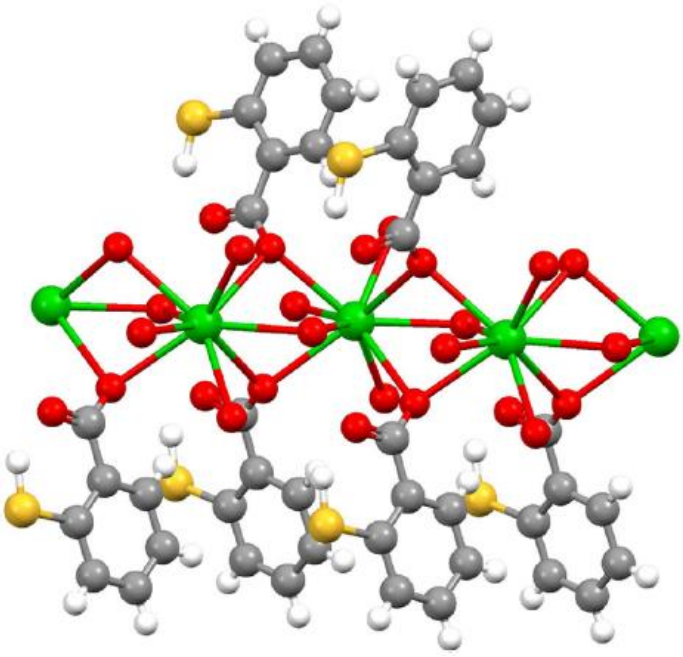

Figure 1.6: Part of the X-ray structure of $[Ba(HSC_6H_4COO)_2(H_2O)_4]_n$. Colour code: barium (green); oxygen (red); carbon (grey); sulfur (yellow); hydrogen (white)

In group 13, $Al(SC_6H_4CO_2)(O^iPr)$ and $Al(SC_6H_4CO_2)(HSC_6H_4CO_2)$ were prepared by the reaction of $Al(O^iPr)_3$ with thiosalicylic acid [16]. Gallium and indium thiosalicylate complexes have also been prepared by reaction of Ga^{3+} and In^{3+} ions towards thiosalicylic acid in ethanol [17]. Thallium(I) and thallium(III) thiosalicylate compounds have also been reported [18,19].

In group 14, a number of silicon thiosalicylate complexes have been prepared and characterised, such as $PhMeSi(SC_6H_4CO_2)$, $Me_2Si(SC_6H_4CO_2)$, $[Me_2NHCH_2Si(SC_6H_4CO_2)_2]$ and $C_6H_4(SSiMe_3)(COOSiMe_3)$ [20,21]. A limited number of germanium thiosalicylate complexes have been reported, with the best well-known one being $Et_2Ge(SC_6H_4CO_2)$ [22]. Complexes of the thiosalicylate ligand with tin have been very extensively studied, mainly on tin in the IV oxidation state. Examples include $(Cy_2NH_2)[Ph_3Sn(SC_6H_4CO_2)]$ and $[Me_2Sn(SC_6H_4CO_2)]$ [23,24]. A limited number of lead thiosalicylate complexes have been studied and no X-ray crystal structures have been reported. The best well-known one is $[Pb(SC_6H_4CO_2)]$ [25].

In group 15, the arsenic thiosalicylate complex $Me_2AsSC_6H_4COOH$ has been synthesised and used for cancer chemotherapy [13]. Some other arsenic thiosalicylate complexes like $As(SC_6H_4COOH)_3$ and $RNHC(O)C_6H_4As(SC_6H_4COOH)_2$ (R = H or Me) have been known for many years, but there are no reports on X-ray structures of these complexes [26]. A number of antimony(III) and bismuth(III) thiosalicylate complexes have been reported, since these metal centres are chemically soft. Examples include $Cl_2Sb(SC_6H_4COOH)$ and $(NH_4)_3[Bi(SC_6H_4CO_2)_3].2H_2O$ [27].

In group 16, $Se(SC_6H_4COOH)_2$ (Figure 1.7) has been prepared by reduction of selenous acid with thiosalicylic acid in methanol and characterised by high performance liquid chromatography (HPLC) [28]. $Te(SC_6H_4COOH)_2$ has been prepared from thiosalicylic acid with sodium tellurite and characterised by NMR spectroscopy [29].

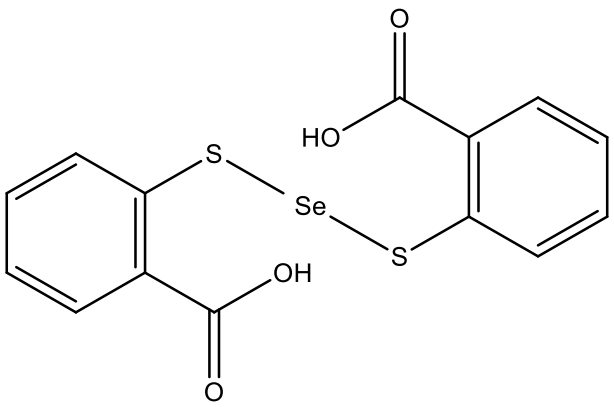

Figure 1.7: Chemical structure of $Se(SC_6H_4COOH)_2$

1.2.2 Complexes of the thiosalicylate ligand with transition metals

This section summarises the coordination chemistry of the thiosalicylate ligand with transition metals, with an emphasis on the best-characterised and best known thiosalicylate complexes.

$Ti(OPr^i)_4$ and $Zr(OPr^i)_4$ can react with thiosalicylic acid to form $M(SC_6H_4CO_2)_2$ or $M(SC_6H_4CO_2)_2(OPr^i)_2$ (M=Ti or Zr) depending on the mole ratio [16]. The titanocene derivative $Cp_2Ti(SC_6H_4CO_2)$ and the related complex $(C_5H_4Me)_2Ti(SC_6H_4CO_2)$ have also been synthesised and characterised by UV-visible spectroscopy [30]. There are no reports on thiosalicylate complexes of hafnium [13].

An early study of thiosalicylate ligands with vanadium investigated the reaction of VO^{2+} ion with thiosalicylic acid giving a common type $VO(SC_6H_4CO_2)L_2$ (L = other donor ligands) [31]. More recently, reaction of the vanadium(III) precursor $[VCl_3(thf)_3]$ (thf = $(CH_2)_4O$) or the vanadium(IV) precursor $[VOCl_4]^{2-}$ with thiosalicylic acid has been studied. Their products $[V_3OCl_4(HSC_6H_4CO_2)_5]^{2-}$ and $[Li_4V_2O_2Cl_4(SC_6H_4CO_2)_4]^{4-}$ were characterised by X-ray structure determinations [32]. There are no reports on thiosalicylate complexes of niobium and tantalum [13].

A limited number of chromium thiosalicylate complexes have been reported, one known example being $[Cr(SC_6H_4CO_2)(H_2NCH_2CH_2NH_2)_2]^+$ [33]. In contrast, there have been extensive studies on molybdenum(VI) thiosalicylate complexes. Examples include $(Et_3NH)_2[MoO_2(SC_6H_4CO_2)_2]$ and the related complex $(Et_3NH)_2[MoO(NNPh_2)(SC_6H_4CO_2)_2]$ [34,35]. Some lower oxidation state

molybdenum(V) and molybdenum(IV)-thiosalicylate complexes have been synthesised and characterised [36]. A number of molybdenum thiosalicylate complexes based on sulfide clusters are also reported, eg $(Et_3NH)_2[Mo_3S_7(SC_6H_4CO_2)_3]$ [37]. There are no reports on thiosalicylate complexes of tungsten [13].

A colourless manganese(II)-thiosalicylate complex $[Mn(SC_6H_4CO_2)_2]^{2-}$ has been characterised. Some manganese(III)-thiosalicylate complex have also been reported, for example the red complex $[Mn(SC_6H_4CO_2)_2]^-$ [38]. Some organometallic manganese-thiosalicylate complexes containing carbonyl ligands have been reported and characterised [39]. The technetium thiosalicylate chemistry is based on a metastable nuclear isomer of Tc-99 which symbolised as ^{99m}Tc. Reduction of $^{99m}TcO_4^-$ with $SnCl_2$ and succinic dihydrazide followed by the addition of phosphine gave the $[^{99m}Tc(N)(L)(SC_6H_4CO_2)]$ [L = $\{Ph_2P(CH_2)_2\}_2O$ or $\{Me_2P(CH_2)_2\}_2NMe$] [40]. For rhenium, reaction of $ReCl(CO)_5$, $[Re_2(\mu\text{-}OH)_3(CO)_6]^-$, $[ReO_2(py)_4]Cl$ or $[ReOCl_5]^{2-}$ with thiosalicylic acid in different reagents gave a variety of rhenium-thiosalicylate complexes [41,42].

A range of iron-thiosalicylate complexes have been synthesised and reported. One example is the "Roussin red ester" complex $[Fe_2(\mu\text{-}SC_6H_4COOH)_2(NO)_4]$, which can be prepared by reaction of $[Fe_2(\mu\text{-}Br)_2(NO)_4]$ with thiosalicylic acid [43]. Iron-sulfide compounds containing thiosalicylate ligands such as $[Fe_2(\mu\text{-}S)_2(SC_6H_4CO_2)_2]^{2-}$ (Figure 1.8) are also known [44]. Reduction of this complex with $[Co(\eta^5\text{-}C_5Me_5)_2]$ gives the reduced species $[Fe_2(\mu\text{-}S)_2(SC_6H_4CO_2)_2]^{3-}$. From this species, iron(II) bis(thiosalicylate) complex $[Fe(SC_6H_4CO_2)_2]^{2-}$ (Figure 1.9) and tetra-ferric cluster $[Fe_4S_6(SC_6H_4CO_2)_2]^{4-}$ were able to be isolated and characterised [45].

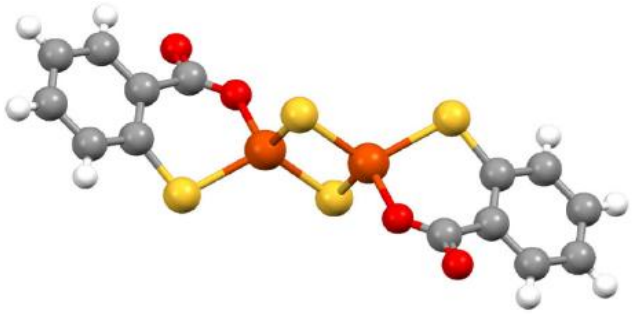

Figure 1.8: The X-ray structure of $[Fe_2(\mu\text{-}S)_2(SC_6H_4CO_2)_2]^{2-}$. Colour code: iron (orange); oxygen (red); sulfur (yellow); carbon (grey); hydrogen (white)

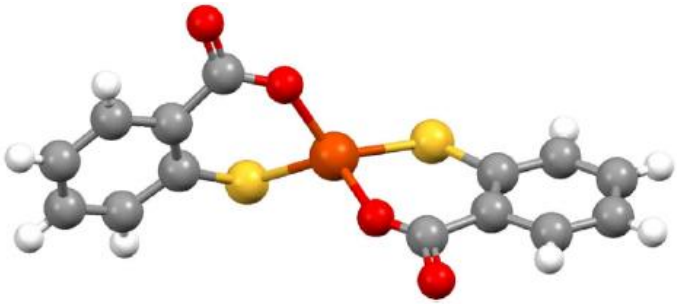

Figure 1.9: The X-ray structure of $[Fe(SC_6H_4CO_2)_2]^{2-}$. Colour code: iron (orange); oxygen (red); sulfur (yellow); carbon (grey); hydrogen (white)

A number of different types of ruthenium-thiosalicylate complexes have been synthesised and reported, some showing anticancer activity. One example is $(Et_4N)[Ru_3(SC_6H_4CO_2H)_2(SC_6H_4CO_2)_4]$ [46]. Ruthenium-thiosalicylate complex $(Et_4N)_{1.5}[Ru(SC_6H_4CO_2)_4(SC_6H_4CO_2H)_2](OAc)_{0.5}.3H_2O$ can react with $Fe(CH_3COCHCOCH_3)_3$ and $(Et_4N)OAc$ in ethylene glycol to give polymeric $(Et_4N)_2[\{Fe(OCH_2CH_2OH)(H_2O)_2\}\{Ru_3(SC_6H_4CO_2)_6\}].2H_2O.C_2H_6O_2$ [47]. Reaction of osmium carbonyls such as the triosmium cluster $[Os_3(CO)_{10}(CH_3CN)_2]$ with thiosalicylic acid forms the osmium-thiosalicylate complex $[\{Os_3H(CO)_{10}\}_2(\mu\text{-}SC_6H_4CO_2)]$ [48].

A number of cobalt(II) and cobalt(III)-thiosalicylate complexes have been reported. One of the best-known cobalt(II) thiosalicylate complexes is $[Co(SC_6H_4CO_2)_2]_n$, which shows antiferromagnetic behaviour [49]. Limited numbers of rhodium and iridium-thiosalicylate complexes have been reported. Recently, $[M(SC_6H_4CO_2)(\eta^5\text{-}C_5Me_5)]_2$ (M = Rh, Ir) have been prepared by reaction of $[MCl_2(\eta^5\text{-}C_5Me_5)]_2$ with thiosalicylic acid and Et_3N base [50].

A variety of different types of nickel(II), palladium(II) and platinum(II)-thiosalicylate complexes have been characterised in early studies. $[Ni(SC_6H_4CO_2)(dppe)]$ has been synthesised by reaction of $[NiCl_2(dppe)]$ with thiosalicylic acid in methanol with pyridine base. [51]. $[Pt(SC_6H_4CO_2)(bipy)]$ was one of the first synthesised and characterised platinum(II)-thiosalicylate complexes [52]. A number of platinum thiosalicylate complexes containing neutral nitrogen-donor ligands, e.g. pyridine, imidazole, etc have also been synthesised [53].

One of the most widely known copper(II)-thiosalicylate complexes is $[Cu_2(HSC_6H_4COOH)_2(H_2O)_6]^{4+}$ [54]. Copper(II)-thiosalicylate complexes can be stabilised by binding with nitrogen-donor ligands [13]. The copper(I)-thiosalicylate complex $[Cu(SC_6H_4COOH)(PPh_3)_3]$ has also been prepared and characterised [55].

There are a wide range of mononuclear and polynuclear silver complexes containing the thiosalicylate ligand, on account of silver ions showing coordination numbers of 2 to 4 and silver's affinity for both sulfur and oxygen donors. One of the most common examples of a mononuclear silver complex containing the thiosalicylate ligand is $[Ag(SC_6H_4COOH)(PPh_3)_3]$, which can be synthesised by reaction of $[AgCl(PPh_3)_3]$ or $[AgCl(PPh_3)_2]_2$ with thiosalicylic acid and sodium hydroxide [56]. $[Ag_4(SC_6H_4CO_2)_2(en)]_n$ (en = $C_2H_4(NH_2)_2$) (Figure 1.10) is one example of a polynuclear silver complex, prepared by reaction of silver nitrate with thiosalicylic acid and ethylenediamine (en) [57].

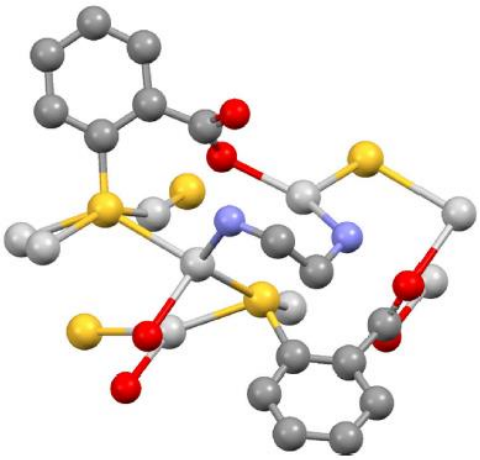

Figure 1.10: Part of the X-ray structure of $[Ag_4(SC_6H_4CO_2)_2(en)]_n$. Colour code: silver (light grey); nitrogen (blue); sulfur (yellow); carbon (grey); oxygen (red)

Silver(I)-thiosalicylate complexes have been found to show antibacterial activity [58].

A number of gold(I)-thiosalicylate complexes have been reported, since gold(I) has very strong affinity for S ligands. The gold(I)-thiosalicylate complex $(Ph_3P)AuSC_6H_4COOH$ has antifungal and antibacterial activity [59]. Some gold(I)-thiosalicylate complexes can be used to generate supramolecular liquid-crystalline aggregates [60]. A number of gold(III)-thiosalicylate complexes containing

cycloaurated ligands have been synthesised and summarised in a review [61]. Cycloaurated ligands are used to stabilise the gold(III) metal centre as it can reduce the positive charge on the gold atom and make it less prone to reduction, and hence less oxidising [62]. This kind of complex has anticancer activity [63]. Gold(III)-thiosalicylate complexes (Figure 1.11) show affinity for thiol-based ligands, unlike platinum anticancer complexes which have affinity for DNA [64].

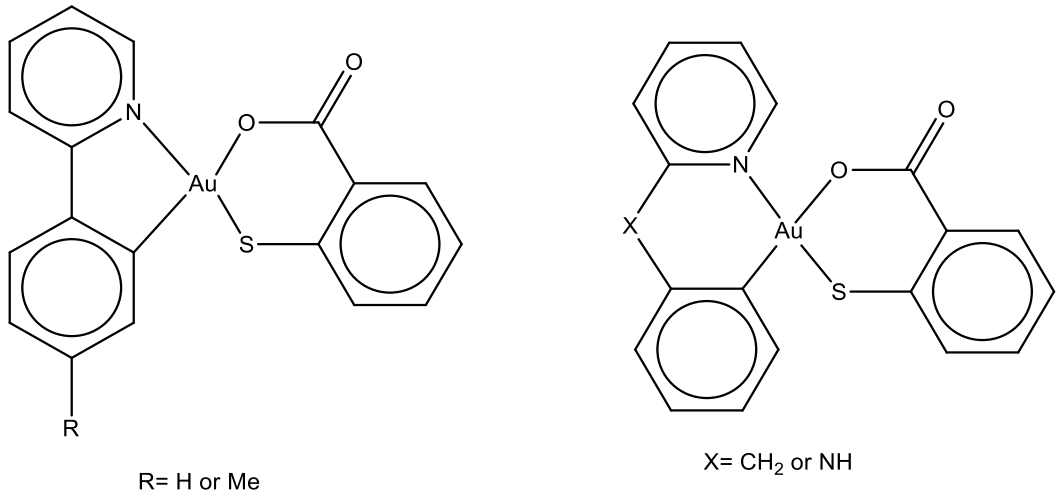

Figure 1.11: Chemical structure of gold(III) thiosalicylate complexes

$[Zn(SC_6H_4CO_2)]$ is one of the well-characterised zinc-thiosalicylate complexes synthesised in different ways and characterised by IR spectroscopy and elemental analysis [65]. A number of zinc-thiosalicylate complexes with an ancillary tris(pyrazolyl)borate ligand have also been investigated and reported [66]. There are only a few studies on cadmium thiosalicylate complexes. $[Cd_2(SC_6H_4CO_2)_2(bipy)_2]$ is one of the best-characterised cadmium-thiosalicylate complexes [67]. In contrast to cadmium, there is an extensive chemistry of mercury with thiosalicylate ligands, since mercury has a strong affinity for thiolate ligands. Mercury-thiosalicylate complexes can be divided into inorganic and organometallic mercury complexes. The best-known example of an inorganic mercury-thiosalicylate complex is $[Hg(SC_6H_4CO_2H)_2Cl]$ [25]. $EtHgSC_6H_4CO_2H$ is the best-known organomercury containing thiosalicylate complex and it has been used as an antibacterial agent [68].

1.3 Electrospray ionisation mass spectrometry

Since 1989, when Fenn introduced electrospray ionisation (ESI), it has become the most widely used soft ionisation technique in biochemical and chemical analysis. Combined with a mass spectrometer (MS), it allows the analysis of samples in solution form [69]. There are two major advantages of using a soft ionisation technique. One is that little or no fragmentation occurs during soft ionisation, as very little residual energy is retained by the analyte. Therefore, this technique is very useful in investigation of large biological molecules, such as proteins. The other advantage of this soft ionisation technique is that weak non-covalent interactions are preserved in the gas phase [70].

1.3.1 ESI-MS ionisation mechanism

There are 3 basic components for ESI-MS: the ion source, mass analyser and detector (Figure 1.12).

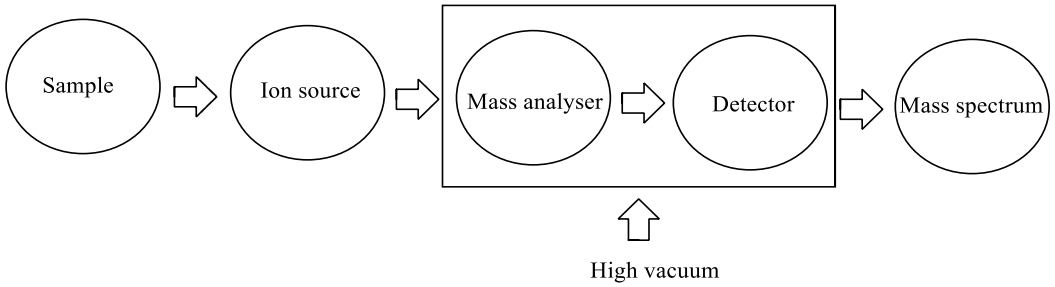

Figure 1.12: The basic components of the ESI-MS

Generally a dilute analyte solution is injected into the ion source at a low flow rate. Within the ESI source, a very high voltage is applied to the tip of the metal capillary and is assisted by a nebulising gas, which breaks the sample solution into an aerosol of highly charged electrospray droplets. Evaporation of the solvent reduces the size of the charged droplets and at the same time increases their surface charge density (Figure 1.13).

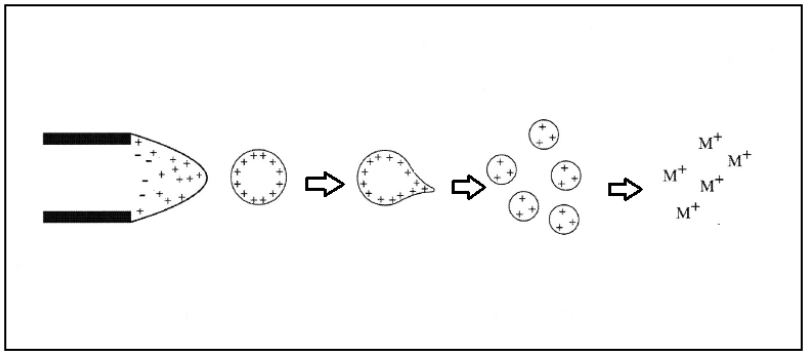

Figure 1.13: The electrospray ionisation process

Finally, when the charged droplets reach a critical point, ions are ejected into the gas phase. Then the emitted ions are accelerated into the mass analyser. The mass analyser is a core component of the ESI-MS. It can separate and sort the ions according to their mass to charge ratio (*m/z* value). The most commonly used mass analyser is a quadrupole mass analyser (Figure 1.14). In this mass analyser, ions travel forward in the z direction with the oscillating pattern in the x-y plane [71]. The different types of ions have different amplitudes of oscillation under different the DC and RF voltages. Specific DC and RF voltages are set to make sure that desirable ions travel along the z-axis without hitting the quadrupole rods, and thus reach the detector.

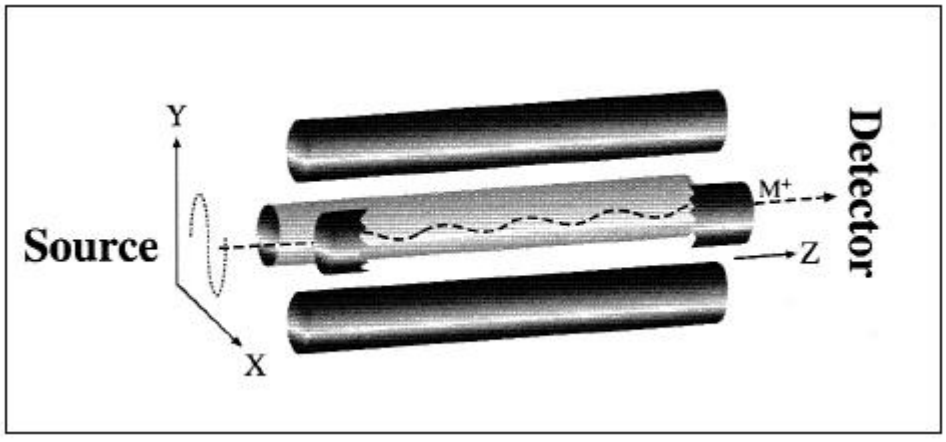

Figure 1.14: Operation of a quadrupole mass analyser

The Time-of-Flight (TOF) mass analyser is the type of mass spectrometer detector used in this research. The principle of TOF is: Ions are formed in pulses and inserted

by an applied electric field into the TOF analyser. At this stage, all the ions have the same kinetic energy and enter the field-free drift tube (Figure 1.15) [72]. Since the ion kinetic energy is $0.5mv^2$, heavier ions have a lower velocity than lighter ions and reach the detector later. The major advantage of a TOF is parallel ion detection. It can detect all the ions present in the source. The TOF analyser is also more sensitive compared to quadrupole mass analyser.

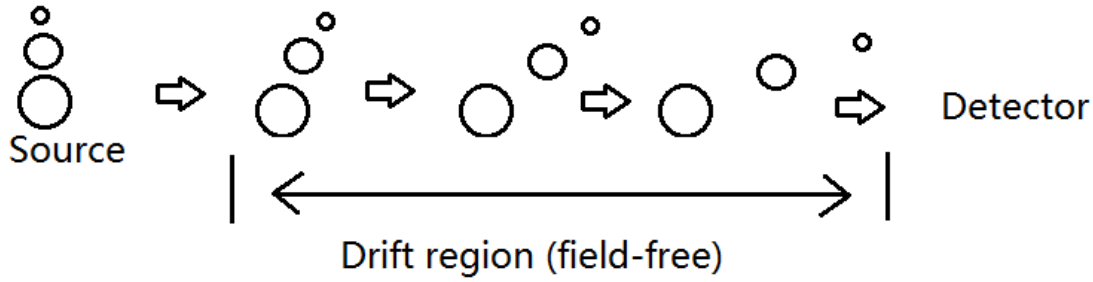

Figure 1.15: Operation of a time-of-flight mass analyser

After the ions pass through the mass analyser, they reach the detector system. At this time, the system will measure their abundance and display the results on a mass spectrum. High vacuum is applied to the mass analyser and detector system since the ions in the gas phase are often short-lived and very reactive.

1.3.2 Applications of ESI-MS in coordination and organometallic chemistry

ESI-MS has been widely used in the study of coordination and organometallic chemistry, and such applications have been reviewed several times [73,74]. In general, ESI-MS is used to detect and analyse various species in sample solution. In coordination and organometallic chemistry, ESI-MS can confirm the stoichiometry of an unknown, newly-synthesised complex [75]. In contrast to NMR, it can be used for paramagnetic samples [74].

Like other MS techniques, ESI-MS can only detect ions. For neutral species further ionisation is required. The most common process for them to be ionised is to abstract a proton from the solvent to give a $[M+H]^+$ ion. On the other hand, neutral species containing –COOH or –OH groups can lose a proton to give a negative ion

$[M-H]^-$. To encourage these ionisation processes, a base (e.g. NH_3) or an acid (e.g. HCOOH) can be added. In some cases, metal ions such as K^+, Na^+ or Ag^+ can also be used, since some metal ions favour binding to "soft" ligand centres and some ions favour binding to "hard" ligand centres [76]. Loss of an anionic ligand like a halide is another common ionisation mechanism, since a number of coordination and organometallic complexes contain halide ligands [74].

1.3.3 ESI-MS behaviour of metallocene compounds

An electrochemical reaction occurs during the analyte through the ESI high-voltage capillary, this reaction can induce an electron flow from or to the metal capillary and redox reactions of the analyte solvent occurs in the ESI capillary [70]. Since the coordinated Cp ligand is not protonatable, the ESI-MS behaviour of metallocene compounds is strongly dependent on the ancillary ligands present. Ferrocene (Cp_2Fe) and a selection of analogues $[Cp_2Fe]BF_4$, $FcCH_2NMe_2$, $FcCH_2P(O)(OPh)_2$, $FcCH_2OH$, $FcCH_2P(CH_2OH)_2$, $FcCH_2PH_2$ [Fc = $(C_5H_5)Fe(C_5H_4)$] have been analysed by ESI-MS [77-80]. In the case of $[Cp_2Fe]BF_4$ neither oxidation nor protonation are needed, since the metallocene is already charged. However, for neutral metallocenes during the ionisation process, oxidation and protonation will compete with each other, depending on the redox potential of the metal centre, the solvent flow rate used by the instrument and the basicity of other ligands. Thus only the protonated $[M+H]^+$ ion was observed when ferrocenyl-amine $FcCH_2NMe_2$ is analysed by ESI-MS, due to the high basicity of the NMe_2 group. In cases of lower basicity, like the phosphonate $FcCH_2P(O)(OPh)_2$, both oxidised $[M]^+$ and protonated $[M+H]^+$ ions can be observed. Osmocene (Cp_2Os) and ruthenocene (Cp_2Ru) have also been investigated by ESI-MS, where the $[Cp_2M]^+$ ion was observed for those complexes [81]. Molybdocene complexes with cysteine and glutathione have been characterised by ESI-MS in positive-ion mode; the results suggest that Cp_2MoCl_2 will coordinate to thiols in *vivo* [82]. Three zirconium metallocene complexes Cp_2ZrMe_2, $(MeCp_2)ZrMe_2$ and $(MeCp)_2Zr(BH_4)_2$ have also been studied by ESI-MS [72,83].

1.3.4 ESI-MS behaviour of Ti compounds

Many Ti compounds have been investigated using ESI-MS. In early studies, titanium trichloride ($TiCl_3$) and titanium tetrachloride ($TiCl_4$) were characterised by ESI-MS, resulting in confirmation of their hydrolysed species [84]. The interaction between Cp_2TiCl_2 and methanol has been investigated by ESI-MS in positive ion mode. Three methoxide species $[TiCp_2(OMe)]^+$, $[TiCp(OMe)(OH_2)(OH)]^+$ and $[Ti(OMe)_3(OH_2)]^+$ have been observed. (Further details of this study are provided in chapter 2) [85]. ESI-MS has been used to study a number of titanium(III) β-diketonate complexes like Cp_2Ti(acetylacetonate) (Figure 1.16) which give the expected $[M]^+$ parent cations in positive mode (i.e. due to the oxidation occurring) [86].

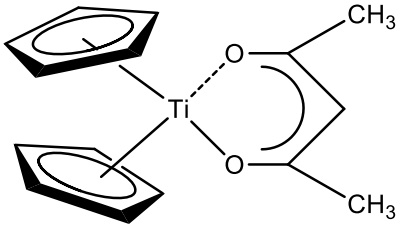

Figure 1.16: Chemical structure of Cp_2Ti(acetylacetonate)

Recently, ESI-MS has been used to investigate a series of different Ti clusters. Ti clusters with 11-12 Ti atoms have been observed in the case of sol-gel solutions based on titanium tetraisopropoxide (TTIP). For sol-gel solutions based on titanium tetrabutoxide (TTB), clusters containing 10-11 Ti atoms were identified. Smaller clusters with 5-7 Ti atoms were identified for sol-gel solutions based on titanium tetraethoxide (TTE). However, a limited number of Ti clusters containing OH groups were observed [87]. A titanium salalen complex has been studied using ESI-MS. The ESI mass spectrum of the salalen ligand (Figure 1.17 a) with titanium isopropoxide in dichloromethane has shown two major signals which indicate the species shown in Figure 1.17 b and c [88].

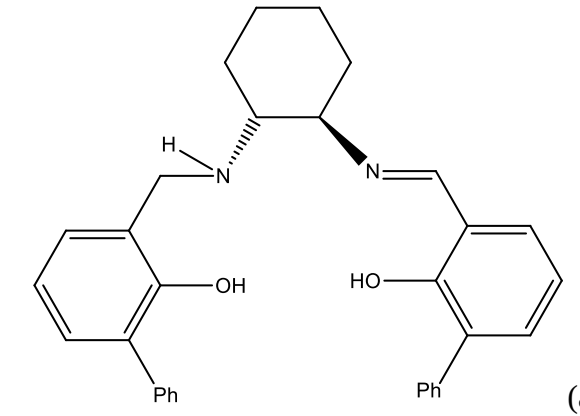

(a)

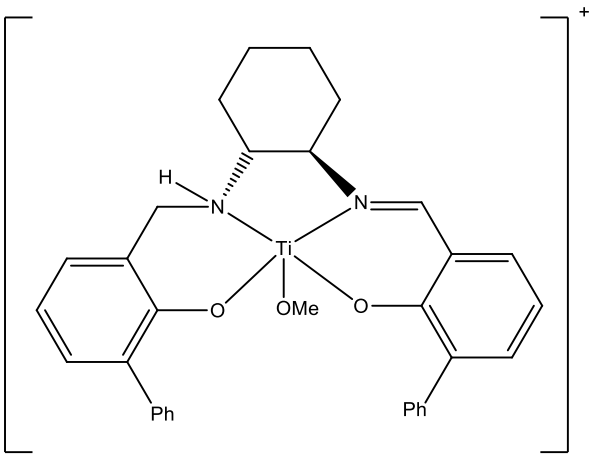

(b)

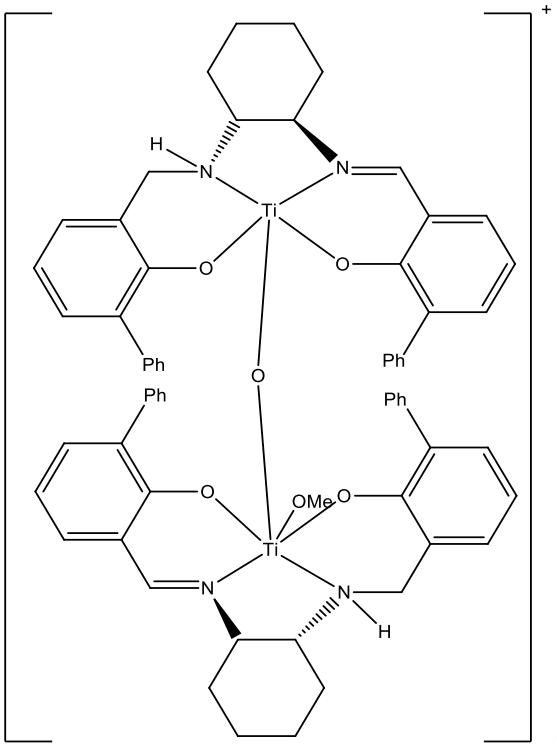

(c)

Figure 1.17: Chemical structure of salalen ligand and two major titanium salalen complex species

ESI-MS has also been used for the analysis of the highly moisture-sensitive metal alkoxide compound $Ti(OEt)_4$. The negative-ion spectra of $Ti(OEt)_4$ show four major species which indicate $[Ti_3(OEt)_{12}(OH)_2Na]^-$, $[Ti_4(OEt)_{16}(OH)_2Na]^-$, $[Ti_5(OEt)_{20}(OH)_2Na]^-$ and $[Ti_6(OEt)_{23}(OH)_4Na_2]^-$ [89].

ESI-MS was used in characterising titanium triethanolamine (tea = $N(CH_2CH_2O^-)_3$) complexes. The results have shown that the present species include the mono and bis titanatrane moieties shown in Figure 1.18. Examples include $(teaTi)_3teaH^+$, $(teaTi)_3(OCH_3)_2^+$ and $(teaTi)teaH_2H^+$ [90].

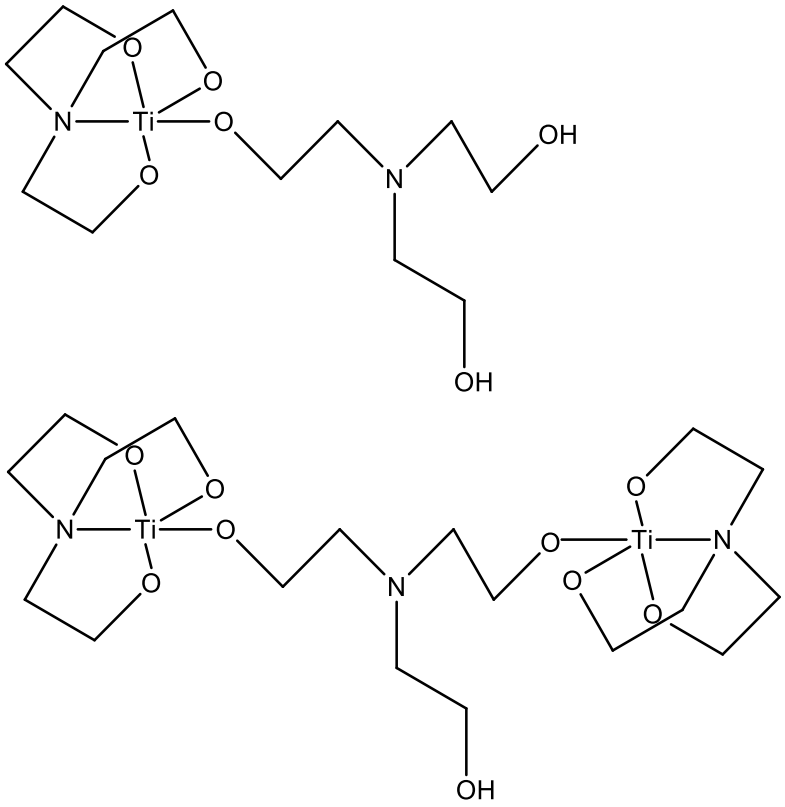

Figure 1.18: Chemical structure of mono and bis titanatrane moieties

Recently, ESI-MS had been used to investigate the binding preferences of titanocene to RNA and DNA. Results from competition experiments in combination with ESI-MS demonstrated titanocene generally strong preference for the binding to phosphate groups adjacent to thymidines in DNA [91].

1.4 Scope of investigation

There are few previous reports of ESI-MS investigations on Cp_2TiCl_2. The aim of this project was therefore to carry out a detailed investigation of the MS characteristics and reactivity of the organometallic compounds Cp_2TiCl_2 and $Cp_2Ti(tsal)$ (Figure 1.19) using ESI-MS. The deep green titanocene derivative $Cp_2Ti(tsal)$ can be prepared by reaction of Cp_2TiCl_2 with thiosalicylic acid in benzene or in a water-chloroform mixture with β-cyclodextrin or in an ethanol-chloroform mixture with sodium hydroxide base [92]. Two Cp ligands in $Cp_2Ti(tsal)$ are similar to those in Cp_2TiCl_2, which are in a bent sandwich configuration coordinated to the Ti. The thiosalicylate ligand binds through the S and carboxylate O to the central metal. This compound is a relatively rare example of a stable (to air and water), chemically hard Ti(IV) centre in combination with a chemically soft thiolate ligand.

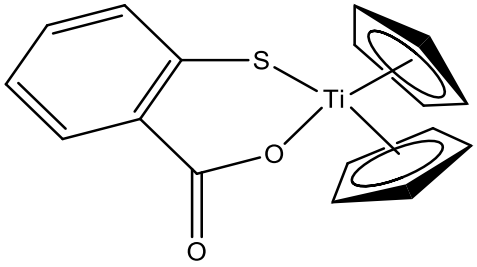

Figure 1.19: Chemical structure of $Cp_2Ti(tsal)$

This project will investigate the behaviour of $Cp_2Ti(tsal)$ in potential reactions with a variety of reagents. These reagents include alkali metal salts and $PhHg^+$. This project will also investigate ligand exchange reactions to see the possibility of the tsal ligand bridging two Cp_2Ti centres. Finally the closely related compounds Cp_2MoCl_2 and $Cp_2Mo(tsal)$ were studied by ESI-MS. Overall, ESI-MS will be utilised as the primary technique in all the investigation of these chemical reactions.

Chapter 2

An investigation of the ESI-MS behaviour of Cp_2TiCl_2

2.1 Introduction

2.1.1 The hydrolysis and alcoholysis reactions of Cp_2TiCl_2 in solution

^{1}H NMR spectroscopy has been previously used to investigate the hydrolysis chemistry of Cp_2TiCl_2 and has shown that $[Cp_2Ti(OH_2)(OH)]^+$ and $[Cp_2(OH_2)Ti\text{-}O\text{-}Ti(OH_2)Cp_2]^{2+}$ are the two major species present in the solution [93]. The pH and chloride concentration influence hydrolysis reactions of Cp_2TiCl_2 in solution. At low pHs, one of the chloride ligands is rapidly hydrolysed and replaced by an aqua or hydroxido ligand, but hydrolysis of the second chloride ligand takes about 50 min. at 35ºC (Figure 2.1) [94]. The rate of hydrolysis is expected to increase at low chloride concentrations and high pH values [94].

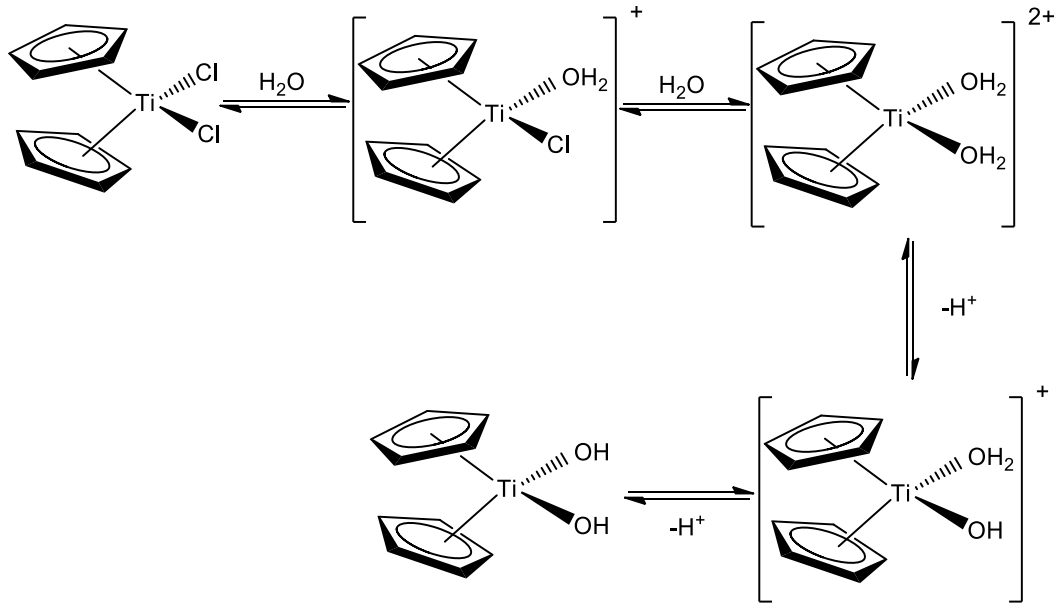

Figure 2.1: Hydrolysis of the chloride ligands of Cp_2TiCl_2

The dihydroxido titanocene species $[Cp_2Ti(OH)_2]$ undergoes further hydrolysis to release a free cyclopentadiene and a hydroxido titanium species (Figure 2.2). The hydrolysis of the Cp ligands is much slower than that hydrolysis of the Cl ligands,

and at low pH values, Cp ligands can be stable over several days [94]. At pH values above 4, insoluble titanium oxido species can be observed due to loss of the Cp ligands and protonation [95].

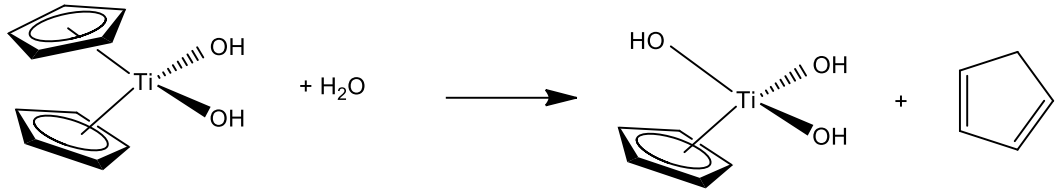

Figure 2.2: Hydrolysis of a Cp ligand of $Cp_2Ti(OH)_2$

There are 11 possible species (Table 2.1) containing Ti(IV) which can be formed when hydrolysis of Cp_2TiCl_2 occurs in water [94]. During this research, some of these species have been observed, but not all of them. Hydrolysis of Cp_2TiCl_2 in water-containing organic solvents has a general trend which involves formation of Ti^{IV}-O^{2-}-Ti^{IV} bridges [3].

Table 2.1: Summary of 11 possible species that can be formed when hydrolysis of Cp_2TiCl_2 occurs in water

Mononuclear species	Dinuclear species	Polymeric species
Cp_2TiCl_2	$Cp_4Ti_2Cl_2O$	$[(CpTiO)_4O_2]_n$
$[Cp_2Ti(OH_2)_2]^{2+}$	$[Cp_4Ti_2(OH_2)_2O]^{2+}$	
$[Cp_2Ti(OH_2)(OH)]^{+}$	$Cp_5Ti_3Cl_3O_2$	
$[CpTi(OH_2)(OH)_2]^{+}$	$Ti_4Cl_4O_4$	
	$[Ti_4(OH_2)_4O_4]^{4+}$	
	$Ti_4(OH)_4O_4$	

2.1.2 Review of the previous ESI-MS investigation of Cp_2TiCl_2

Solutions of Cp_2TiCl_2 in alcohols have been investigated previously using ESI-MS [85]. Previously, research has shown that the alcohols can accelerate the catalytic action of Cp_2TiCl_2 and increase its cytotoxicity [94,96]. ESI-MS in positive-ion mode had been used to investigate the behaviour of solutions of Cp_2TiCl_2 in CH_3OH and proved Cp_2TiCl_2 in CH_3OH accelerated catalytic Mannich reactions [96]. Two major species were found at *m/z* 241.07 and *m/z* 209.04 which correspond to the ions $[Cp_2Ti(OCH_3)_2+H]^+$ and $[Cp_2TiOCH_3]^+$ respectively [96]. After 3 weeks of

aging, the Cp_2TiCl_2 solutions in methanol and ethanol were also analysed by ESI-MS. The result showed no doubly-charged ions and chlorides were absent from all species. In CH_3OH, there were four major methoxide species observed: $[Cp_2Ti(OCH_3)]^+$ (*m/z* 209), $[CpTi(OCH_3)(OH_2)(OH)]^+$ (*m/z* 179), $[Ti(OCH_3)_3(OH_2)]^+$ (*m/z* 159) and $[Ti(OCH_3)_3]^+$ (*m/z* 141). The species observed in ethanol were similar to those in CH_3OH [85]. The literature reports that methanolic solutions of Cp_2TiCl_2 will generate species $[OTiH]^+$ (*m/z* 65) and $[Cp_2TiH]^+$ (*m/z* 179) via ESI [97]. Cp_2TiCl_2 solutions in acetonitrile with formic acid gives the $[Cp_2Ti(O_2CH)]^+$ (*m/z* 223) ion via ESI [97].

The reaction of ethanol with Cp_2TiCl_2 has also been studied by ^1H NMR and HRMS; the result shows the species $[Cp_2Ti(OCH_2CH_3)_2+H]^+$ can be formed. This result clearly demonstrates that ethoxyl groups can bind with the Cp_2Ti moiety and the ethanol is not just an inert solvent for the Cp_2TiCl_2 complex [98].

2.1.3 Project outline

This research project carried out a much more in-depth investigation on solutions of Cp_2TiCl_2 in alcohols. An ESI source coupled with a high resolution TOF mass spectrometer was used for investigating the ESI-MS behaviour of the Cp_2TiCl_2 complex. A suitable solvent is very important for the ESI-MS studies; in this case Cp_2TiCl_2 was dissolved in methanol, ethanol, propan-1-ol and butan-1-ol. At the same time, bis(ethylcyclopentadienyl) titanium(IV) dichloride $(EtCp)_2TiCl_2$ (EtCp = $C_5H_4CH_2CH_3$) (Figure 2.3) was also studied by ESI-MS. Comparison of the ESI-MS spectra of Cp_2TiCl_2 with $(EtCp)_2TiCl_2$ ESI-MS spectra was used to confirm the identity of some unknown species.

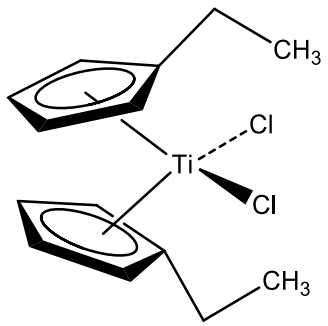

Figure 2.3: Chemical structure of $(EtCp)_2TiCl_2$

2.2 Experimental

The chemicals, solvents and instruments used during this research are listed in sections 2.2.1 and 2.2.2.

2.2.1 Chemicals and solvents

Powdered bis(cyclopentadienyl)titanium(IV) dichloride was obtained from Ralph N. Emanuel Ltd, Alperton, Middlesex, UK and bis(ethylcyclopentadienyl) titanium(IV) dichloride was purchased from Alfa Aesar. Univar grade methanol used was distilled. Ethanol, propan-1-ol and butan-1-ol used were of laboratory reagent grade. Deuterated methanol used was of greater than 99.8 atom % D grade from Sigma-Aldrich.

2.2.2 ESI-MS instrumentation

In this research, ESI-MS data were collected using a Bruker MicrOTOF mass spectrometer. Mass spectra were collected in positive-ion mode, and low range and wide range methods were used. The parameters of these two methods are shown in Table 2.2.

Table 2.2: Operating conditions of the ESI-MS in positive ion mode

Acquisition parameter	Low range method	Wide range method
Scan start	50 *m/z*	500 *m/z*
Scan end	800 *m/z*	1500 *m/z*
End plate offset	-500 V	-500 V
Capillary	4500 V	4500 V
Capillary exit	60-250 V	60-250 V
Nebuliser pressure	0.4 Bar	0.4 Bar
Dry gas flow rate	4.0 L/min	4.0 L/min
Dry temperature	180 °C	180 °C
Skimmer 1	20-80 V	20-80 V
Skimmer 2	22.5 V	24.5 V
Hexapole 1	-25.5 V	-25.5 V
Hexapole RF	80 Vpp	600 Vpp
Lens 1 transfer	49 µs	63 µs
Lens 1 pre pulse	5 µs	11 µs

In this case, the capillary exit voltage was varied from 60 to 250 V. The capillary exit voltage should be approximately three times higher than the skimmer 1 voltage. Table 2.3 shows a full summary of capillary exit and skimmer 1 voltages used for this research. Using a higher capillary exit voltage typically produces more fragmentation.

Table 2.3: Summary of capillary exit and skimmer 1 voltages used

Capillary Exit Voltage	Skimmer 1 Voltage
60	20
100	30
150	50
180	60
210	70
250	80

The instrument-based software micrOTOFcontrol was used to collect data which were further analysed using software mMass [99].

2.2.3 Experimental procedure

The instrument was calibrated prior to use with calibration solution (0.002 mol L^{-1} sodium formate). Typically a tiny amount (i.e. 0.1 mg) of analyte was diluted to *ca.* 1.5 mL with the solvent in a plastic Eppendorf tube and then centrifuged to remove any insoluble matter before analysis.

During the investigation of intensity of $[Cp_2Ti(OR)]^+$ ion in various alcohols where exact by 2 mg of Cp_2TiCl_2 in 1 mL of various alcohols and spectra recorded at a capillary exit voltage of 150 V.

In this research no visible insoluble material was present in any of the sample solutions. Samples were injected into the spectrometer via a syringe pump with a flow rate of 180 μL/hour. Before each operation, CH_3OH was used to flush the instrument system for approximate by half an hour to reduce contamination.

2.3 Results and discussion

2.3.1 Isotope pattern of titanium and the effect of additional chlorine

There are 5 stable isotopes for naturally occurring titanium; ^{46}Ti, ^{47}Ti, ^{48}Ti, ^{49}Ti and ^{50}Ti. ^{48}Ti is the dominant isotope with 73.72% natural abundance. The atomic mass, natural abundance and the relative intensities of each Ti isotope are given in Table 2.4.

Table 2.4: Naturally-occurring isotopes of titanium

Isotope	Atomic Mass	Natural Abundance%	*MS%
^{46}Ti	45.95	8.25	11.2
^{47}Ti	46.95	7.44	10.1
^{48}Ti	47.95	73.72	100.0
^{49}Ti	48.95	5.41	7.3
^{50}Ti	49.94	5.18	7.0

*relative abundances are normalised

A set of peaks containing different isotopes but with the same chemical formula is known as the isotope pattern. The isotope pattern is a result of the relative abundance of the isotopes and their masses. Figure 2.4 shows the theoretical titanium isotope pattern with 5 isotope peaks and ^{48}Ti at *m/z* 47.95 with the highest intensity.

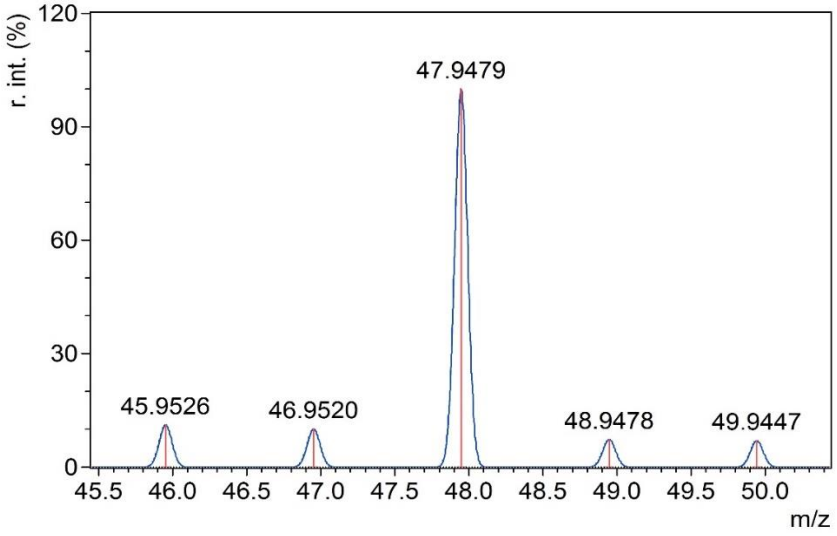

Figure 2.4: Titanium isotope pattern

In this particular study, chlorine is the other element having more than one isotope in any significant abundance, ^{35}Cl and ^{37}Cl. Table 2.5 gives the details of these isotopes.

Table 2.5: Naturally-occurring isotopes of chlorine

Isotope	Atomic Mass	Natural Abundance%	*MS%
^{35}Cl	34.97	75.78	100.0
^{37}Cl	36.97	24.22	32.0

*relative abundances are normalised

In the mass spectrum, these two isotopes are observed as two peaks separated by *m/z* 2 and with a relative intensity ratio of 3:1. Based on this characteristic, any ion with a single chlorine atom will have a distinctive isotope pattern. One example is the Cp_2TiCl^+ ion at *m/z* 213. Figure 2.5 (A) shows the calculated isotope pattern of Cp_2TiCl^+ and (B) is the experimental isotope pattern of Cp_2TiCl^+ ion from Cp_2TiCl_2 dissolved in CH_3OH.

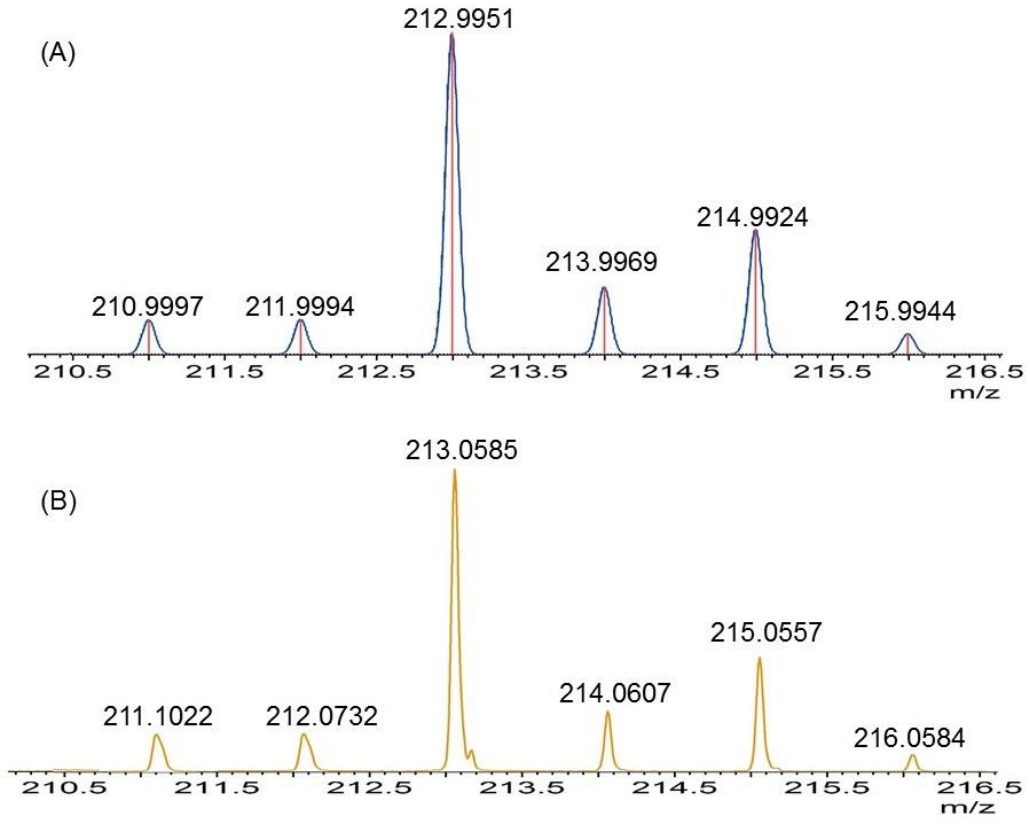

Figure 2.5: Cp_2TiCl^+ ion isotope pattern. (A) Calculated isotope pattern of Cp_2TiCl^+ (B) Experimental isotope pattern of Cp_2TiCl^+

If an ion contains two chlorine atoms, there will be 3 major peaks in the molecular ion region with 2 *m/z* units gaps between them and their peak heights ratio will be 9:6:1. The presence of chlorine in any Ti-containing ions is therefore easily determined by its distinctive effect on the isotope pattern.

2.3.2 Analysis of a freshly-prepared solution of Cp_2TiCl_2 in methanol with low and wide range method

Positive-ion ESI-MS spectra for Cp_2TiCl_2 in methanol solution using the low range method (Table 2), recorded at a range of capillary exit voltages, are given in Figure 2.6.

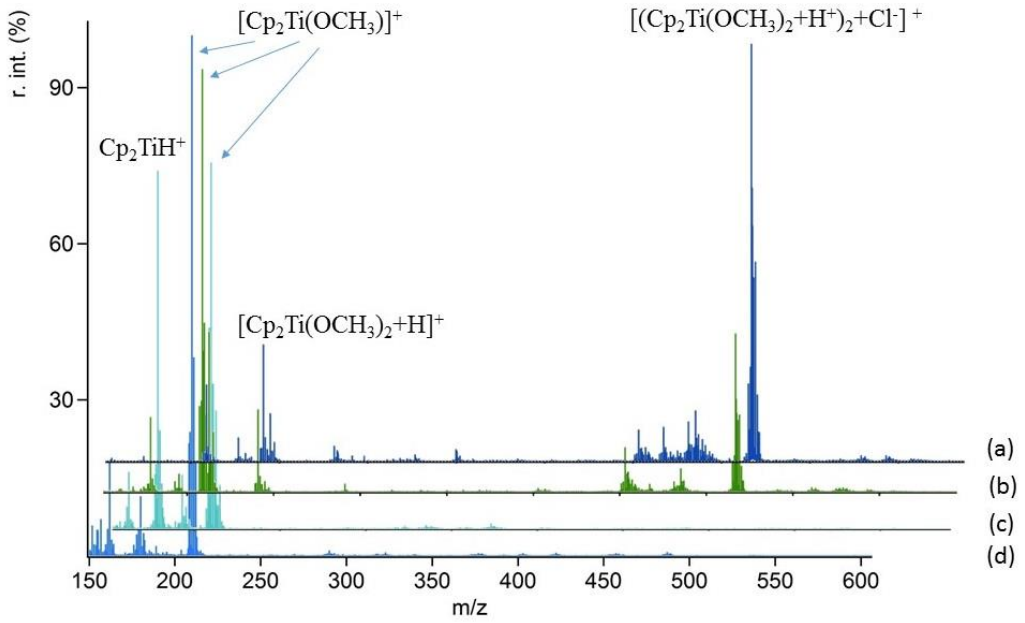

Figure 2.6: Positive-ion ESI mass spectra of a freshly-prepared solution of Cp_2TiCl_2 in methanol with low range method at capillary exit voltages of (a) 60 V, (b) 100 V, (c) 180 V and (d) 250 V

The results show that there are two main groups of ions, one group of species at *m/z* 200-300 and the other group of species only observed at low capillary exit voltages (60 and 100 V, Figure 2.6a and b respectively), at *m/z* 400-550. As the capillary exit voltage increases, the intensity of the low *m/z* range species increases and high *m/z* range species decrease.

To investigate larger Ti clusters which contain three or more Ti required the use of the wide range method. In this research, the wide range method has a maximum at *m/z* 1500. Positive-ion ESI-MS spectra for Cp_2TiCl_2 in methanol solution with the wide range method, recorded at a range of capillary exit voltages, are given in Figure 2.7.

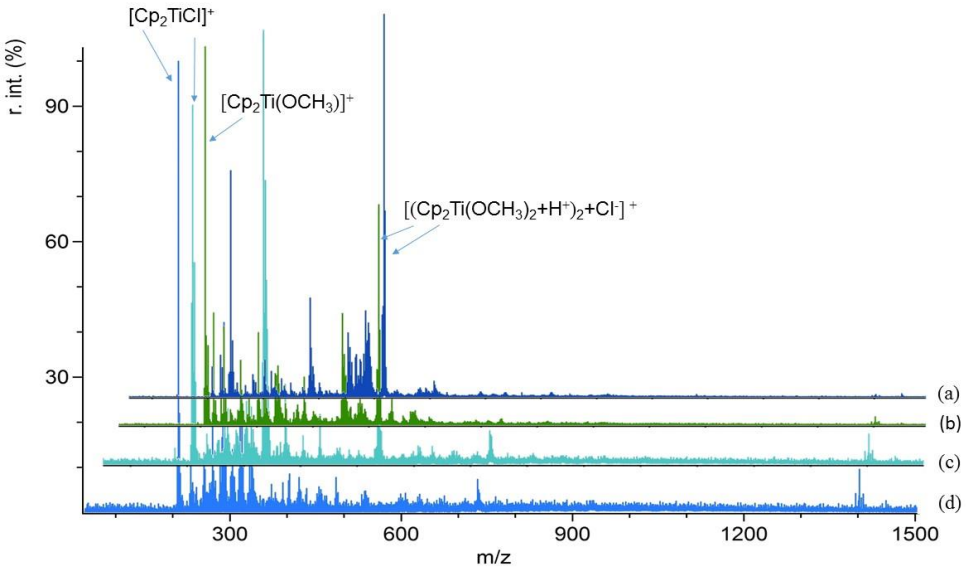

Figure 2.7: Positive-ion ESI mass spectra of a freshly-prepared solution of Cp_2TiCl_2 in methanol with wide range method at capillary exit voltages of (a) 60 V, (b) 100 V, (c) 180 V, and (d) 250 V

The resultant spectra show all the species are concentrated under *m/z* 600. A low intensity ion at *m/z* 1400 was observed when employing a 100 V or higher capillary exit voltages, but this ion does not contain Ti. Most of these species were also observed with the low range method and low range method refers to a limited *m/z* range. The single-crystal X-ray structure of the trinuclear $[Cp_3Ti_3O(OCH_3)_6](I_3)$ complex has been reported [3]. This complex was synthesised by reaction of Cp_2TiI_2 with methanol [3]. The ion $[Cp_3Ti_3O(OCH_3)_6]^+$ at expected *m/z* 541.07 was not observed in the spectra of Cp_2TiCl_2 in methanol, but it was observed during the investigation of the reactivity of $Cp_2Ti(tsal)$ towards soft electrophiles (Section 3.3.5).

Positive-ion ESI mass spectra of a freshly-prepared solution of Cp_2TiCl_2 in methanol acquired with the low range method at capillary exit voltages of 90 V and 120 V are shown in Figure 2.8 and Figure 2.9. The major species at low *m/z* range containing one titanium centre are $[Cp_2TiH]^+$ (*m/z* 179.09), $[Cp_2Ti(OCH_3)]^+$ (*m/z* 209.11), $[Cp_2TiCl]^+$ (*m/z* 213.06) and $[Cp_2Ti(OCH_3)_2+H]^+$ (*m/z* 241.14). Their corresponding species can also observed in deuterated methanol (Section 2.3.11).

The insert to Figure 2.8 shows an isotope pattern comparison of the experimentally observed *m/z* 179 (Figure 2.8A) and the calculated *m/z* 179 (Figure 2.8B) for Cp_2TiH^+. The experimentally observed *m/z* 209 is shown in Figure 2.8C while calculated *m/z* 209 was shown in Figure 2.8D for $Cp_2Ti(OCH_3)^+$. In Figure 2.9, the insert in this figure is an isotope pattern comparison of (A) the experimentally observed *m/z* 213 and (B) the calculated *m/z* 213 for Cp_2TiCl^+. (C) the experimentally observed *m/z* 241 and (D) the calculated *m/z* 241 for $[Cp_2Ti(OCH_3)_2+H]^+$.

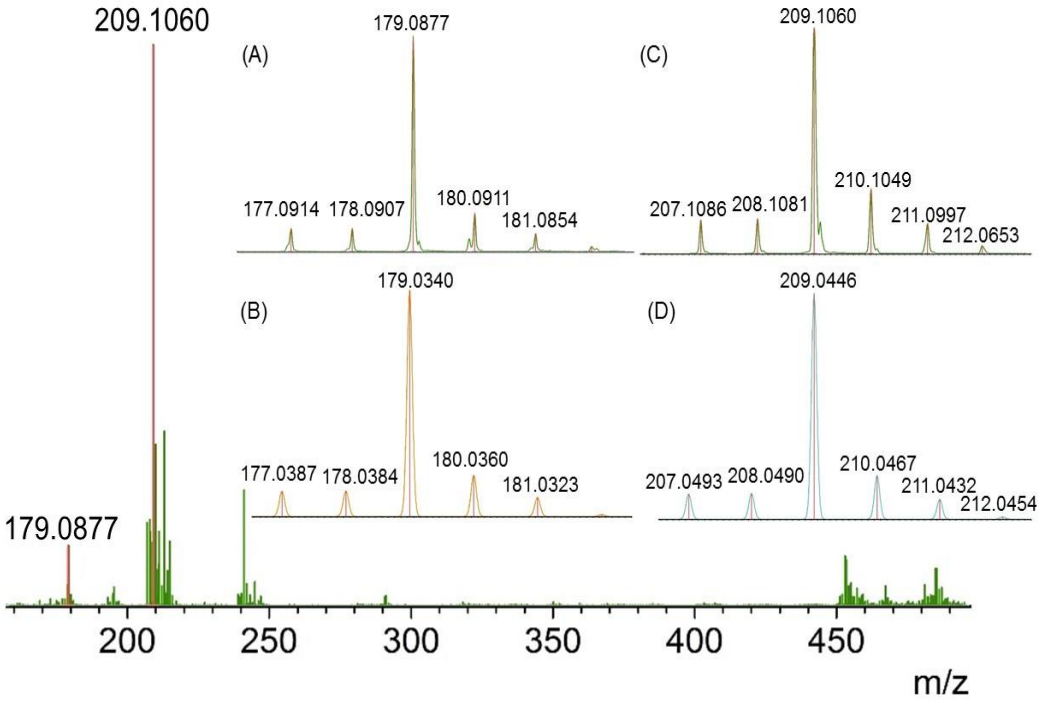

Figure 2.8: Positive-ion ESI mass spectrum of a freshly-prepared solution of Cp_2TiCl_2 in methanol with low range method at a capillary exit voltage of 90 V. The insert in this figure is an isotope pattern comparison of A the experimentally observed *m/z* 179 ion and B the calculated *m/z* 179 ion for Cp_2TiH^+. C shows the experimentally observed *m/z* 209 ion and D shows the calculated *m/z* 209 ion for $Cp_2Ti(OCH_3)^+$

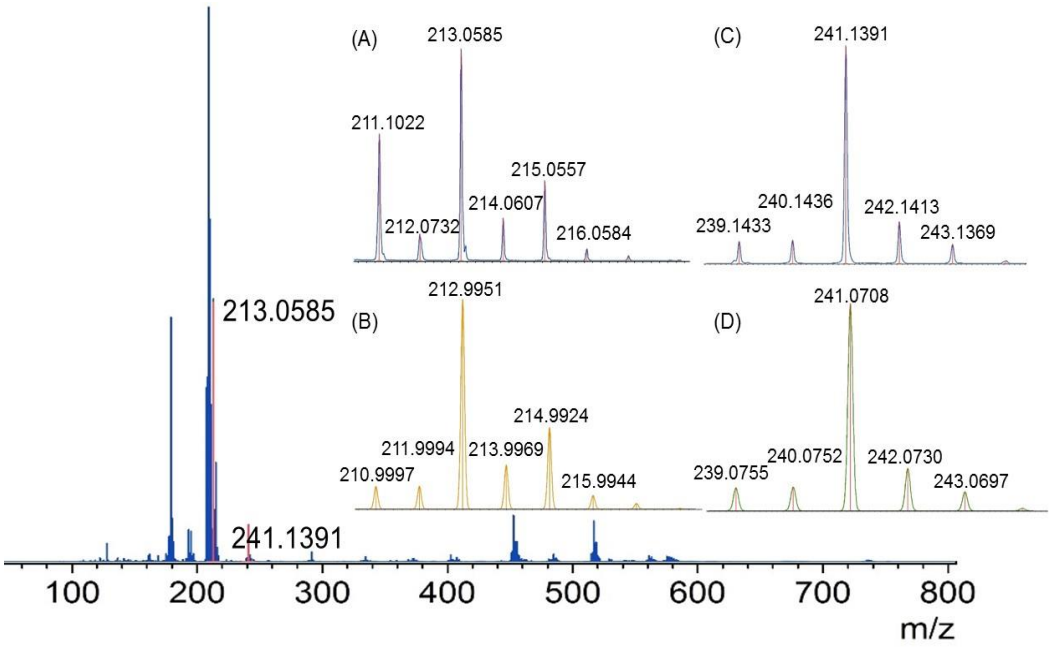

Figure 2.9: Positive-ion ESI mass spectrum of a freshly-prepared solution of Cp_2TiCl_2 in methanol with low range method at a capillary exit voltage of 120 V. The insert in this figure is an isotope pattern comparison of A the experimentally observed *m/z* 213 ion and B the calculated *m/z* 213 ion for Cp_2TiCl^+. C shows the experimentally observed *m/z* 241 ion and D shows the calculated *m/z* 241 ion for $[Cp_2Ti(OCH_3)_2+H]^+$

In Figure 2.9, as the other major ion $[Cp_2Ti(OCH_3)]^+$ was at *m/z* 209, the experimentally observed *m/z* 211 peak in (A) was much higher than the calculated *m/z* 211 peak in (B).

2.3.3 Beta-hydride elimination

$[Cp_2TiH]^+$ is one of the major species at low *m/z* range containing one titanium centre, this ion is proposed to be formed by β-hydride elimination (Figure 2.10).

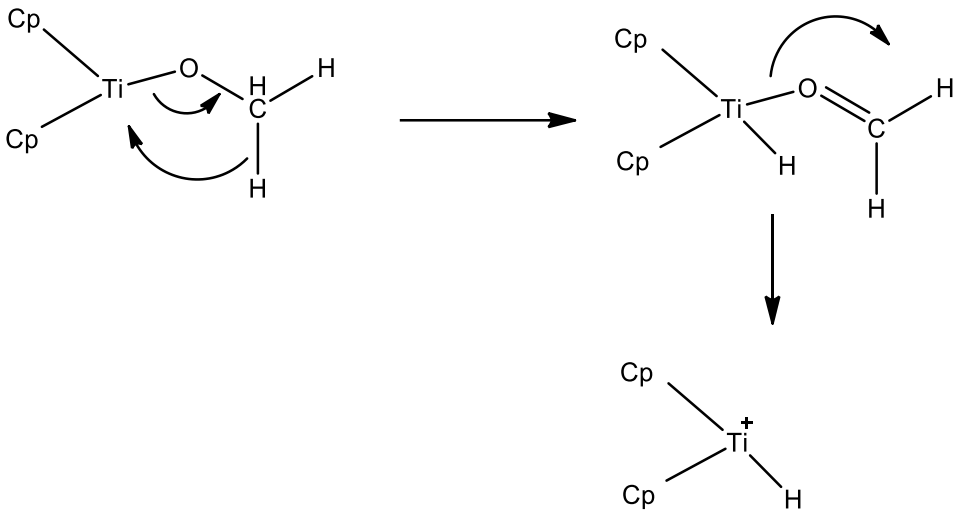

Figure 2.10: Formation of $[Cp_2TiH]^+$ from $[Cp_2Ti(OCH_3)]^+$ species by β -hydride elimination

Beta elimination is the major decomposition pathway for alkyl groups which have a hydrogen on the β-carbon. The characteristic of this elimination is cleavage of σ bond and formation of a π bond. The most famous type of β-elimination is β-hydride elimination. This reaction converts an alkyl group bonded to a metal centre into an alkene and metal-bonded hydride, which involves the formation of an M-H bond and π bond (Figure 2.11) [100].

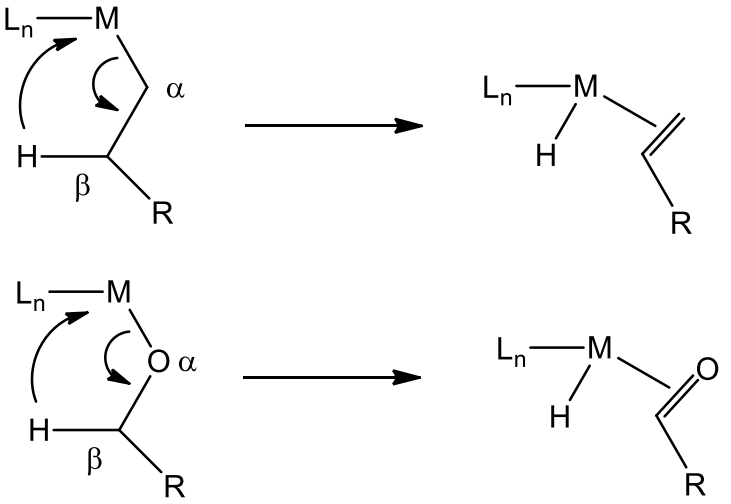

Figure 2.11: β-hydride elimination

2.3.4 Reduction reaction during ESI-MS analysis

The complex isotope pattern at *m/z* 209/210 at a capillary exit voltage of 150 V, that appeared was initially thought to be from 2 overlapping Ti species (Figure

2.12C). In fact, reduction of titanocene(IV) during ESI-MS analysis has been observed during this research. As the capillary exit voltage is increased, the relative intensity of titanocene(III) species increases. In this case, at low capillary exit voltages the titanocene(IV) species $[Cp_2Ti(OCH_3)]^+$ was observed at *m/z* 209, but as the capillary exit voltage was increased, the intensity of an overlapping *m/z* 210 peak increased (Figure 2.12). At a high capillary exit voltage (250 V, Figure 2.12d), complete reduction occurs and this *m/z* 210 ion is proposed to be the titanocene(III) species $[Cp_2Ti(CH_3OH)]^+$.

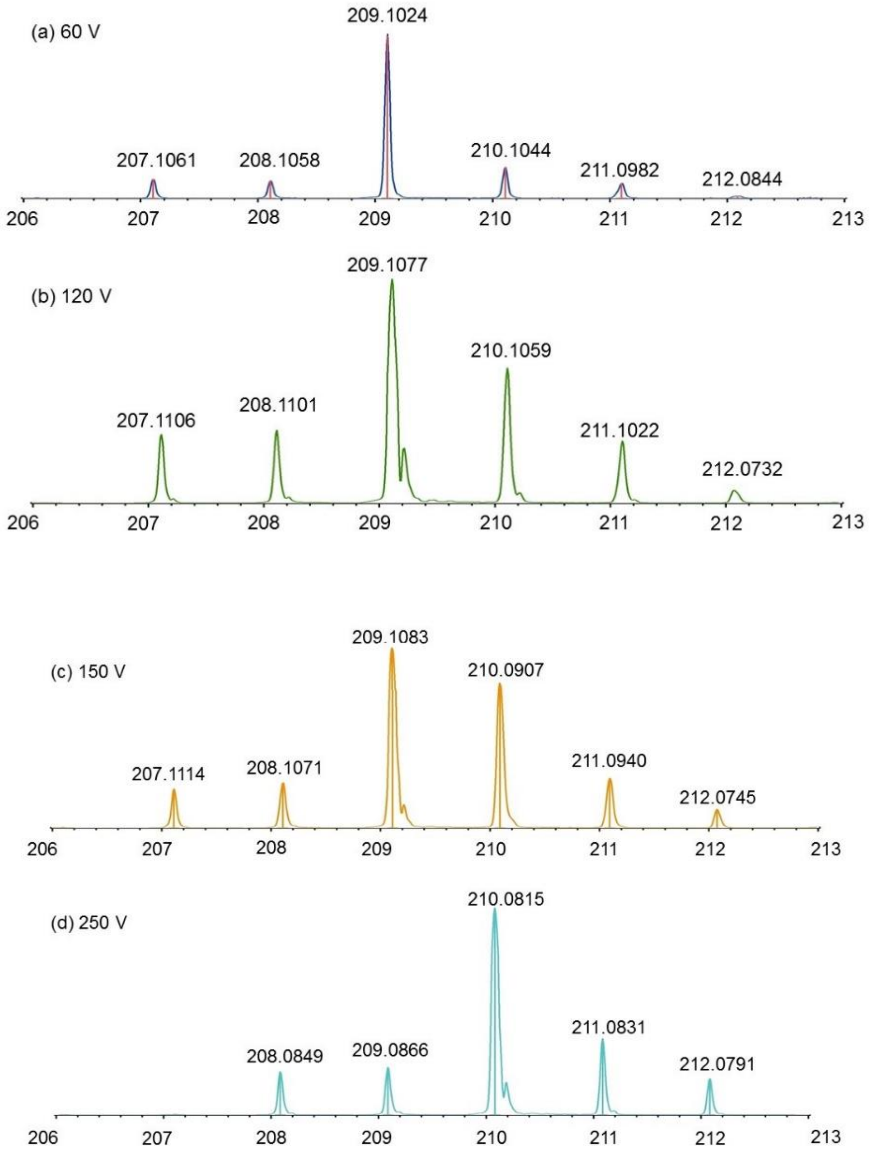

Figure 2.12: Positive-ion ESI mass spectrum of *m/z* 209 and 210 peaks of a freshly-prepared solution of Cp_2TiCl_2 in methanol with low range method at different capillary exit voltages

Titanocene(III) complexes are usually highly oxygen-sensitive and can be easily prepared by stirring the titanocene(IV) precursor and zinc or manganese dust. The applications of titanocene(III) complexes in the field of organic synthesis had been investigated and essentially Cp_2TiCl as a powerful tool in organic synthesis [101]. $Cp_2Ti(CO)_2$ is another important titanocene complex in a lower oxidation state.

This reduction reaction also occurs for other metal complexes at high voltages during ESI-MS analysis. One example is the reduction of a copper(II) chloride solution; at high voltages the bare Cu^+ ion has been observed. Another example is $InCl_3$ in methanol at high voltages where reduction to In^+ has been observed. Reduction of metal ions such as mercury(II) and iron(III) also occur readily in ESI-MS [72]. Also even for lanthanide ions, where the trivalent state dominates the aqueous chemistry of these ions, the Ln^+ ions can be obtained under highly fragmenting conditions. This has been described in the literature as 'bare metal ion' mode [102].

2.3.5 An investigation of dinuclear species observed in the ESI mass spectra of a freshly-prepared solution of Cp_2TiCl_2 in methanol

The major species at high *m/z* containing two titanium centres were only observed at low capillary exit voltages, ie $[Cp_4Ti_2Cl(OCH_3)_2]^+$ (*m/z* 453.18), $[Cp_4Ti_2(OCH_3)_3(OH)+H]^+$ (*m/z* 467.22), $[Cp_4Ti_2(OCH_3)_4+H]^+$ (*m/z* 481.24), $[Cp_4Ti_2Cl(OCH_3)_3+H]^+$ (*m/z* 485.19) and $[(Cp_2Ti(OCH_3)_2+H^+)_2+Cl^-]^+$ (*m/z* 517.23). Unfortunately just based on ESI mass spectrum, $[OCH_3+H]^+$ and $[CH_3OH]^+$ ions can't be distinguished. An illustrative spectrum is shown in Figure 2.13.

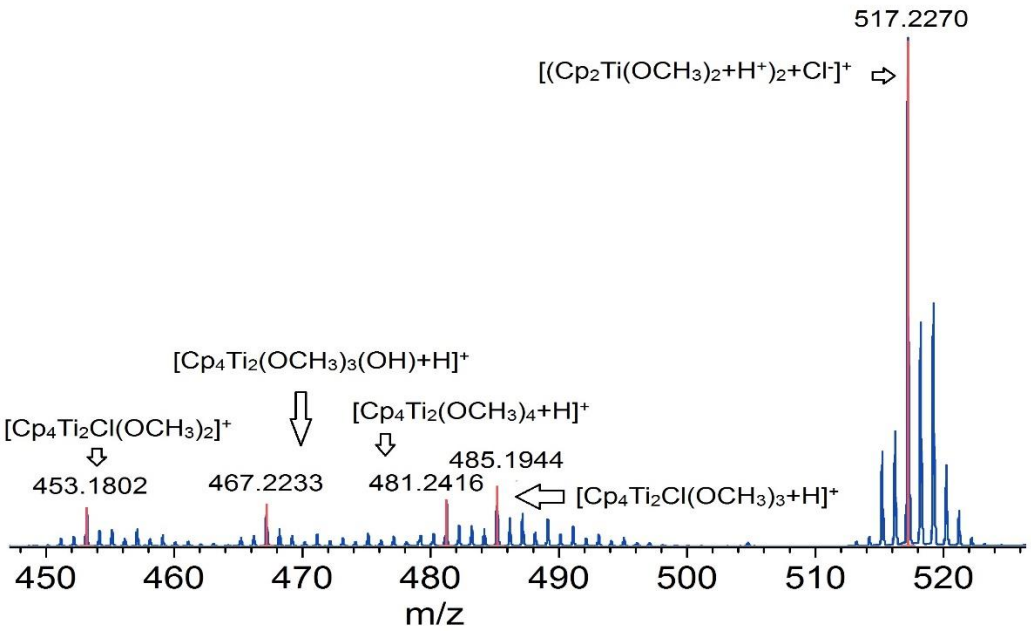

Figure 2.13: Part of the positive-ion ESI mass spectrum of a freshly-prepared solution of Cp_2TiCl_2 in methanol at mass range 440 to 530 *m/z* at a capillary exit voltage of 60 V

Dinuclear Cp_2Ti-X-$TiCp_2$ species have been synthesised previously. One example is $[Cp_2Ti(\mu\text{-}S)_2TiCp_2]$; this labile complex was synthesised as an intermediate in the reaction of $[Cp_2Ti(N^tBu)(py)]$ with an excess of MeSH or H_2S [103]. The bimetallic titanocene alkoxide species $Cp_2Ti(Ph)(\mu\text{-}OCH_2C(CH_3)_2CH_2O)(Ph)TiCp_2$ has also been reported, formed by the reaction of Cp_2TiPh_2 with 2,2-dimethylpropane-1,3-diol [104]. The X-ray crystallographic structure determination of the oxo-bridged titanium(III) complex $[Cp_2Ti]_2(\mu\text{-}O)$ has been reported [105]. This complex can be formed by the reaction of Cp_2Ti with N_2O [106].

2.3.6 An investigation of the effects of the capillary exit voltage to the peak relative intensity

The relative intensity of major species in low *m/z* range for a freshly-prepared solution of Cp_2TiCl_2 in CH_3OH varies with the capillary exit voltage. Figure 2.14 shows the relationship between relative intensity and capillary exit voltage.

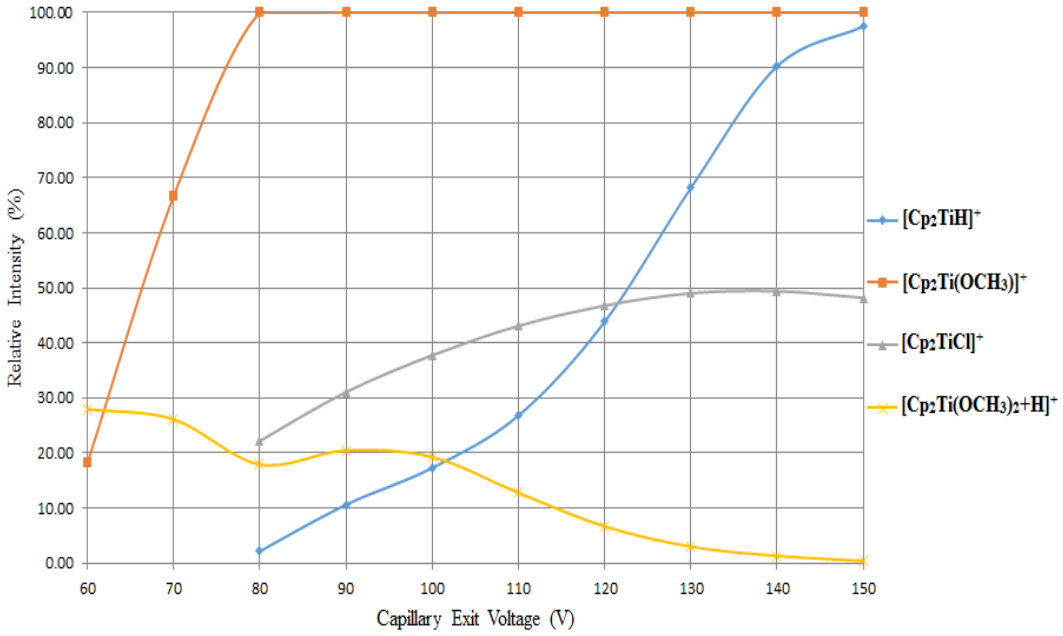

Figure 2.14: Relative intensity vs capillary exit voltage of major species in low *m/z* range for a freshly-prepared solution of Cp_2TiCl_2 in CH_3OH

This result shows that, as capillary exit voltage increases, the relative intensity of $[Cp_2TiH]^+$, $[Cp_2Ti(OCH_3)]^+$ and $[Cp_2TiCl]^+$ increases but that of $[Cp_2Ti(OCH_3)_2+H]^+$ decreases.

The relative intensities of these high *m/z* species also varies with the capillary exit voltage. Figure 2.15 shows the relationship between relative intensity and capillary exit voltage for major species at high *m/z* range.

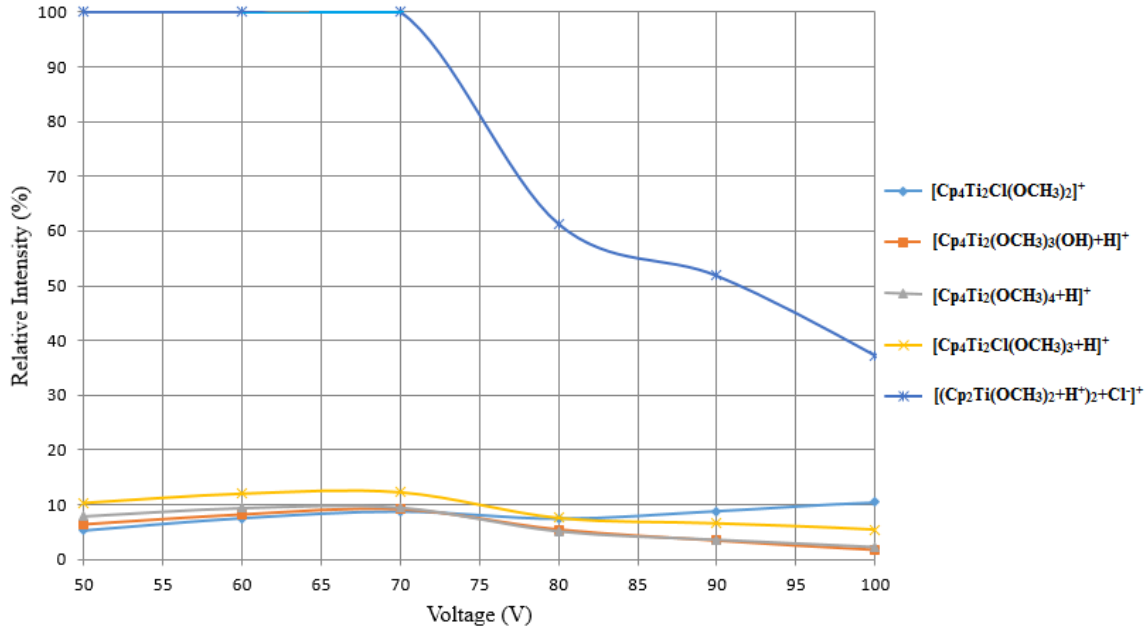

Figure 2.15: Relative intensity vs capillary exit voltage of major species in high *m/z* range for a freshly-prepared solution of Cp_2TiCl_2 in CH_3OH

This figure shows that, as the capillary exit voltage increases, the relative intensity of $[(Cp_2Ti(OCH_3)_2+H^+)_2+Cl^-]^+$ will rapidly decrease. The relative intensity of other major species at high *m/z* range is almost constant.

2.3.7 An investigation of the effects of the time to the peak intensity

The intensity of major species also changes with time. In this case, solutions of Cp_2TiCl_2 in CH_3OH were left 8 hours and spectra were recorded every two hours from time zero, using a capillary exit voltage of 60 V. Figure 2.16 shows how the major species ($[Cp_2Ti(OCH_3)]^+$, $[Cp_2Ti(OCH_3)_2+H]^+$ and $[(Cp_2Ti(OCH_3)_2+H^+)_2+Cl^-]^+$) change in absolute intensity over this period of time.

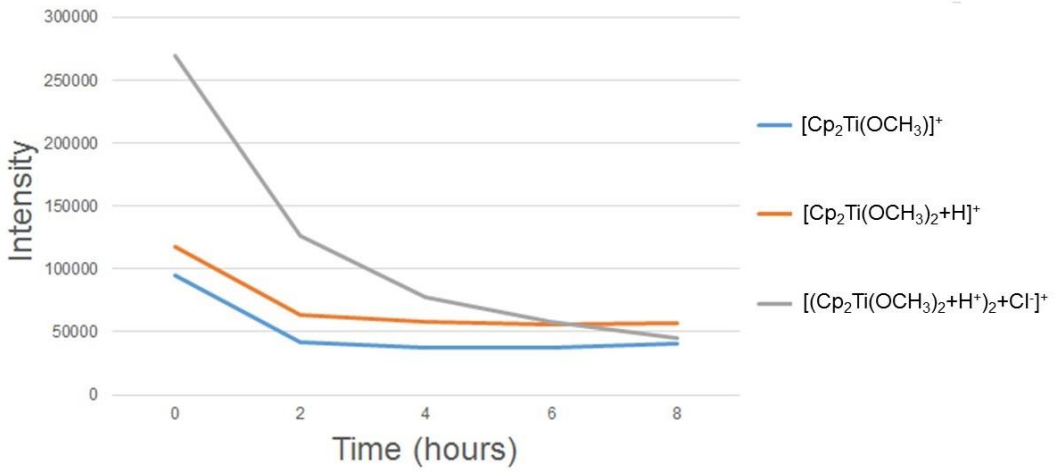

Figure 2.16: Intensity vs time for some major species

The result shows that all the intensity of major species decreased with time, with a significant decrease in the first 2 hours. After 2 hours $[Cp_2Ti(OCH_3)]^+$ and $[Cp_2Ti(OCH_3)_2+H]^+$ ions became relatively stable but the intensity of the larger ion $[(Cp_2Ti(OCH_3)_2+H^+)_2+Cl^-]^+$ is still decreasing.

2.3.8 Analysis of a freshly-prepared solution of $(EtCp)_2TiCl_2$ in methanol with low range method

The major species containing Cp groups observed in positive-ion ESI mass spectra of Cp_2TiCl_2 were confirmed by running the spectrum of $(EtCp)_2TiCl_2$ in methanol solution. Mass-shifted corresponding species should be seen in the ESI mass spectra of $(EtCp)_2TiCl_2$ if the assignments are correct. Figure 2.17 shows mass spectra of Cp_2TiCl_2 and $(EtCp)_2TiCl_2$ with low range method at a capillary exit voltage of 60 V. The spectra have a similar appearance with two groups of species, one group at lower *m/z* values and the other group at higher *m/z* values. All the major species in Cp_2TiCl_2 mass spectra can also observed in ESI mass spectra of $(EtCp)_2TiCl_2$, with the latter mass-shifted in $(EtCp)_2TiCl_2$ mass spectra. At lower *m/z* values, major species shift by *m/z* 56 i.e. Cp and EtCp differ by 28 mass units so Cp_2 and $(EtCp)_2$ differ by two times 28 mass units, i.e. 56 mass units. For example $[Cp_2Ti(OCH_3)]^+$ (*m/z* 209.10) and $[(EtCp)_2Ti(OCH_3)]^+$ (*m/z* 265.10); the intensity of this ion was larger for the EtCp compound. At higher *m/z* values, major species increase in mass by 112 units as they contain four Cp groups, such as $[(Cp_2Ti(OCH_3)_2+H^+)_2+Cl^-]^+$

(*m/z* 517.23) and $[((EtCp)_2Ti(OCH_3)_2+H^+)_2+Cl^-]^+$ (*m/z* 629.23), but this time the intensity of this ion is smaller for the EtCp compound.

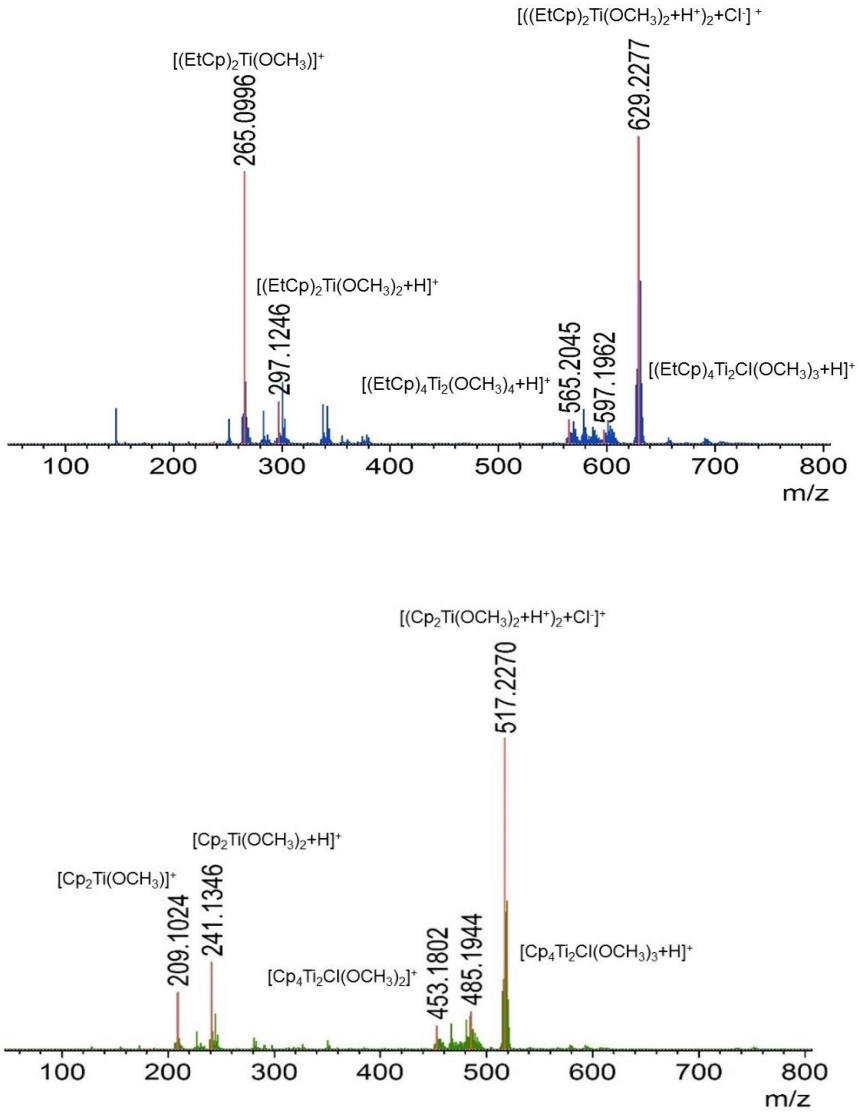

Figure 2.17: ESI mass spectra of $(EtCp)_2TiCl_2$ (Top) and Cp_2TiCl_2 (Bottom) with low range method at a capillary exit voltage of 60 V

Different capillary exit voltages were also used to record the spectra of $(EtCp)_2TiCl_2$. Table 2.6 summarises all the corresponding species which were observed at various voltages.

Table 2.6: Summary of corresponding species formed by Cp_2TiCl_2 and $(EtCp)_2TiCl_2$

	Cp_2TiCl_2 species	***m/z***	**$(EtCp)_2TiCl_2$ species**	***m/z***
1 Ti	$[Cp_2Ti(OCH_3)]^+$	209.04	$[(EtCp)_2Ti(OCH_3)]^+$	265.11
	$[Cp_2Ti(OCH_3)(OH)H]^+$	227.06	$[(EtCp)_2Ti(OCH_3)(OH)H]^+$	283.12
	$[Cp_2Ti(OCH_3)_2H]^+$	241.07	$[(EtCp)_2Ti(OCH_3)_2H]^+$	297.13
	$[Cp_2TiCl(OCH_3)H]^+$	245.02	$[(EtCp)_2TiCl(OCH_3)H]^+$	301.08
	$[Cp_2TiCl_2H]^+$	248.97	$[(EtCp)_2TiCl_2H]^+$	305.03
	$[Cp_2TiCl]^+$	213.00	$[(EtCp)_2TiCl]^+$	269.06
	$[Cp_2Ti(OH)]^+$	195.03	$[(EtCp)_2Ti(OH)]^+$	251.09
	$[Cp_2Ti(OH)_2H]^+$	213.04	$[(EtCp)_2Ti(OH)_2H]^+$	269.10
2 Ti	$[Cp_4Ti_2(OCH_3)_4H]^+$	481.13	$[(EtCp)_4Ti_2(OCH_3)_4H]^+$	593.26
	$[Cp_4Ti_2(OCH_3)_3]^+$	449.11	$[(EtCp)_4Ti_2(OCH_3)_3]^+$	561.23
	$[Cp_4Ti_2(OCH_3)_3ClH]^+$	485.08	$[(EtCp)_4Ti_2(OCH_3)_3ClH]^+$	597.21
	$[Cp_4Ti_2(OCH_3)_2Cl]^+$	453.06	$[(EtCp)_4Ti_2(OCH_3)_2Cl]^+$	565.18
	$[Cp_4Ti_2(OCH_3)_2Cl_2H]^+$	489.04	$[(EtCp)_4Ti_2(OCH_3)_2Cl_2H]^+$	601.16
	$[Cp_4Ti_2(OCH_3)_2(OH)]^+$	435.09	$[(EtCp)_4Ti_2(OCH_3)_2(OH)]^+$	547.22
	$[Cp_4Ti_2(OCH_3)_2(OH)_2H]^+$	453.10	$[(EtCp)_4Ti_2(OCH_3)_2(OH)_2H]^+$	565.23

2.3.9 Analysis of solutions of Cp_2TiCl_2 in other alcohols using ESI-MS

The analysis of the spectra of Cp_2TiCl_2 dissolved in other alcohols, namely in ethanol, propan-1-ol and butan-1-ol solution can also help to confirm the identity of some species and explore the behaviour in larger chain alcohols. Spectra of Cp_2TiCl_2 in various alcohols at a capillary exit voltage of 60 V are shown in Figure 2.18. For example, one major species observed in methanol was $[Cp_2Ti(OCH_3)]^+$ (*m/z* 209.10); when the spectrum was recorded in ethanol as the solvent, the analogous species $[Cp_2Ti(OCH_2CH_3)]^+$ was observed at *m/z* 223.10. The corresponding species $[Cp_2Ti(OR)]^+$ can also be observed in propan-1-ol at *m/z* 237.05 and in butan-1-ol at *m/z* 251.07.

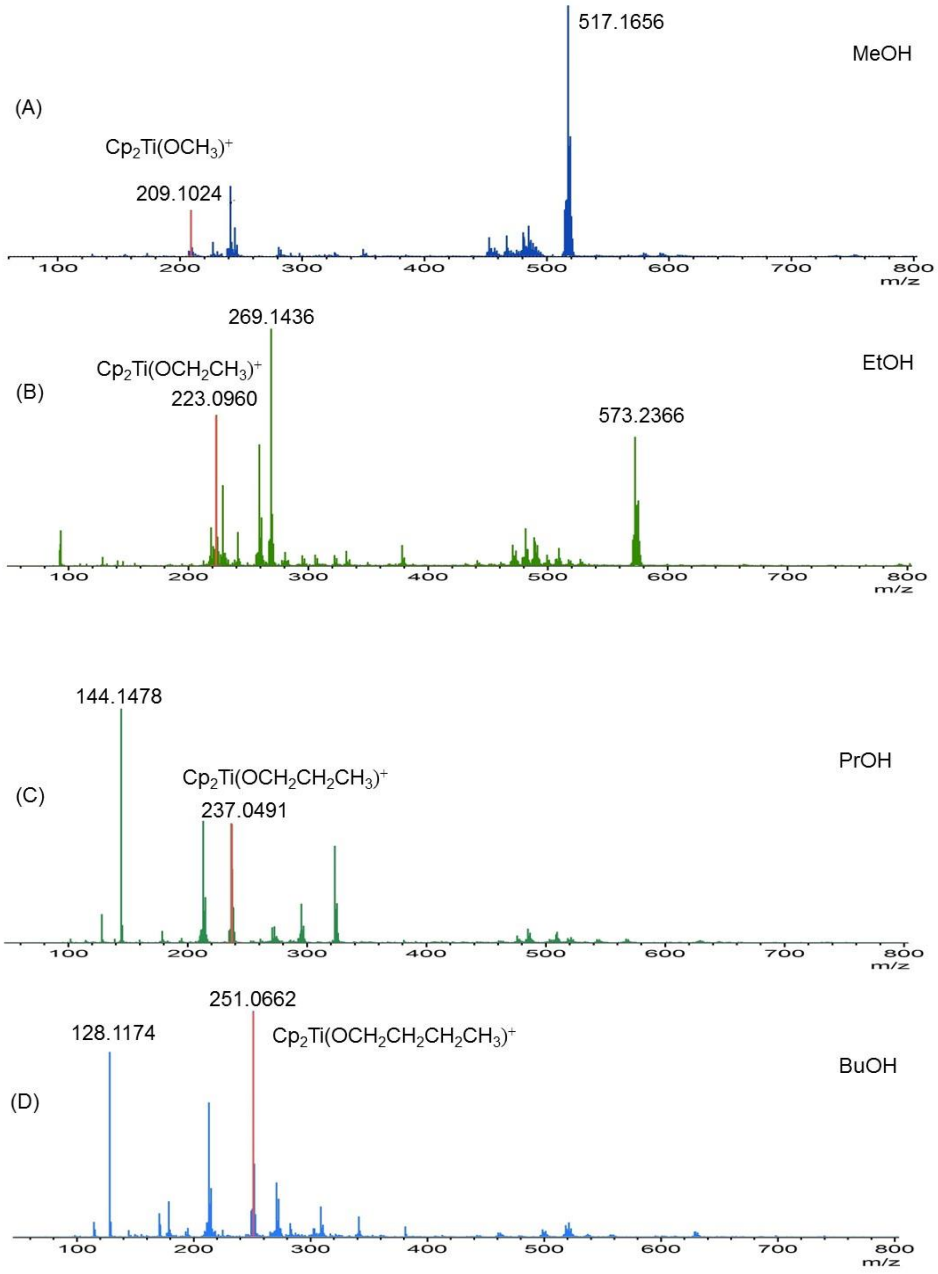

Figure 2.18: Positive-ion ESI mass spectra of a freshly-prepared solution of Cp_2TiCl_2 in (A) methanol, (B) ethanol, (C) propan-1-ol and (D) butan-1-ol at a capillary exit voltage of 60 V

All the major species observed at a capillary exit voltage of 60 V with low and wide range methods in various alcohols are summarised in Table 2.7. Some of these species are not present in the propan-1-ol and butan-1-ol solutions, possibly due to the greater steric size of these larger alcohols.

Table 2.7: Summary of corresponding species of Cp_2TiCl_2 in various alcohols at a capillary exit voltage of 60 V with low and wide range methods. (---- not observed)

Species	Methanol (*m/z*)	Ethanol (*m/z*)	Propan-1-ol (*m/z*)	Butan-1-ol (*m/z*)
$[Cp_2Ti(OR)]^+$	209.07	223.10	237.05	251.07
$[Cp_2Ti(OR)OH+H]^+$	227.08	241.11	----	----
$[Cp_2Ti(OR)_2+H]^+$	241.10	269.14	297.11	325.15
$[Cp_2Ti(OR)Cl+H]^+$	245.05	259.08	273.03	287.05
$[Cp_2TiCl_2+ROH+H]^+$	281.03	295.06	309.01	323.04
$[Cp_4Ti_2(OR)_2Cl]^+$	453.13	481.17	509.15	537.15
$[Cp_4Ti_2(OR)Cl_2]^+$	457.08	471.10	485.03	499.05
$[Cp_4Ti_2(OR)(OH)Cl_2+H]^+$	475.07	489.10	503.04	517.07
$[Cp_4Ti_2(OR)_3Cl+H]^+$	485.13	527.20	----	----
$[Cp_4Ti_2(OR)_2Cl_2+H]^+$	489.10	517.14	545.02	----
$[(Cp_2Ti(OR)_2+H^+)_2+Cl]^-$	517.17	573.26	629.25	----

The intensities of different ions change when the alcohol is changed. Solutions of Cp_2TiCl_2 in various alcohols (methanol, ethanol, propan-1-ol and butan-1-ol) at concentration of 2 mg mL^{-1} at a capillary exit voltage of 150 V were analysed on same day, intensity of $[Cp_2Ti(OR)]^+$ ion in various alcohols are given in Table 2.8.

The result shown that $[Cp_2Ti(OR)]^+$ ion has highest intensity in CH_3OH at capillary exit voltage of 150 V with low range method and in ethanol its intensity will decreased by a half. Intensities of this ion in propan-1-ol also dropped by half compared to it in ethanol. The literature reports that butanols are much less volatile than ethanol [107] and volatility could affect ion production [108], therefore why the lowest intensities in butan-1-ol.

Table 2.8: Intensity of $Cp_2Ti(OR)^+$ in various alcohols at a capillary exit voltage of 50 V with low range method

	Methanol	Ethanol	Propan-1-ol	Butan-1-ol
$[Cp_2Ti(OR)]^+$	(*m/z* 209)	(*m/z* 223*)*	(*m/z* 237)	(*m/z* 251)
Intensity (counts per second)	$1.76x10^6$	$9.18x10^5$	$4.68x10^5$	$2.79x10^4$

2.3.10 Analysis of freshly-prepared solutions of Cp_2TiCl_2 and $(EthylCp)_2TiCl_2$ in a non-protic solvent using ESI-MS

The mass spectra of freshly-prepared solutions of Cp_2TiCl_2 and $(EtCp)_2TiCl_2$ in a non-protic solvent were also investigated during this research. Acetonitrile was used as the non-protic solvent because it is a coordinating solvent but without alkoxide groups to complicate the spectra. Positive-ion ESI mass spectra of freshly-prepared solutions of Cp_2TiCl_2 and $(EtCp)_2TiCl_2$ in acetonitrile with low range method at a capillary exit voltage of 60 V are shown in Figure 2.19 and Figure 2.20 respectively.

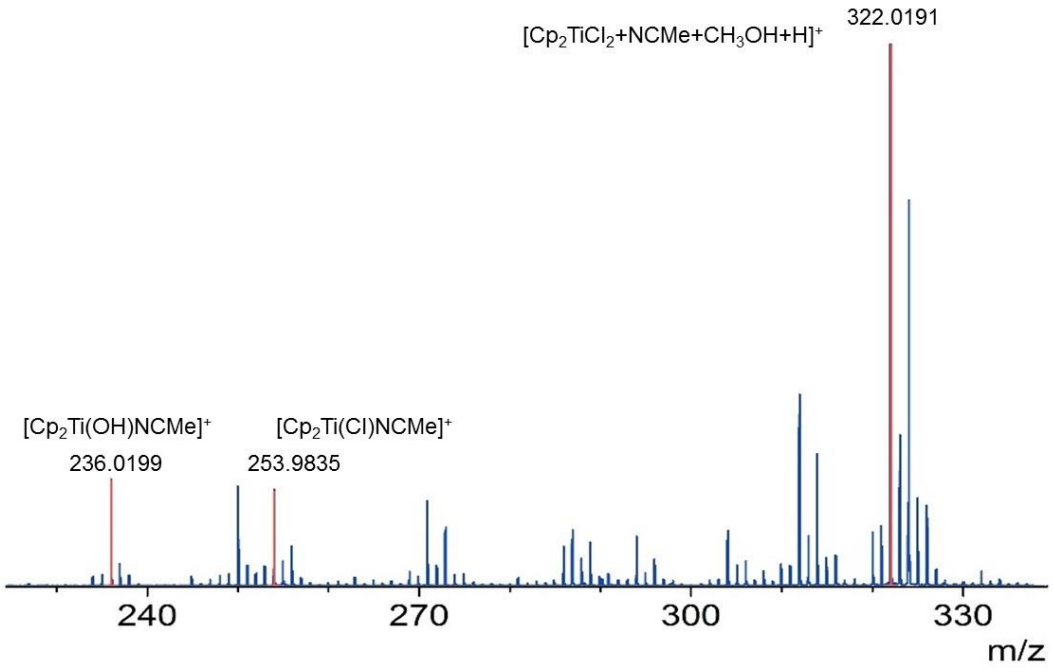

Figure 2.19: Positive-ion ESI mass spectrum of Cp_2TiCl_2 in acetonitrile at a capillary exit voltage of 60 V with low range method

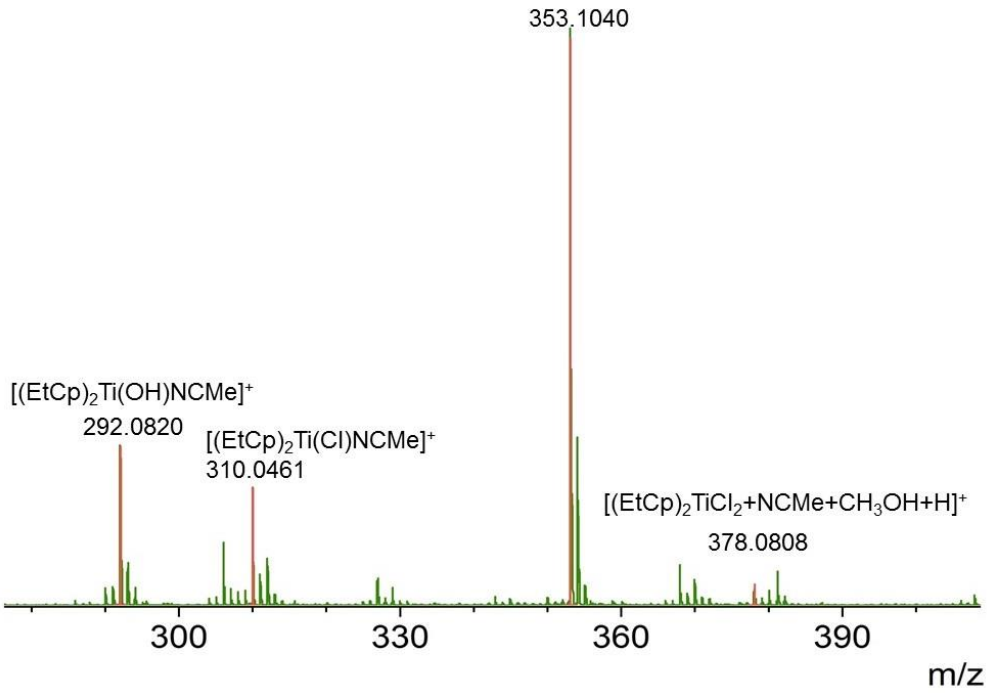

Figure 2.20: Positive-ion ESI mass spectrum of $(EtCp)_2TiCl_2$ in acetonitrile at a capillary exit voltage of 60 V with low range method. *m/z* 353.10 ion does not contain Ti

The results indicate that acetonitrile can easily react with Cp_2TiCl_2 and $(EtCp)_2TiCl_2$. Referring to Section 2.3.1, the result clearly shows that some isotope pattern of Cl-containing ions had been observed. For instance, the ion $[Cp_2Ti(Cl)NCMe]^+$ at *m/z* 253.98 in Figure 2.19, the isotope pattern at *m/z* 253.98 and *m/z* 255.98 that represent the M and M+2 in a 3:1 ratio which indicates the presence of one Cl atom. Mass-shifted corresponding species $[(EtCp)_2Ti(Cl)NCMe]^+$ at *m/z* 310.05 in Figure 2.20 also observed in the ESI mass spectra of $(EtCp)_2TiCl_2$ in acetonitrile. In Figure 2.20, a high intensity ion at *m/z* 353.10 was observed and this ion does not contain Ti.

The $[Cp_2Ti(Cl)NCMe]^+$ complex has been previously characterised by an X-ray structure determination which shows the Ti atom and acetonitrile ligand are nearly collinear and the Ti atom exhibits a distorted tetrahedral coordination [109]. The crystal and molecular structure of Ti(III) complex $[Cp_2Ti(NCMe)_2]^+$ has also been established. The coordination geometry of the Ti atom is pseudotetrahedral from an X-ray structure determination [110]. The other example of cationic Ti(III) acetonitrile complex is $[Cp_2Ti(NCMe)(THF)]^+$, which has been characterised by X-

ray crystallography, this complex adopts a pseudotetrahedral structure similar to $[Cp_2Ti(NCMe)_2]^+$ and the acetonitrile ligand is nearly linear [111].

2.3.11 Analysis of a freshly-prepared solution of Cp_2TiCl_2 in deuterated methanol using ESI-MS

The analysis of the spectra of Cp_2TiCl_2 dissolved in deuterated methanol (CD_3OD) was also investigated to confirm the identity of some species. Spectra of Cp_2TiCl_2 in CD_3OD at a capillary exit voltage of 90 V are given in Figure 2.21a.

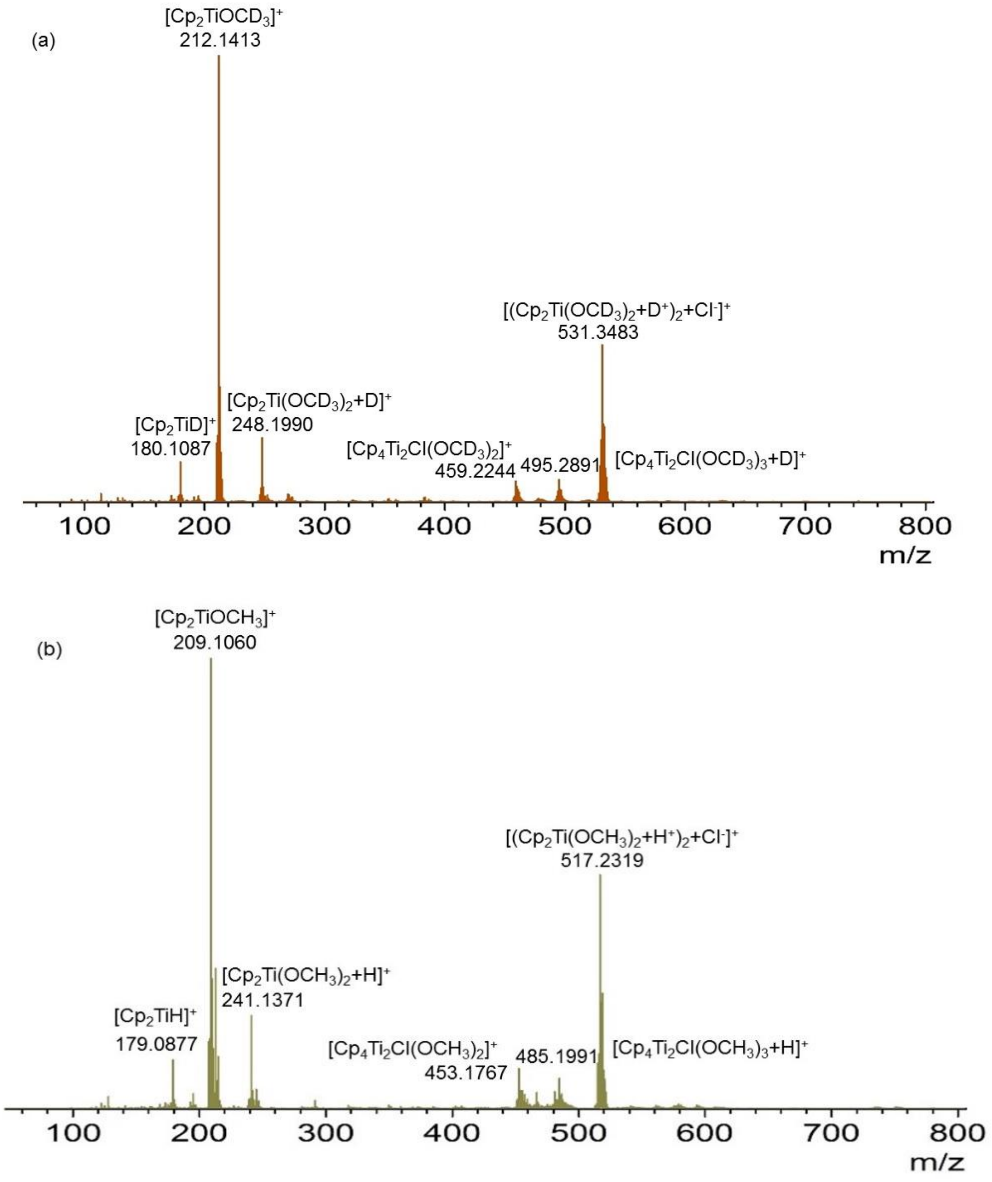

Figure 2.21: Positive-ion ESI mass spectra of Cp_2TiCl_2 a) in CD_3OD b) in CH_3OH at a capillary exit voltage of 90 V with low range method

All the major species in the mass spectra of Cp_2TiCl_2 in CH_3OH can also observed in mass spectra of Cp_2TiCl_2 in CD_3OD and with the latter mass-shifted in CD_3OD mass spectra. The species with -OCH_3 group will shift by *m/z* 3 i.e. -OCH_3 and -OCD_3 differ by 3 mass units. For example, one major species observed in CH_3OH was $Cp_2Ti(OCH_3)^+$ (*m/z* 209.11); when the spectrum was recorded in CD_3OD as the solvent, the analogous species $Cp_2Ti(OCD_3)^+$ was observed at the expected *m/z* 212.14.

Table 2.9 summarises all the corresponding species which were observed in CH_3OH and CD_3OD.

Table 2.9: Summary of corresponding species of Cp_2TiCl_2 in CH_3OH and CD_3OD at a capillary exit voltage of 90 V with low range method

Cp_2TiCl_2 in CH_3OH	***m/z***	**Cp_2TiCl_2 in CD_3OD**	***m/z***
$[Cp_2TiH]^+$	179.09	$[Cp_2TiD]^+$	180.11
$[Cp_2Ti(OCH_3)]^+$	209.11	$[Cp_2Ti(OCD_3)]^+$	212.14
$[Cp_2Ti(OCH_3)_2+H]^+$	241.14	$[Cp_2Ti(OCD_3)_2+D]^+$	248.20
$[Cp_4Ti_2Cl(OCH_3)_2]^+$	453.18	$[Cp_4Ti_2Cl(OCD_3)_2]^+$	459.22
$[Cp_4Ti_2Cl(OCH_3)_3+H]^+$	485.20	$[Cp_4Ti_2Cl(OCD_3)_3+D]^+$	495.29
$[(Cp_2Ti(OCH_3)_2+(H)^+)_2+Cl^-]^+$	517.23	$[(Cp_2Ti(OCD_3)_2+D^+)_2+Cl^-]^+$	531.35

At a capillary exit voltage of 180 V, a new species at *m/z* 211 was observed (Figure 2.22B). Compared to the species $[Cp_2Ti(OCD_3)]^+$ (*m/z* 212) observed at low voltages, this species has decreased by 1 *m/z* unit.

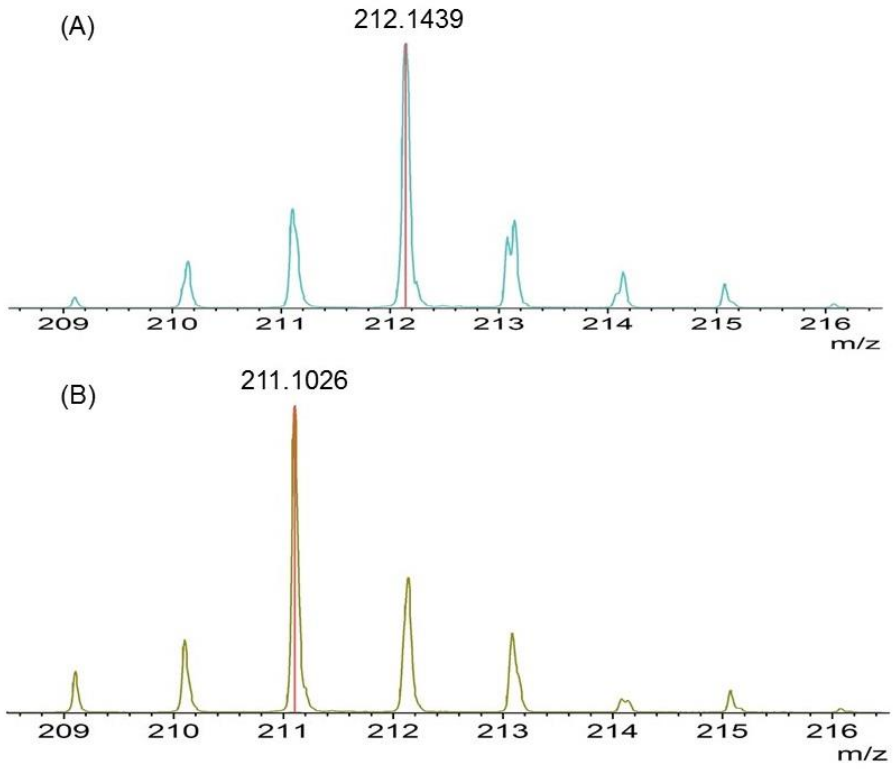

Figure 2.22: Positive-ion ESI mass spectra of *m/z* 212 and 211 peaks of a freshly-prepared solution of Cp_2TiCl_2 in CD_3OD at a capillary exit voltage of (A) 150 V and (B) 180 V with low range method

Since in CH_3OH, the species $[Cp_2Ti(OCH_3)]^+$ at *m/z* 209 is observed at a capillary exit voltage of 150 V which corresponds to the species $[Cp_2Ti(OCD_3)]^+$ at *m/z* 212 in CD_3OD. As the capillary exit voltage increased to 180 V, titanocene(III) species $[Cp_2Ti(CH_3OH)]^+$ at *m/z* 210 was proposed to be observed (Section 2.3.4). However, the *m/z* unit increased by 1 as the capillary exit voltage increased (Figure 2.23).

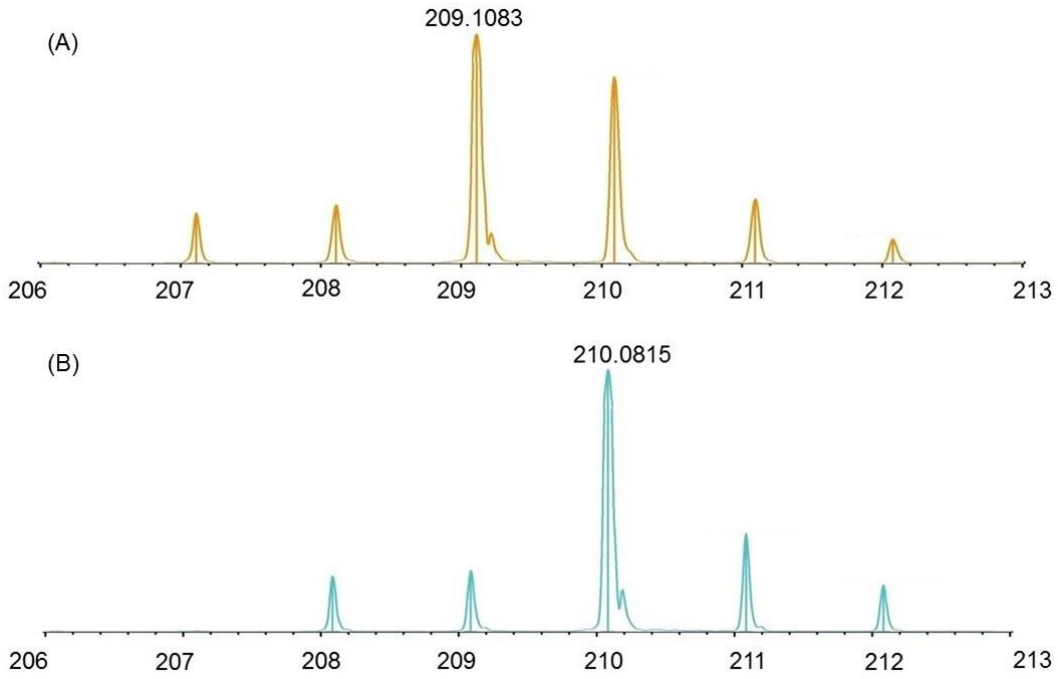

Figure 2.23: Positive-ion ESI mass spectrum of *m/z* 209 and 210 peaks of a freshly-prepared solution of Cp_2TiCl_2 in CH_3OH at capillary exit voltages of (A) 150 V and (B) 180 V with low range method

Another possible explanation is the ion at *m/z* 210 in CH_3OH could be a superoxo complex $Cp_2TiO_2^+$ and the ion at *m/z* 211 in CD_3OD is a protonated peroxo species (Isotope pattern comparison provided by Ryland Fortney-Zirker) (Figure 2.24). The source of H^+ ions could be from residual water in the instrument (e.g. drying gas).

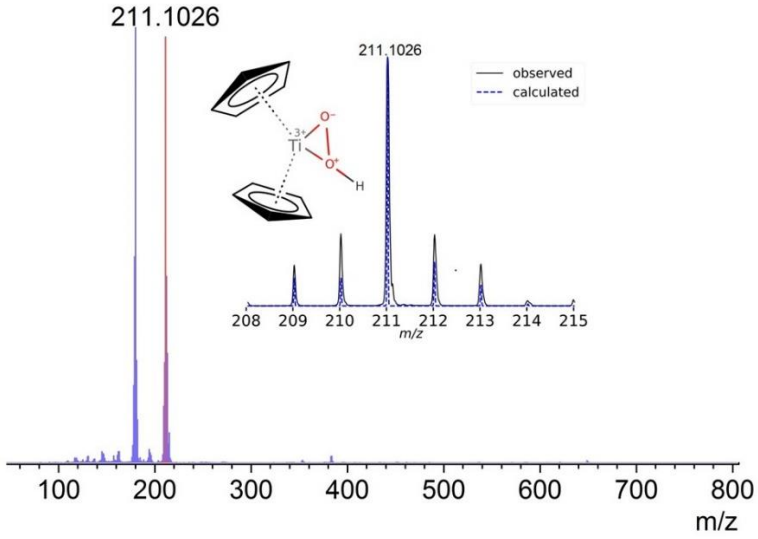

Figure 2.24: Positive-ion ESI mass spectrum of Cp_2TiCl_2 in CD_3OD at a capillary exit voltage of 180 V with low range method. The insert shows an isotope pattern comparison of the experimentally and the calculated protonated peroxo species at m/z 211

The source of oxygen in the protonated peroxo species could be from the nitrogen generator. There would be oxygen in the nitrogen feed for the ESI-MS from the nitrogen generator. The nitrogen generator unit used during this research has the practical oxygen ranges from about 2.5% to 5%.

There are no reports on Cp_2Ti(peroxy) species, but a similar complex $(C_5Me_4{}^iPr)_2TiO_2$ has been synthesised and characterised by the NMR spectroscopy and X-ray diffraction and confirms the side-on hapticity of the peroxide ligand [112].

Overall, compared to the ESI mass spectra of Cp_2TiCl_2 in CH_3OH at low capillary exit voltage, mass-shifted corresponding species can be observed in the ESI mass spectra of Cp_2TiCl_2 in CD_3OD, but the presence of *m/z* 211 in CH_3OH and *m/z* 210 in CD_3OD at a capillary exit voltage of 180 V, looks like Cp_2TiCl_2 in CH_3OH and CD_3OD behave differently at high capillary exit voltage. The further experiment was done to run the spectrum of Cp_2TiCl_2 in CH_3OH with 1 drop of dilute hydrogen peroxide, but the peroxy species was not observed at low capillary exit voltages.

2.4 Discussion

The positive-ion ESI-MS spectra for Cp_2TiCl_2 and $(EtCp)_2TiCl_2$ in methanol, ethanol, propan-1-ol or butan-1-ol, recorded at a range of capillary exit voltages, have identified some major species containing one or two Ti centres, but these species containing two Ti centres disappeared when the capillary exit voltage was greater than 150 V. Larger Ti clusters which contain three or more Ti centres were not observed. The presence of Ti species containing OH groups indicated that rapid hydrolysis of the Cp_2TiCl_2 occurred and OR groups indicated alcoholysis of the Cp_2TiCl_2 occurred. The hydrolysis of the Cp ligands is much slower than that hydrolysis of the Cl ligands.

To confirm the identity of some species observed in the mass spectra of Cp_2TiCl_2 in methanol, various alcohols, deuterated methanol and $(EtCp)_2TiCl_2$ have been used. Most of corresponding species can be observed. The relative intensity of major species can be influenced by the capillary exit voltage and aging of the sample in the solvent. Reduction of titanium(IV) during ESI-MS analysis was also observed when the capillary exit voltage was greater than 150 V and other tentative

suggestion is that a protonated peroxo species is formed at a high capillary exit voltage.

Chapter 3

An investigation of the ESI-MS behaviour of $Cp_2Ti(SC_6H_4CO_2)$

3.1 Introduction

3.1.1 Review of the previous investigation of $Cp_2Ti(tsal)$

Bis(cyclopentadienyl) thiosalicylatotitanium(IV) is the organotitanium compound with the formula $Cp_2Ti(SC_6H_4CO_2)$, commonly abbreviated as $Cp_2Ti(tsal)$. $Cp_2Ti(tsal)$ exists as a deep green coloured solid and has been characterised by NMR and IR spectroscopies [92]. $Cp_2Ti(tsal)$ has been previously synthesised by reaction of Cp_2TiCl_2 with thiosalicylic acid in benzene and with anhydrous ammonia gas as base (Scheme 3.1) [113].

$$Cp_2TiCl_2 + HSC_6H_4COOH + 2NH_3 \longrightarrow Cp_2Ti(SC_6H_4COO) + 2NH_4Cl$$

Scheme 3.1: Formation of $Cp_2Ti(tsal)$ from Cp_2TiCl_2 and thiosalicylic acid

$Cp_2Ti(tsal)$ can be also synthesised by reaction of Cp_2TiCl_2 with thiosalicylic acid in a water-chloroform mixture with β-cyclodextrin [13].

The thiosalicylate in $Cp_2Ti(tsal)$ acts as a bidentate ligand and forms a puckered six-membered ring with the titanium atom as shown by the X-ray structure determination (Figure 3.1) [92]. The coordination geometry of the Ti atom is pseudotetrahedral and the distances between the Ti and two Cp rings are different; presumably from Ti to the centroid of the Cp rings are 2.0707 Å and 2.0627 Å [114]. This complex exhibits a 3D framework constructed through weak interactions, which are four intermolecular C-H…π interactions and two types of intermolecular hydrogen bonds (C13-H13…O2 and C8-H8…S1) [92].

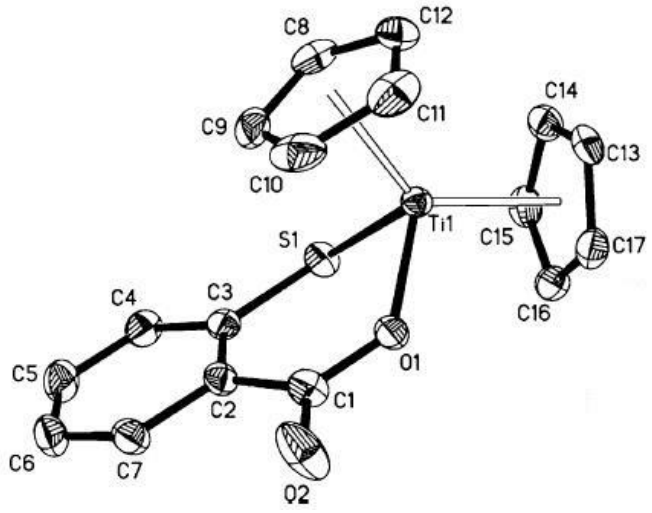

Figure 3.1: Molecular structure of $Cp_2Ti(tsal)$

The electron ionisation mass spectrum of this compound was reported in 1969 [113]. The metal-containing ion peaks are summarised in Table 3.1.

Table 3.1: Metal-containing ions recorded in the mass spectrum of $Cp_2Ti(tsal)$

Ions	*m/z*	Relative intensity (%)
$C_{17}H_{14}O_2STi^+$	330	79
$C_{16}H_{13}STi^+$	285	2.7
$C_{11}H_9STi^+$	221	100
$C_9H_7STi^+$	195	9
$C_{10}H_{10}Ti^+$	178	35
$C_5H_5STi^+$	145	10.3
$C_5H_5Ti^+$	113	8

The electron ionisation mass spectrum of $Cp_2Ti(tsal)$ gave a molecular ion peak at *m/z* 330 which showed the compound to be monomeric with a closed ring structure [113]. The proposed fragmentation pattern for $Cp_2Ti(tsal)$ is shown in Figure 3.2.

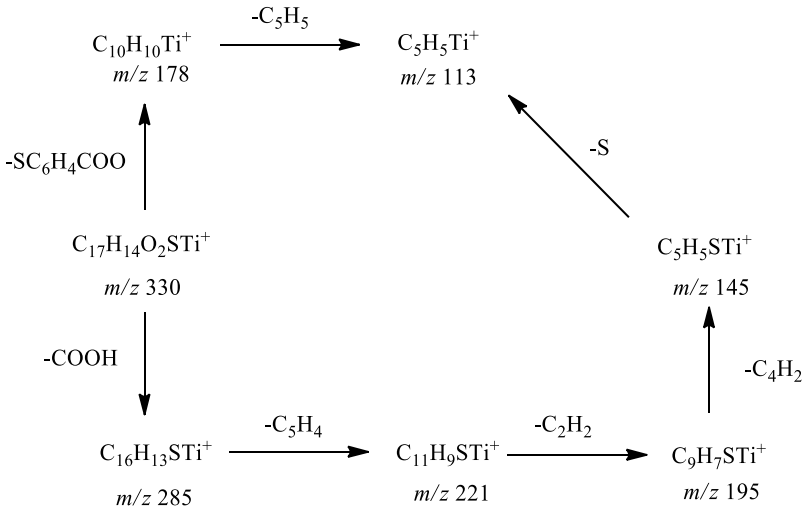

Figure 3.2: The proposed fragmentation pattern for $Cp_2Ti(tsal)$

3.1.2 Project outline

Titanium is normally considered to be a chemically very hard metal centre [115]. Because the high polarisability of the chalcogen atoms, thiolate is generally soft [116], so it is interesting that $Cp_2Ti(tsal)$ is a rare example which contains a Ti-S bond and it is very stable and can even be made in water [117]. This research project carried out a much more in-depth investigation into the ESI-MS behaviour of the $Cp_2Ti(tsal)$ complex. At the same time, a new complex bis(ethylcyclopentadienyl) thiosalicylatotitanium(IV) $(EtCp)_2Ti(tsal)$ ($EtCp = C_5H_4CH_2CH_3$) (Figure 3.3) was synthesised and also studied by ESI-MS. Comparison of the ESI-MS spectra of $Cp_2Ti(tsal)$ with those of $(EtCp)_2Ti(tsal)$ was used to confirm the identity of some unknown species. The further experiment was done to run the spectrum of the mixed solution of Cp_2TiCl_2 and $Cp_2Ti(tsal)$ in CH_3OH, to investigate the possibility of the tsal ligand bridging two Cp_2Ti centres. Characterisation of $Cp_2Ti(tsal)$ using ESI mass spectrometry in the presence of added alkali metal salts and the reactivity of $Cp_2Ti(tsal)$ towards soft electrophiles have also been studied.

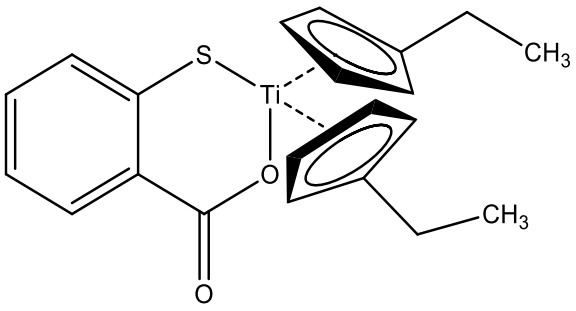

Figure 3.3: Chemical structure of $(EtCp)_2Ti(tsal)$

3.2 Experimental

The chemicals, solvents and instruments used during this research are listed in sections 3.2.1 to 3.2.4.

3.2.1 Chemicals and solvents

Powdered bis(cyclopentadienyl)titanium(IV) dichloride was obtained from Ralph N. Emanuel Ltd, Alperton, Middlesex, UK and bis(ethylcyclopentadienyl) titanium(IV) dichloride was purchased from Alfa Aesar, alkali metal salts: LiCl, KCl, RbCl and CsCl were all purchased from Ajax Finechem. NaCl was purchased from Dominion Salt Limited. PhHgCl was purchased from BDH. FcHgCl was synthesised according to the literature method [118]. Univar grade methanol used was distilled. Ethanol used was of laboratory reagent grade. Dichloromethane was obtained from Merck KGaA. Petroleum spirits and toluene were purchased from Ajax Finechem with analytical reagent grade.

3.2.2 ESI-MS instrumentation

As described for the ESI-MS investigation of Cp_2TiCl_2 (Section 2.2.2), ESI-MS instrumentation was the same as in this previous chapter.

3.2.3 NMR instrumentation

^1H NMR spectroscopy was performed on the University of Waikato School of Sciences Bruker AVIII (400) NMR spectrometer running Topspin 3.5 pl 7 software. The spectrometer was fitted with a 5 mm ATMA BBI probe operating at 300 MHz for ^1H spectroscopy and spectra were recorded using deuterated chloroform ($CDCl_3$) as the solvent.

3.2.4 Melting point and IR instrumentation

Melting point was recorded using Buchi M-560 Melting Point instrument. IR spectrum was recorded in the 4000-400 cm^{-1} region as KBr discs on a Perkin Elmer Spectrum 100 FT-IR spectrometer.

3.2.5 Experimental procedures

3.2.5.1 Synthesis of $Cp_2Ti(tsal)$

$Cp_2Ti(tsal)$ was synthesised by a modification of literature methods [13]. Cp_2TiCl_2 (1094 mg, 4.39 mmol) and thiosalicylic acid (680 mg, 4.41 mmol) were suspended in ethanol (30 mL) in a 50 mL round bottom flask with a magnetic stirrer, resulting in a red suspension. KOH (493 mg, 8.79 mmol) was added and the red suspension quickly changed into a deep green supension. The mixture was stirred for 4 hours, then allowed to evaporate to dryness. The solid residue was extracted with 60 mL of a 1:1 mixture of toluene and CH_2Cl_2, the resulting deep green solution was filtered to remove KCl, washed successively with CH_2Cl_2 (10 mL) and the filtrate evaporated to dryness in a fumehood. The dark green residue was recrystallised by dissolving in CH_2Cl_2 (30 mL) followed by addition of petroleum spirits (50 mL). The solid was filtered off, washed with 10 mL of petroleum spirits, and dried under vacuum to give a dark green, almost black, microcrystalline $Cp_2Ti(tsal)$ solid (yield ca. 770 mg, 53%) [92].

3.2.5.2 Synthesis of $(EtCp)_2Ti(tsal)$

Equimolar amounts of $(EtCp)_2TiCl_2$ (100 mg, 0.328 mmol) and thiosalicylic acid (50.5 mg, 0.328 mmol) were suspended in ethanol (30 mL) in a 50 mL round bottom flask with a magnetic stirrer, resulting in a red suspension. KOH (36.8 mg, 0.656 mmol) was added and the red suspension quickly changed into a deep green suspension. The mixture was stirred for 4 hours, then allowed to evaporate to dryness. The solid was extracted with 60 mL of a 1:1 mixture of toluene and CH_2Cl_2. The resulting deep green solution was filtered to remove KCl, washed successively with 10 mL of CH_2Cl_2, and then the solvent evaporated in a fumehood to give final dark green solid (yield ca. 70 mg, 55%). Melting point of $(EtCp)_2Ti(tsal)$ 115-118 °C.

3.2.5.3 Investigation of the possibility of the tsal ligand bridging two Cp_2Ti centres

Equimolar amounts of Cp_2TiCl_2 (18.9 mg, 0.076 mmol) and Cp_2Ti(tsal) (25 mg, 0.076 mmol) were dissolved in dichloromethane (25 mL) in a 50 mL round bottom flask with a magnetic stirrer and stirred for 24 hours, giving a clear deep green solution. The solution was diluted with methanol and then analysed by positive-ion ESI-MS. The same experimental procedure was performed but using pure methanol as the solvent.

3.2.5.4 Characterisation of Cp_2Ti(tsal) using ESI mass spectrometry in the presence of added alkali metal salt

Cp_2Ti(tsal) (10 mg, 0.030 mmol) was dissolved in 10 mL of CH_3OH in a 25 mL glass vial and shaken gently for about one minute. Alkali metal chloride MCl (10 mg) (M= Li, Na, K, Rb, Cs) respectively were added into the Cp_2Ti(tsal) CH_3OH solution. Then, several drops of water were added to help dissolve alkali metal chloride. The resulting deep green solutions were respectively analysed by positive-ion ESI-MS.

3.2.5.5 Investigation of the reactivity of Cp_2Ti(tsal) towards soft electrophiles

Equimolar amounts of Cp_2Ti(tsal) (5 mg, 0.015 mmol) and PhHgCl (4.7 mg, 0.015 mmol) were suspended in CH_3OH (20 mL) in a 50 mL round bottom flask with a magnetic stirrer and stirred for 2 hours. The resulting brown precipitate was filtered and then extracted with 60 mL of a 1:1 mixture of toluene and CH_2Cl_2 and then analysed by ESI-MS.

3.3 Results and discussion

3.3.1 An investigation of the ESI-MS behaviour of Cp_2Ti(tsal)

3.3.1.1 Analysis of a freshly-prepared solution of Cp_2Ti(tsal) in methanol with low range method

The positive-ion ESI-MS spectrum for Cp_2Ti(tsal) in methanol solution using the low range method, recorded at a capillary exit voltage of 150 V, is given in Figure 3.4.

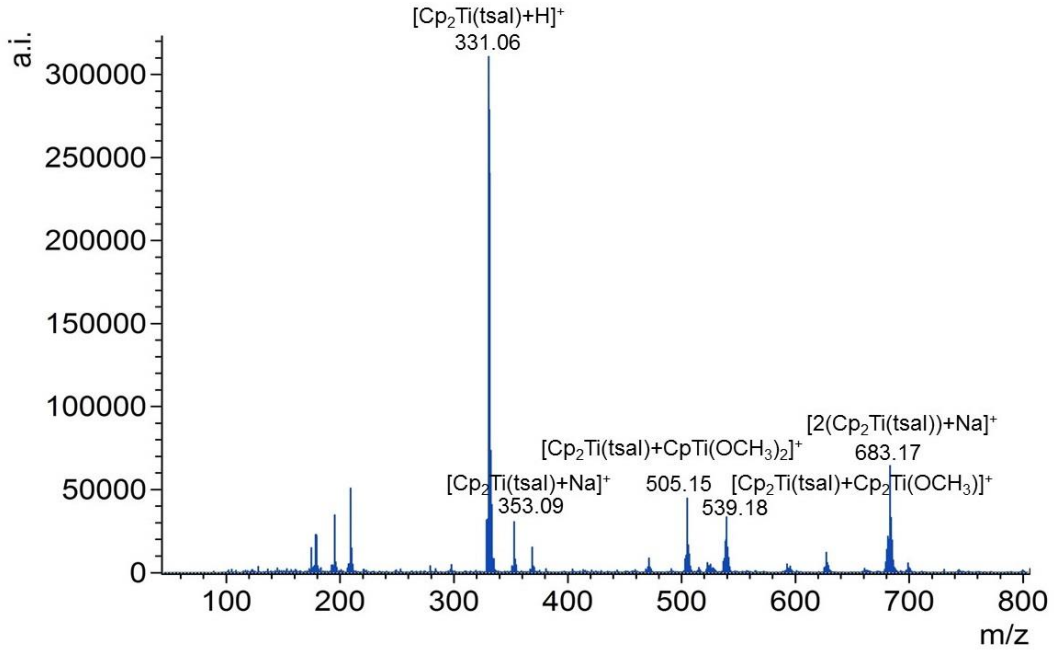

Figure 3.4: Positive-ion ESI mass spectrum of a freshly-prepared solution of $Cp_2Ti(tsal)$ in methanol with low range method at a capillary exit voltage of 150 V

The results show that species at *m/z* 100-300 do not contain the tsal group and these species were also observed in the spectrum of Cp_2TiCl_2 in methanol solution using the low range method (Section 2.3.2). At *m/z* 300-800, all the major species contain the tsal group. An ion at *m/z* 331.06 is assigned as $[Cp_2Ti(tsal)+H]^+$ (calculated *m/z* 331.03) (Figure 3.5).

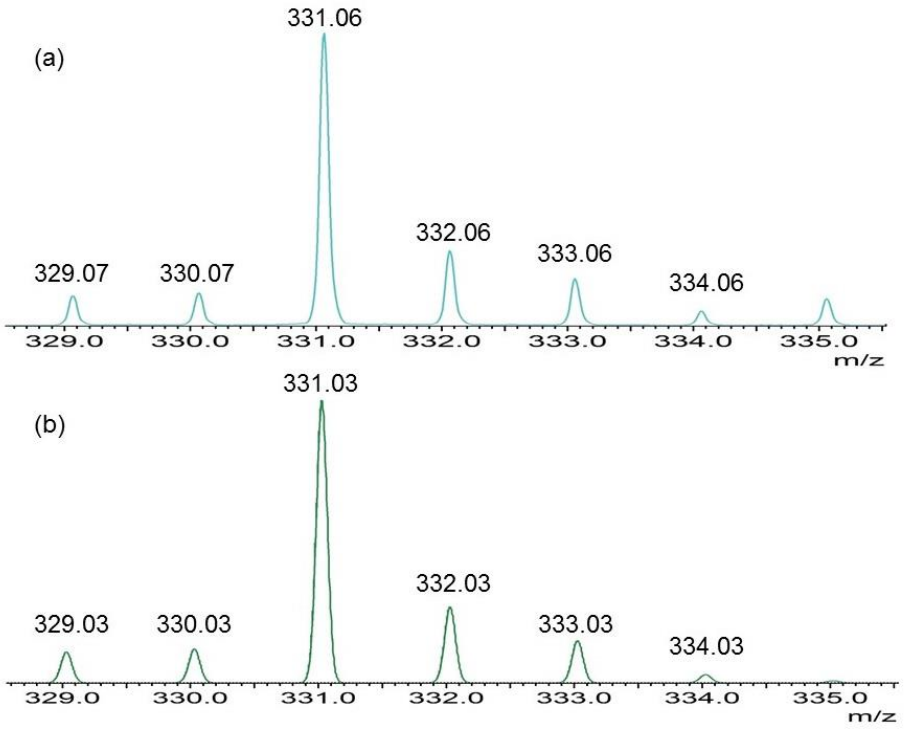

Figure 3.5: An isotope pattern comparison for $[Cp_2Ti(tsal)+H]^+$ (a) experimental (*m/z* 331.06) and (b) calculated (*m/z* 331.03)

Table 3.2 summarises all the major species contain the tsal group which were observed at a capillary exit voltage of 150 V with low method.

Table 3.2: Summary of species containing the tsal group observed at a capillary exit voltage of 150 V in a freshly-prepared solution of $Cp_2Ti(tsal)$ in methanol with low range method

Species	Experimental (*m/z*)	Calculated (*m/z*)
$[Cp_2Ti(tsal)+H]^+$	331.06	331.03
$[Cp_2Ti(tsal)+Na]^+$	353.09	353.01
$[Cp_2Ti(tsal)+CpTi(OCH_3)_2]^+$	505.15	505.04
$[Cp_2Ti(tsal)+Cp_2Ti(OCH_3)]^+$	539.18	539.06
$[2(Cp_2Ti(tsal))+Na]^+$	683.17	683.03

The positive-ion ESI-MS spectrum for $Cp_2Ti(tsal)$ in methanol solution using the low range method, recorded at a capillary exit voltage of 180 V, are given in Figure 3.6.

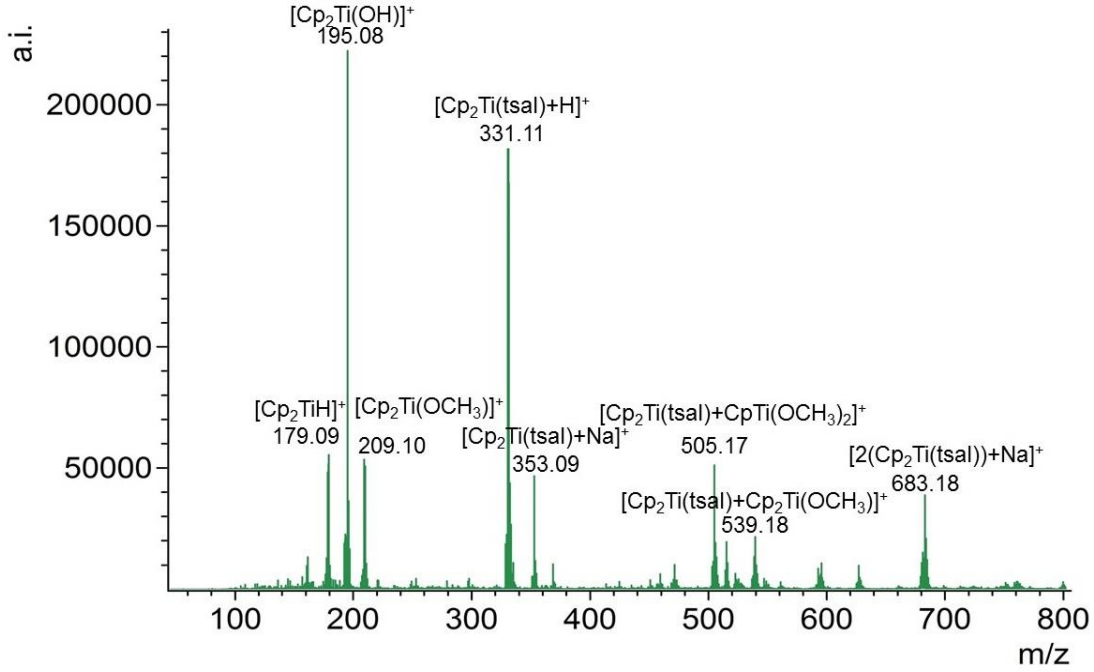

Figure 3.6: Positive-ion ESI mass spectrum of a freshly-prepared solution of $Cp_2Ti(tsal)$ in methanol with low range method at a capillary exit voltage of 180 V

The result shows that the intensities of species at *m/z* 100-300 increased as the capillary exit voltage increased. All the major species containing the tsal group were also observed at a capillary exit voltage of 150 V, but their intensities decreased as the capillary exit voltage increased. Table 3.3 summarises all the major species containing the tsal group which were observed at a capillary exit voltage of 180 V with low method.

Table 3.3: Summary of species containing the tsal group observed at a capillary exit voltage of 180 V in a freshly-prepared solution of $Cp_2Ti(tsal)$ in methanol with low range method

Species	Experimental (*m/z*)	Calculated (*m/z*)
$[Cp_2Ti(tsal)+H]^+$	331.11	331.03
$[Cp_2Ti(tsal)+Na]^+$	353.09	353.01
$[Cp_2Ti(tsal)+CpTi(OCH_3)_2]^+$	505.17	505.04
$[Cp_2Ti(tsal)+Cp_2Ti(OCH_3)]^+$	539.18	539.06
$[2(Cp_2Ti(tsal))+Na]^+$	683.18	683.03

The positive-ion ESI-MS spectrum for $Cp_2Ti(tsal)$ in methanol solution using the low range method, recorded at a capillary exit voltage of 220 V, are given in Figure 3.7.

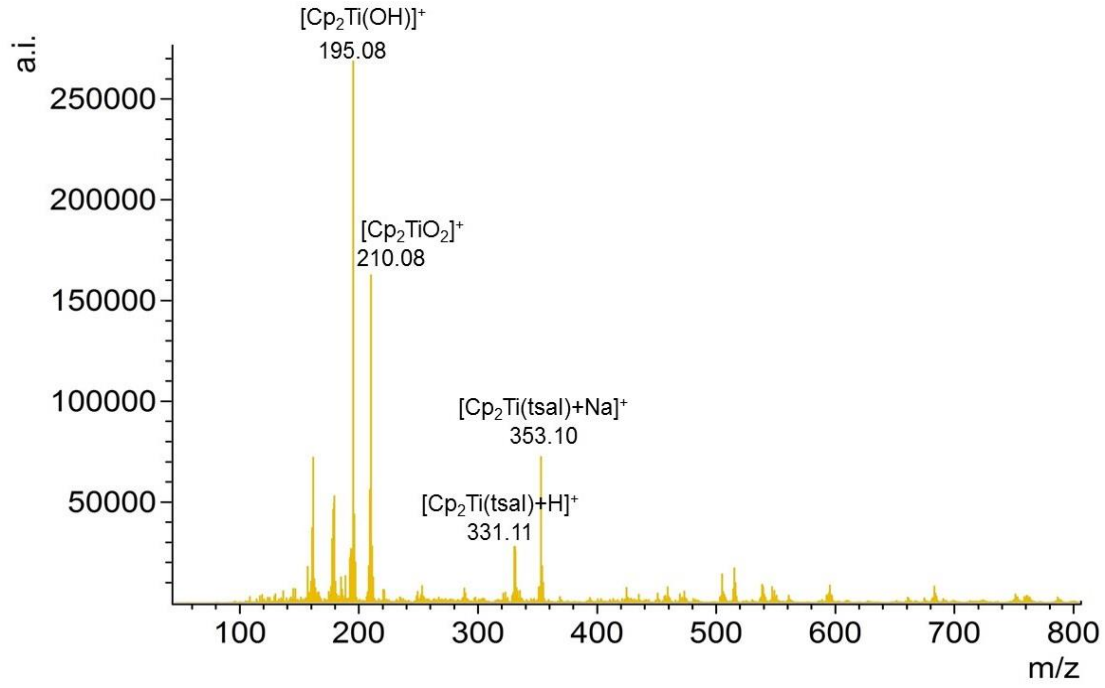

Figure 3.7: Positive-ion ESI mass spectrum of a freshly-prepared solution of $Cp_2Ti(tsal)$ in methanol with low range method at a capillary exit voltage of 220 V

The results show that only two major species contain the tsal group; $[Cp_2Ti(tsal)+H]^+$ and $[Cp_2Ti(tsal)+Na]^+$ were observed at *m/z* 331.11 and *m/z* 353.10 at the capillary exit voltage of 220 V.

Overall, as the capillary exit voltage increases, the intensity of the low *m/z* range species increases and high *m/z* range species which contain the tsal group decrease.

3.3.1.2 Analysis of a freshly-prepared solution of $Cp_2Ti(tsal)$ in methanol with wide range method

In this research, the wide range method has a maximum at *m/z* 1500. Positive-ion ESI-MS spectra for $Cp_2Ti(tsal)$ in methanol solution using the wide range method, recorded at a capillary exit voltage of 100 V, are given in Figure 3.8

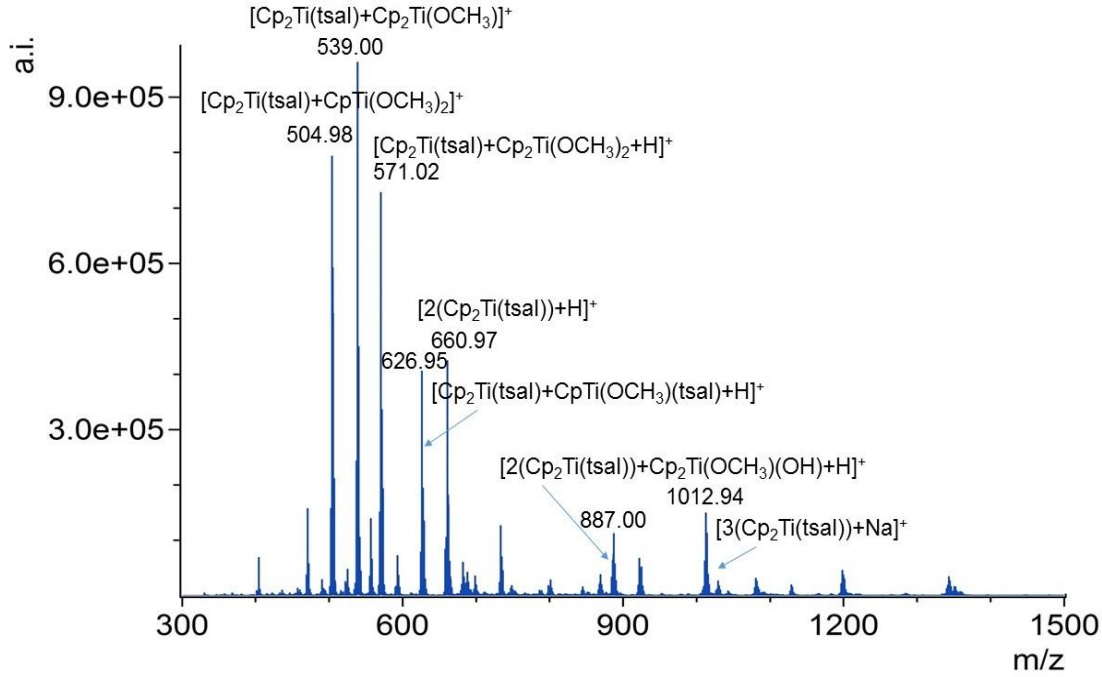

Figure 3.8: Positive-ion ESI mass spectrum of a freshly-prepared solution of $Cp_2Ti(tsal)$ in methanol with wide range method at a capillary exit voltage of 100 V

The result shows that some of these species were also observed with the low range method. Some new species like $[2(Cp_2Ti(tsal))+Cp_2Ti(OCH_3)(OH)+H]^+$ (*m/z* 887.00) and $[3(Cp_2Ti(tsal))+Na]^+$ (*m/z* 1012.94) were observed when using the wide range method. Table 3.4 summarises all the major species contain the tsal group which were observed at a capillary exit voltage of 100 V with wide method.

Table 3.4: Summary of species containing the tsal group observed at a capillary exit voltage of 100 V of a freshly-prepared solution of $Cp_2Ti(tsal)$ in methanol with wide range method

Species	Experimental (*m/z*)	Calculated (*m/z*)
$[Cp_2Ti(tsal)+CpTi(OCH_3)_2]^+$	504.98	505.04
$[Cp_2Ti(tsal)+Cp_2Ti(OCH_3)]^+$	539.00	539.06
$[Cp_2Ti(tsal)+Cp_2Ti(OCH_3)_2+H]^+$	571.02	571.09
$[Cp_2Ti(tsal)+CpTi(OCH_3)(tsal)+H]^+$	626.95	627.03
$[2(Cp_2Ti(tsal))+H]^+$	660.97	661.05
$[2(Cp_2Ti(tsal))+Cp_2Ti(OCH_3)(OH)+H]^+$	887.00	887.10
$[3(Cp_2Ti(tsal))+Na]^+$	1012.94	1013.05

Positive-ion ESI-MS spectrum for $Cp_2Ti(tsal)$ in methanol solution using the wide range method, recorded at a capillary exit voltage of 180 V, are given in Figure 3.9.

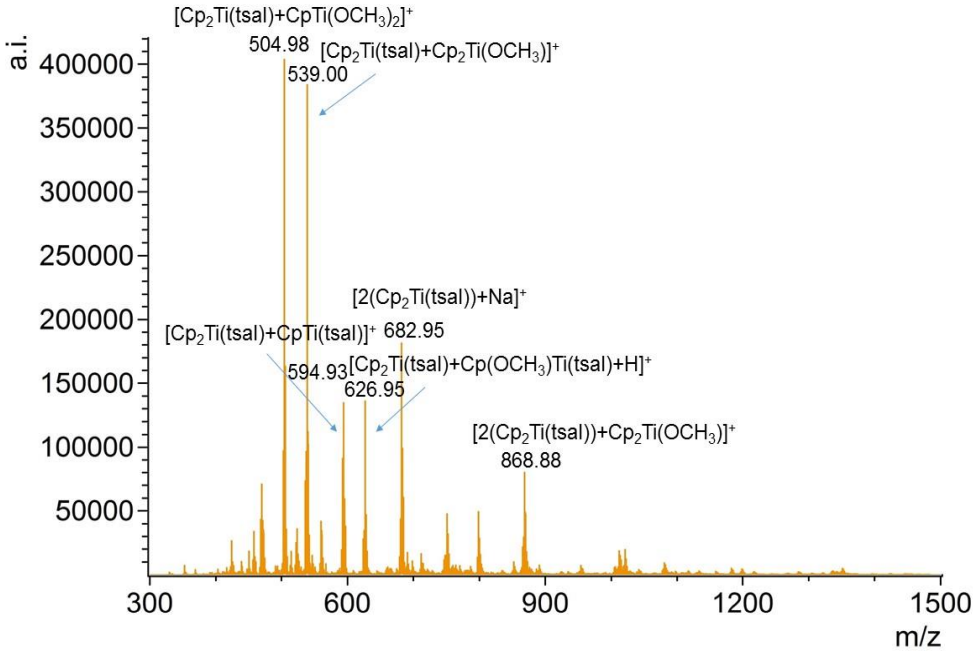

Figure 3.9: Positive-ion ESI mass spectrum of a freshly-prepared solution of $Cp_2Ti(tsal)$ in methanol with wide range method at a capillary exit voltage of 180 V

The results show that $[Cp_2Ti(tsal)+CpTi(OCH_3)_2]^+$ (*m/z* 504.98) and $[Cp_2Ti(tsal)+Cp_2Ti(OCH_3)]^+$ (*m/z* 539.00) were also observed with the low range method. Some new species like $[Cp_2Ti(tsal)+CpTi(tsal)]^+$ (*m/z* 594.93), $[2(Cp_2Ti(tsal))+Na]^+$ (*m/z* 682.95) and $[2(Cp_2Ti(tsal))+Cp_2Ti(OCH_3)]^+$ (*m/z* 868.88)

were observed when using higher voltage. Table 3.5 summarises all the major species that contain the tsal group which were observed at a capillary exit voltage of 180 V with wide method.

Table 3.5: Summary of species containing the tsal group observed at a capillary exit voltage of 180 V of a freshly-prepared solution of $Cp_2Ti(tsal)$ in methanol with wide range method

Species	Experimental (*m/z*)	Calculated (*m/z*)
$[Cp_2Ti(tsal)+CpTi(OCH_3)_2]^+$	504.98	505.04
$[Cp_2Ti(tsal)+Cp_2Ti(OCH_3)]^+$	539.00	539.06
$[Cp_2Ti(tsal)+CpTi(tsal)]^+$	594.93	595.00
$[Cp_2Ti(tsal)+CpTi(OCH_3)(tsal)+H]^+$	626.95	627.03
$[2(Cp_2Ti(tsal))+Na]^+$	682.95	683.03
$[2(Cp_2Ti(tsal))+Cp_2Ti(OCH_3)]^+$	868.88	869.09

The positive-ion ESI-MS spectrum for $Cp_2Ti(tsal)$ in methanol solution using the wide range method, recorded at a capillary exit voltage of 240 V, is given in Figure 3.10.

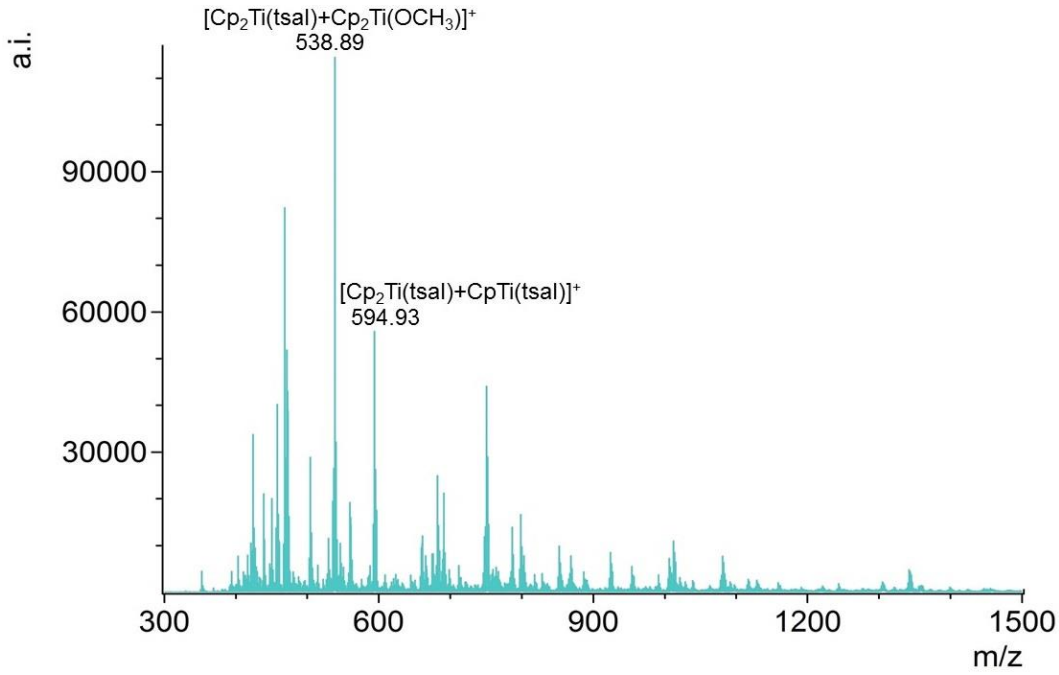

Figure 3.10: Positive-ion ESI mass spectrum of a freshly-prepared solution of $Cp_2Ti(tsal)$ in methanol with wide range method at a capillary exit voltage of 240 V

The result shows that $[Cp_2Ti(tsal)+Cp_2Ti(OCH_3)]^+$ (*m/z* 538.89) and $[Cp_2Ti(tsal)+CpTi(tsal)]^+$ (*m/z* 594.93) were also observed at low capillary exit voltages. As for the low range method, when the capillary exit voltage increases, the intensity of the major species with high *m/z* will decrease.

3.3.1.3 Analysis of a freshly-prepared solution of $Cp_2Ti(tsal)$ in ethanol using ESI-MS

The analysis of the spectra of $Cp_2Ti(tsal)$ dissolved in ethanol solution can also help to confirm the identity of some species and explore the behaviour in larger chain alcohols. Spectra of $Cp_2Ti(tsal)$ in ethanol at various capillary exit voltages are shown in Figure 3.11. For example, one major species observed in methanol was $[Cp_2Ti(tsal)+Cp_2Ti(OCH_3)]^+$ (*m/z* 539.12); when the spectrum was recorded in ethanol as the solvent, the analogous species $[Cp_2Ti(tsal)+Cp_2Ti(OCH_2CH_3)]^+$ was observed at *m/z* 553.18.

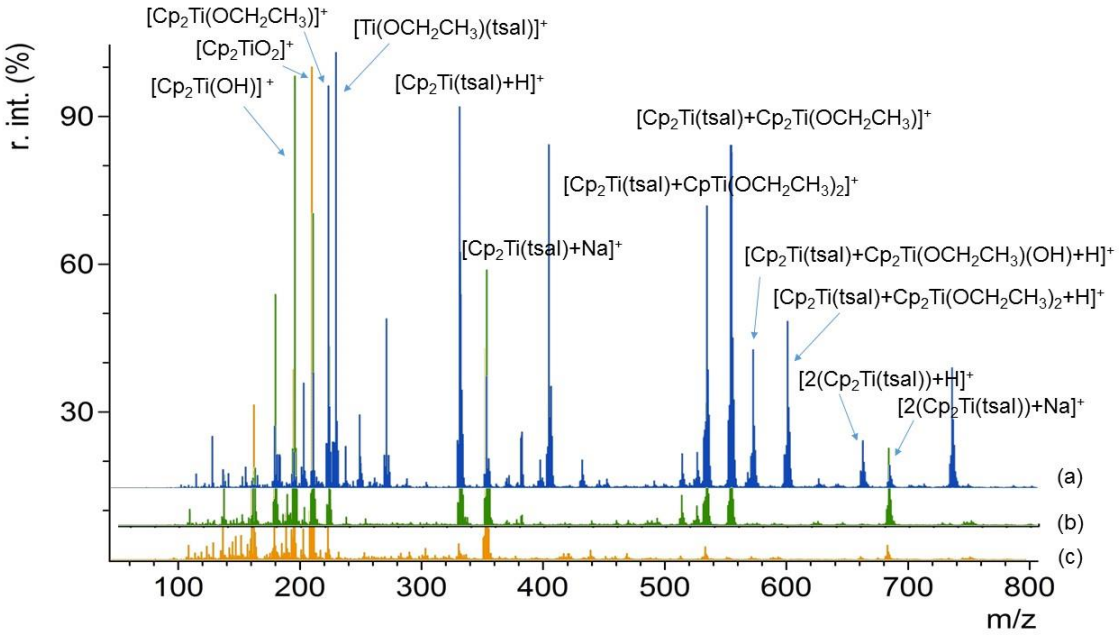

Figure 3.11: Positive-ion ESI mass spectra of a freshly-prepared solution of $Cp_2Ti(tsal)$ in ethanol with low range method at capillary exit voltages of (a) 100 V, (b) 180 V and (c) 240 V

All the corresponding major species observed at various capillary exit voltages with low method in methanol and ethanol are summarised in Table 3.6.

Table 3.6: Summary of corresponding species of $Cp_2Ti(tsal)$ in methanol and ethanol at a capillary exit voltage of 100 V with low range method

Species	Methanol (*m/z*)	Ethanol (*m/z*)
$[Cp_2Ti(OR)]^+$	209.07	223.10
$[Cp_2Ti(tsal)+CpTi(OR)_2]^+$	505.09	533.17
$[Cp_2Ti(tsal)+Cp_2Ti(OR)]^+$	539.12	553.18
$[Cp_2Ti(tsal)+Cp_2Ti(OR)(OH)+H]^+$	557.13	571.19
$[Cp_2Ti(tsal)+Cp_2Ti(OR)_2+H]^+$	571.15	599.23

3.3.2 An investigation of the ESI-MS behaviour of $(EtCp)_2Ti(tsal)$

3.3.2.1 Introduction

$(EtCp)_2Ti(tsal)$ is a new compound that has never been synthesised before. During this research, $(EtCp)_2Ti(tsal)$ was synthesised using the same method for $Cp_2Ti(tsal)$. Experimental procedures have been described in section 3.2.5.2. This new complex was characterised by elemental analysis, ESI-MS, melting point, ^1H NMR and Infra-red (IR) spectroscopy.

Elemental analysis were completed in duplicate by the University of Otago Chemistry Department Microanalytical Laboratory. Found: C, 62.93% and H, 5.88%. $(EtCp)_2Ti(tsal)$ requires C, 65.29% and H, 5.74%. The percentage compositions obtained in the elemental analyses of this complex did not match those required within experimental error limits 1%. This inconsistency may have been due to unreacted $(EtCp)_2TiCl_2$ in the finial product. The presence of $(EtCp)_2TiCl_2$ was confirmed in the proton NMR spectrum. Integration showed the ratio of $(EtCp)_2TiCl_2$: $(EtCp)_2Ti(tsal)$ was approximately 1:4. The calculated percentages of carbon in $(EtCp)_2TiCl_2$ and $(EtCp)_2Ti(tsal)$ are 55.12% and 65.29% respectively, but if 20% of $(EtCp)_2TiCl_2$ is present in the final product $(EtCp)_2Ti(tsal)$, the calculated carbon percentage should be (55.12%×20%) + (65.29%×80%) = 63.26%. Likewise, the percentages of hydrogen in $(EtCp)_2TiCl_2$ and $(EtCp)_2Ti(tsal)$ are 5.95% and 5.74%, but if there is 20% of $(EtCp)_2TiCl_2$ in the final product $(EtCp)_2Ti(tsal)$, the calculated percentages of hydrogen in $(EtCp)_2Ti(tsal)$ should be (5.95%×20%) + (5.74%×80%) = 5.78%. The calculated C, 63.26% and H, 5.78% now compare well with experimental results C, 62.93%

and H, 5.88%, confirming 20% of starting material $(EtCp)_2TiCl_2$ in the final product $(EtCp)_2Ti(tsal)$.

The ^1H NMR spectrum for $(EtCp)_2Ti(tsal)$ is shown in Figure 3.12, showed ten discernible chemical environments. The doublet of doublets at 8.4 ppm and 7.5 ppm were assigned to the benzene ring protons close to the S and O. The other two protons on the benzene ring were assigned at 7.4 ppm and 7.2 ppm as the triplets. The protons on the Cp rings were assigned at 6.2 ppm. CH_2 and CH_3 groups from $(EtCp)_2Ti(tsal)$ were assigned at 2.5 ppm and 1.1 ppm. The correct chemical shift for these protons in starting material $(EtCp)_2TiCl_2$ were also observed. The signal at 6.4 ppm was assigned as the protons on the Cp rings of contaminant $(EtCp)_2TiCl_2$. CH_2 and CH_3 groups from $(EtCp)_2TiCl_2$ were assigned at 2.8 ppm and 1.2 ppm. The ratio of $(EtCp)_2TiCl_2$ integration to $(EtCp)_2Ti(tsal)$ integration was 1:4.

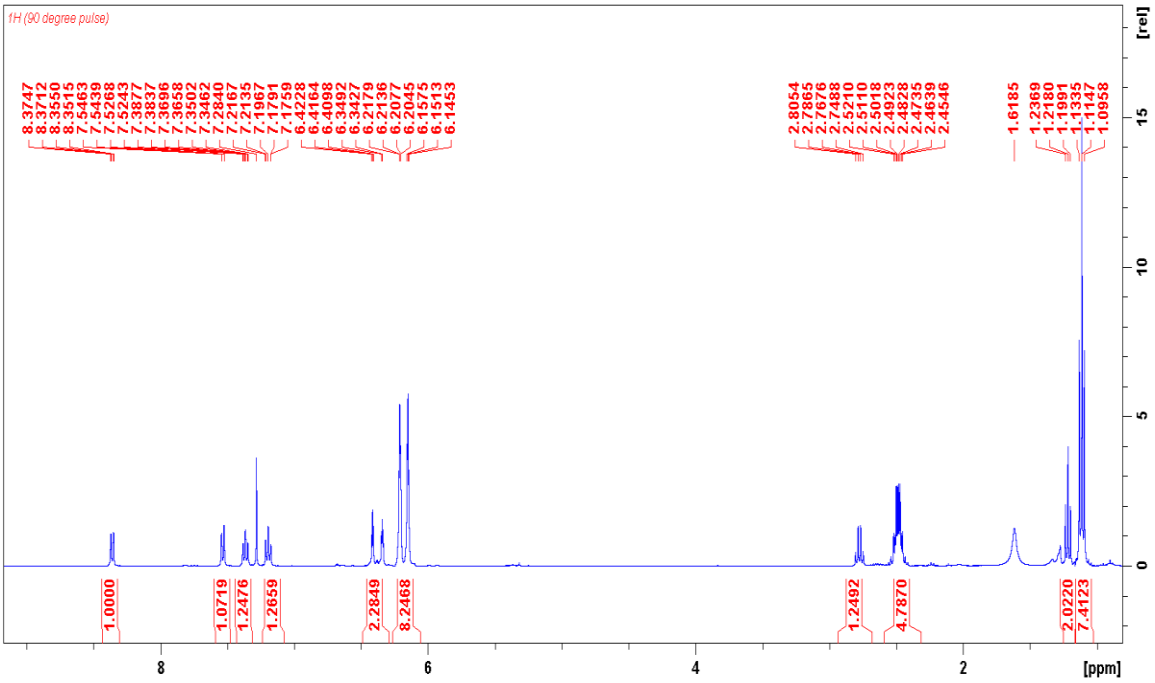

Figure 3.12: ^1H NMR spectrum for $(EtCp)_2Ti(tsal)$

IR spectroscopy shows that strong bands observed at 1624 and 1293 cm^{-1} are attributed to the C=O and C-O stretching vibrations which are characteristic absorptions of the COO group [119]. The C-H stretching frequency at 2970 cm^{-1} is indicative of the cyclopentadienyl ring and 1428 cm^{-1} due to C-C stretching of π-bond further confirm the presence of the Cp group [119,120]. The weak bands at 1600-1300 cm^{-1} region that characterises the benzene ring [121].

3.3.2.2 Analysis of a freshly-prepared solution of $(EtCp)_2Ti(tsal)$ in methanol with low range method

The major species containing Cp groups observed in positive-ion ESI mass spectrum of $Cp_2Ti(tsal)$ were confirmed by running the spectrum of $(EtCp)_2Ti(tsal)$ in methanol solution. Mass-shifted corresponding species should be seen in the ESI mass spectrum of $(EtCp)_2Ti(tsal)$ if the assignments are correct. Figure 3.13 shows mass spectra of $Cp_2Ti(tsal)$ and $(EtCp)_2Ti(tsal)$ with low range method at a capillary exit voltage of 100 V.

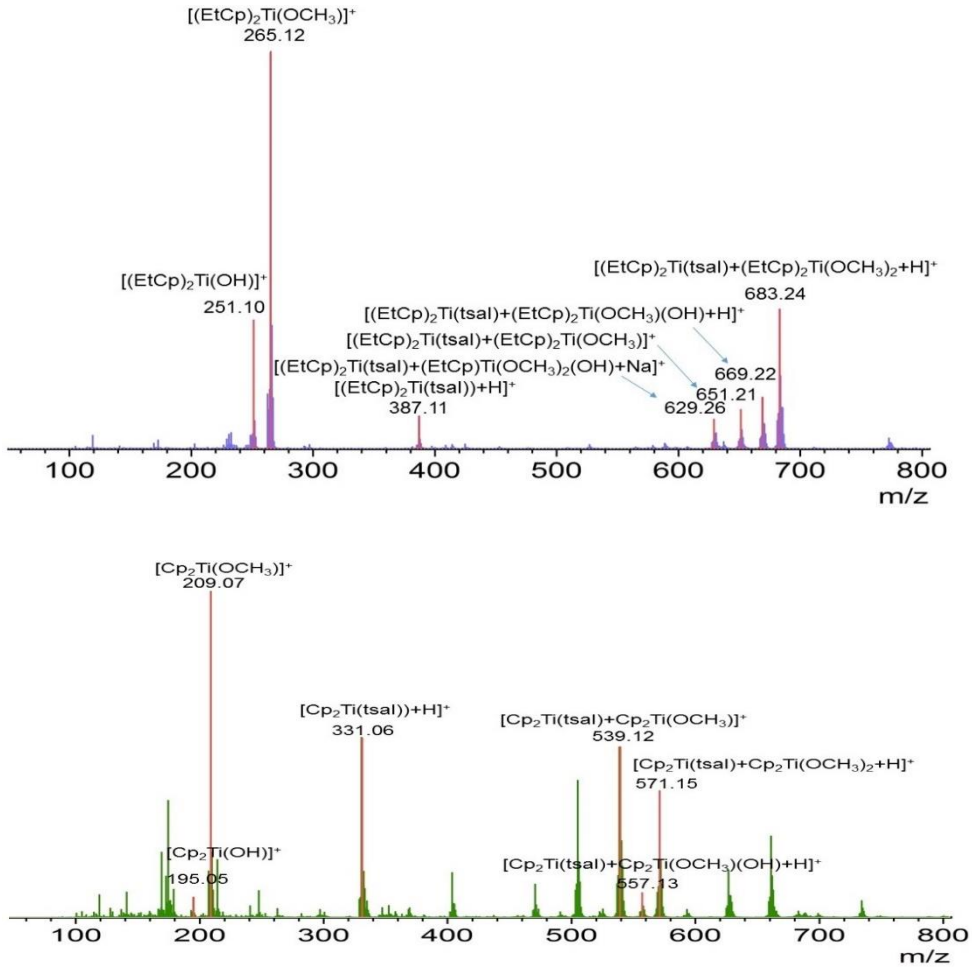

Figure 3.13: ESI mass spectra of $(EtCp)_2Ti(tsal)$ (Top) and $Cp_2Ti(tsal)$ (Bottom) with low range method at a capillary exit voltage of 100 V

Some analogues of the major species in $Cp_2Ti(tsal)$ mass spectra can also be observed in ESI mass spectra of $(EtCp)_2Ti(tsal)$, with the latter mass-shifted in $(EtCp)_2Ti(tsal)$ mass spectra. For example $[Cp_2Ti(tsal)+H]^+$ (*m/z* 331.06) and

$[(EtCp)_2Ti(tsal)+H]^+$ (*m/z* 387.11); the intensity of this ion was larger for the Cp compound. At higher *m/z* values, major species increase in mass by 112 units as they contain four Cp groups, such as $[Cp_2Ti(tsal)+Cp_2Ti(OCH_3)_2+H]^+$ (*m/z* 571.15) and $[(EtCp)_2Ti(tsal)+(EtCp)_2Ti(OCH_3)_2+H]^+$ (*m/z* 683.24).

Different capillary exit voltages were also used to record the spectra of $(EtCp)_2Ti(tsal)$. As the capillary exit voltage increased to 180 V, a weak peak at *m/z* 305.00 was observed and assigned to the $[(EtCp)_2TiCl_2+H]^+$ ion which confirmed impurity in the sample of $(EtCp)_2Ti(tsal)$. Table 3.7 summarises all the corresponding species which were observed at various voltages.

Table 3.7: Summary of corresponding species formed by Cp_2TiCl_2 and $(EtCp)_2TiCl_2$

	$Cp_2Ti(tsal)$ species	***m/z***	**$(EtCp)_2Ti(tsal)$ species**	***m/z***
1 Ti	$[Cp_2Ti(OH)]^+$	195.05	$[(EtCp)_2Ti(OH)]^+$	251.10
	$[Cp_2Ti(OCH_3)]^+$	209.07	$[(EtCp)_2Ti(OCH_3)]^+$	265.12
	$[Cp_2Ti(tsal)+H]^+$	331.06	$[(EtCp)_2Ti(tsal)+H]^+$	387.11
2 Ti	$[Cp_2Ti(tsal)+H]^+$	481.13	$[(EtCp)_4Ti_2(OCH_3)_4H]^+$	593.26
	$[Cp_2Ti(tsal)+CpTi(OCH_3)_2]^+$	505.09	$[(EtCp)_2Ti(tsal)+(EtCp)Ti(OCH_3)_2]^+$	589.16
	$[Cp_2Ti(tsal)+Cp_2Ti(OCH_3)]^+$	539.12	$[(EtCp)_2Ti(tsal)+(EtCp)_2Ti(OCH_3)]^+$	651.21
	$[Cp_2Ti(tsal)+Cp_2Ti(OCH_3)(OH)+H]^+$	557.13	$[(EtCp)_2Ti(tsal)+(EtCp)_2Ti(OCH_3)(OH)+H]^+$	669.22
	$[Cp_2Ti(tsal)+Cp_2Ti(OCH_3)_2+H]^+$	571.15	$[(EtCp)_2Ti(tsal)+(EtCp)_2Ti(OCH_3)_2+H]^+$	683.24

3.3.3 Investigation of the possibility of the tsal ligand bridging two Cp_2Ti centres

Positive-ion ESI-MS spectra for $Cp_2Ti(tsal)$ in methanol solution using the low range method, recorded at a capillary exit voltage of 150 V, shows the species $[Cp_2Ti(tsal)+CpTi(OCH_3)_2]^+$ at *m/z* 505.15. This suggests a dinuclear species, because one of the Ti centres $[CpTi(OCH_3)_2]^+$ is not coordinatively saturated, as it is in $Cp_2Ti(tsal)$. Therefore mixtures of $Cp_2Ti(tsal)$ and Cp_2TiCl_2 were investigated,

by reacting $Cp_2Ti(tsal)$ with Cp_2TiCl_2 in a 1:1 molar ratio and analysing the resulting reaction mixture by ESI-MS. Experimental procedures are described in section 3.2.5.3. One possibility for the tsal ligand bridging two Cp_2Ti centres is shown in Figure 3.14.

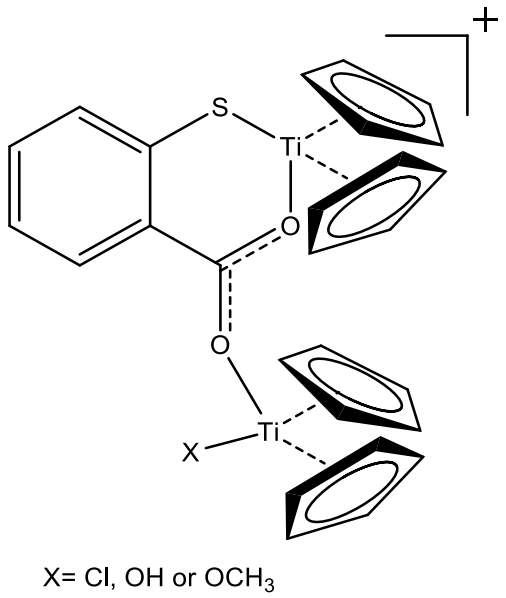

Figure 3.14: A possible structure of the ion formed by reaction of $Cp_2Ti(tsal)$ with Cp_2TiCl_2 to form the tsal ligand bridging two Cp_2Ti centres

In the positive-ion ESI-MS spectrum for the mixture of $Cp_2Ti(tsal)$ with Cp_2TiCl_2 using dichloromethane as solvent and then diluted with methanol, recorded at a capillary exit voltage of 150 V with low range method (Figure 3.15), a very weak ion at *m/z* 543.14 was assigned to the $Cp_2Ti(tsal)Cp_2TiCl^+$ ion (calculated *m/z* 543.02). The isotope pattern of this ion is significantly different than others due to the presence of Cl isotopes (Figure 3.16).

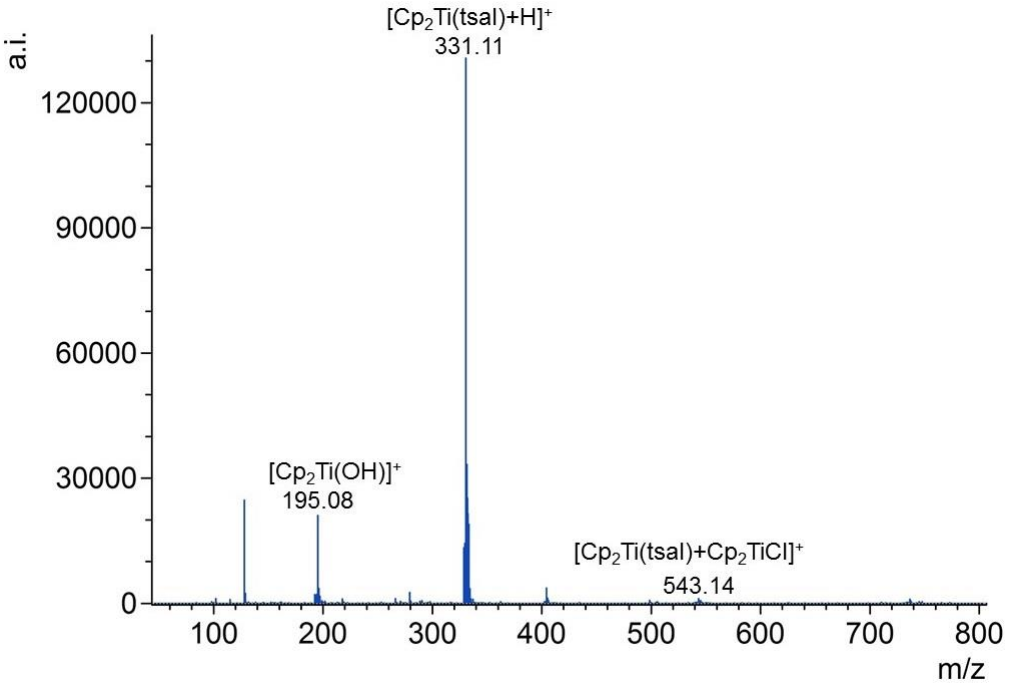

Figure 3.15: Positive-ion ESI mass spectrum (low range method) of a freshly-prepared solution of $Cp_2Ti(tsal)$ with Cp_2TiCl_2 in dichloromethane and diluted with methanol at a capillary exit voltage of 150 V.

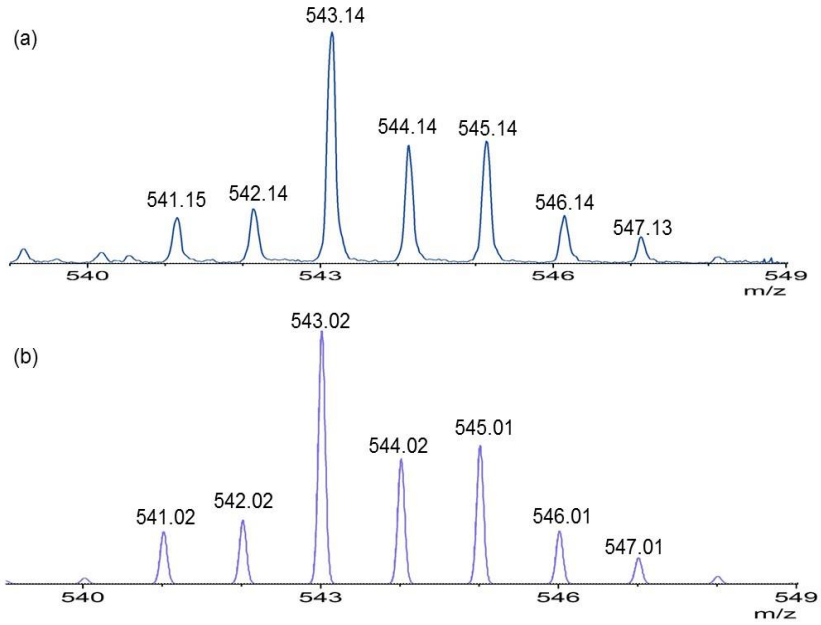

Figure 3.16: An isotope pattern comparison for $Cp_2Ti(tsal)Cp_2TiCl^+$ (a) experimental (*m/z* 543.14) and (b) calculated (*m/z* 543.02)

When the solvent was changed to methanol, $Cp_2Ti(tsal)Cp_2Ti(OH)^+$ (*m/z* 525.14) and $Cp_2Ti(tsal)Cp_2Ti(OCH_3)^+$ (*m/z* 539.16) ions were observed at a capillary exit voltage of 150 V using the low range method. The intensity of

$Cp_2Ti(tsal)Cp_2Ti(OCH_3)^+$ ion was much higher than the $Cp_2Ti(tsal)Cp_2Ti(OH)^+$ ion (Figure 3.17).

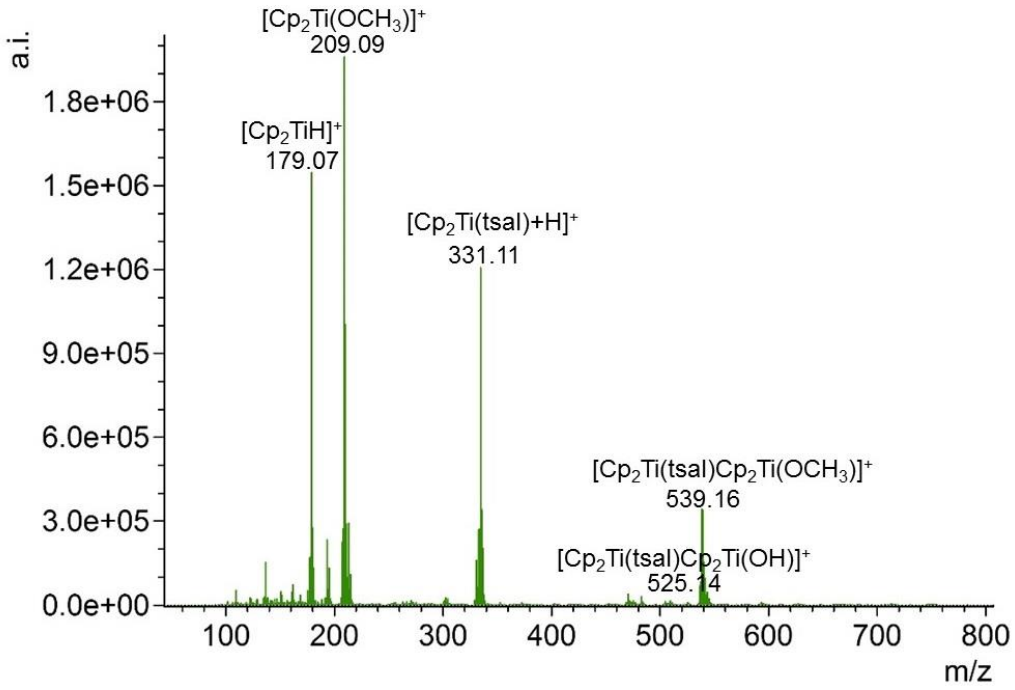

Figure 3.17: Positive-ion ESI mass spectrum of a freshly-prepared solution of $Cp_2Ti(tsal)$ with Cp_2TiCl_2 in methanol with low range method at a capillary exit voltage of 150 V

Figure 3.18 (a) shows the experimental isotope pattern of $Cp_2Ti(tsal)Cp_2Ti(OCH_3)^+$ and (b) is the calculated isotope pattern of $Cp_2Ti(tsal)Cp_2Ti(OCH_3)^+$.

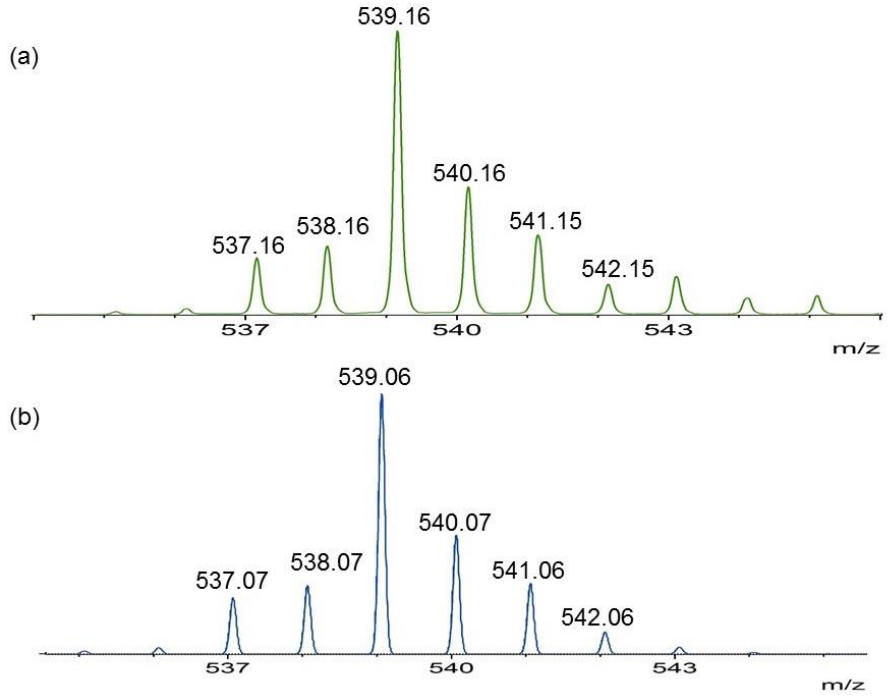

Figure 3.18: An isotope pattern comparison for $Cp_2Ti(tsal)Cp_2Ti(OCH_3)^+$ (a) experimental (*m/z* 539.16) and (b) calculated (*m/z* 539.06)

Comparing Figure 3.15 and 3.17, when using dichloromethane as the solvent, the ESI mass spectrum is much cleaner and doesn't show the multitude of hydrolysis or solvolysis species. When methanol is used as a solvent, more species can be observed.

3.3.4 Investigation of $Cp_2Ti(tsal)$ using ESI mass spectrometry in the presence of added alkali metal salts

Alkali metal cations can promote the formation of aggregate ions from a wide range of neutral molecules in MS. For example, in the presence of alkali metal cations, the self-aggregation of the nucleobases and nucleosides has been studied by the ESI-MS [122,123]. Therefore, it is significant to investigate the ESI-MS spectrum of $Cp_2Ti(tsal)$ in the presence of alkali metal salts. Experimental procedures have been described in section 3.2.5.4.

3.3.4.1 Investigation of $Cp_2Ti(tsal)$ using ESI mass spectrometry in the presence of LiCl

Figure 3.19 compares ESI-MS spectra of $Cp_2Ti(tsal)$ in the presence and absence of LiCl. The LiCl ionisation aid is clearly very effective at forming lithiated ions in the spectrum.

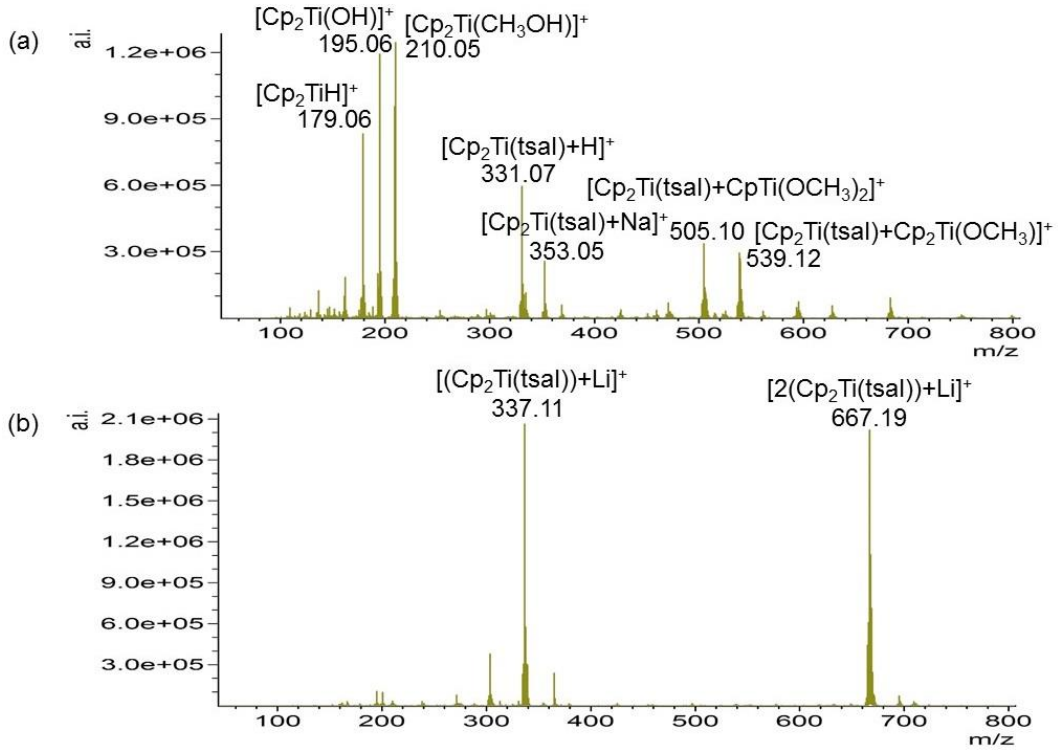

Figure 3.19: Positive-ion ESI mass spectra of a freshly-prepared solution of $Cp_2Ti(tsal)$ without (a) and with LiCl (b) in methanol using low range method at a capillary exit voltage of 180 V

Positive-ion ESI mass spectra for $Cp_2Ti(tsal)$ with LiCl in methanol solution using the wide range method, recorded at capillary exit voltages of 60 V, 90 V and 180 V, and using the low range method, recorded at a capillary exit voltage of 180 V, are given in Figure 3.20.

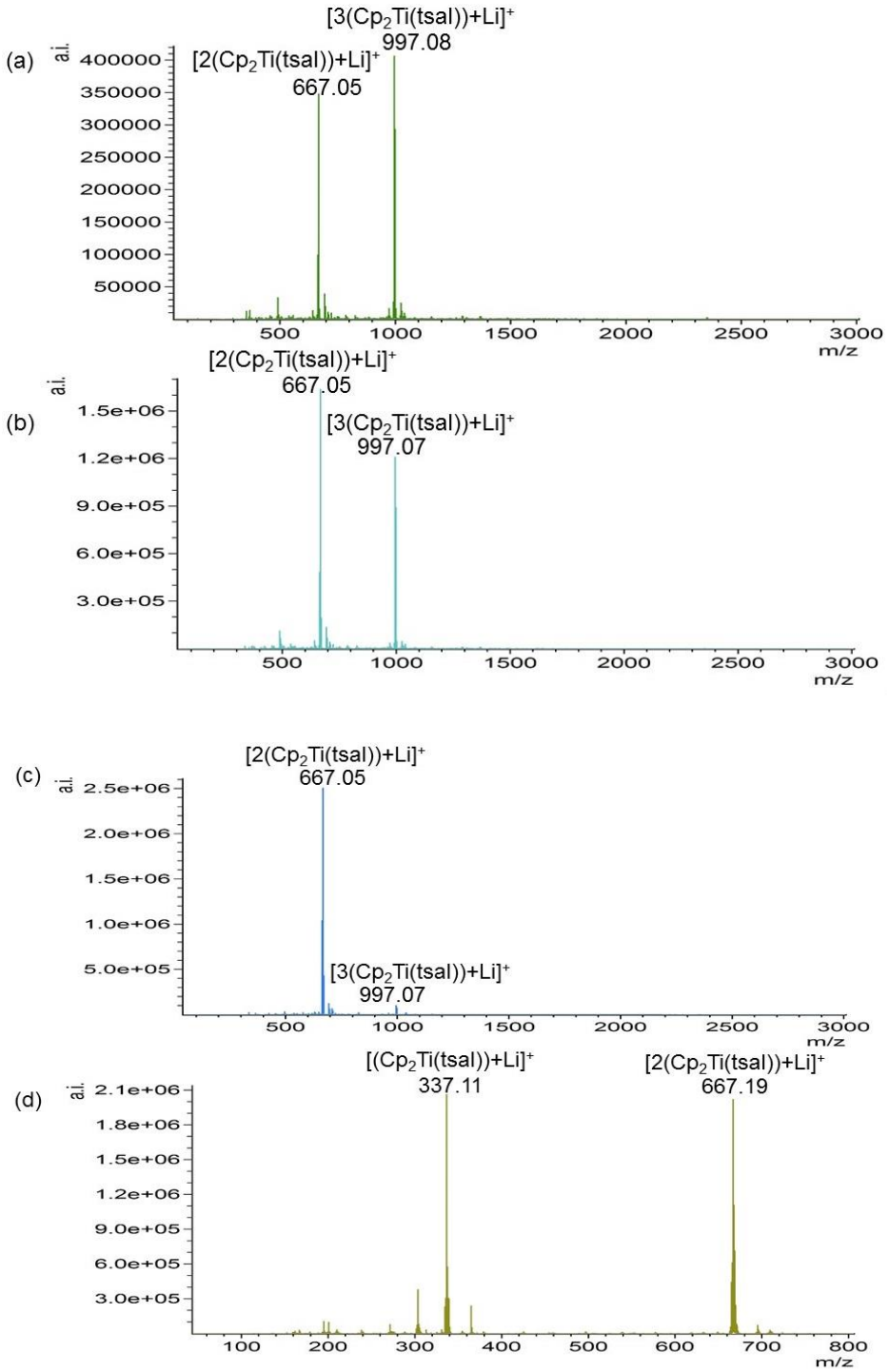

Figure 3.20: Positive-ion ESI mass spectra of a freshly-prepared solution of $Cp_2Ti(tsal)$ with LiCl in methanol with wide range method at capillary exit voltages of (a) 60 V, (b) 90 V and (c) 180 V. Low range method at capillary exit voltage of (d) 180 V

The results show that the $[(Cp_2Ti(tsal))+Li]^+$ (*m/z* 337.11) ion was observed at a capillary exit voltage of 180 V with low range method. The larger ions $[2(Cp_2Ti(tsal))+Li]^+$ and $[3(Cp_2Ti(tsal))+Li]^+$ can be observed using wide range

method. The intensity of $[2(Cp_2Ti(tsal))+Li]^+$ ion increased and $[3(Cp_2Ti(tsal))+Li]^+$ ion decreased as the capillary exit voltage increased.

3.3.4.2 Investigation of $Cp_2Ti(tsal)$ using ESI mass spectrometry in the presence of NaCl and KCl

Positive-ion ESI-MS spectra for $Cp_2Ti(tsal)$ with NaCl and KCl in methanol solution using the wide range method, recorded at a capillary exit voltages of 60 V and 180 V, are given in Figure 3.21.

The results show that the $[(Cp_2Ti(tsal))+Na]^+$ ion was observed at low capillary exit voltages with low intensities. The larger ions $[2(Cp_2Ti(tsal))+Na]^+$, $[3(Cp_2Ti(tsal))+Na]^+$ and $[4(Cp_2Ti(tsal))+Na]^+$ can be observed at a capillary exit voltage of 60 V using wide range method. As the capillary exit voltage increased to 180 V, only $[2(Cp_2Ti(tsal))+Na]^+$ ion can be observed.

In the case of KCl, the $[(Cp_2Ti(tsal))+K]^+$ ion was observed at various capillary exit voltages with low intensities. The larger ion $[2(Cp_2Ti(tsal))+K]^+$ was the major ion at various capillary exit voltages with relatively high intensities. The larger ions $[3(Cp_2Ti(tsal))+K]^+$ (*m/z* 1029.02) and $[4(Cp_2Ti(tsal))+K]^+$ (*m/z* 1359.03) can be observed at a capillary exit voltage of 60 V and they will disappear at high capillary exit voltages.

Overall, the spectra become much simpler compared to the spectra without NaCl and KCl added.

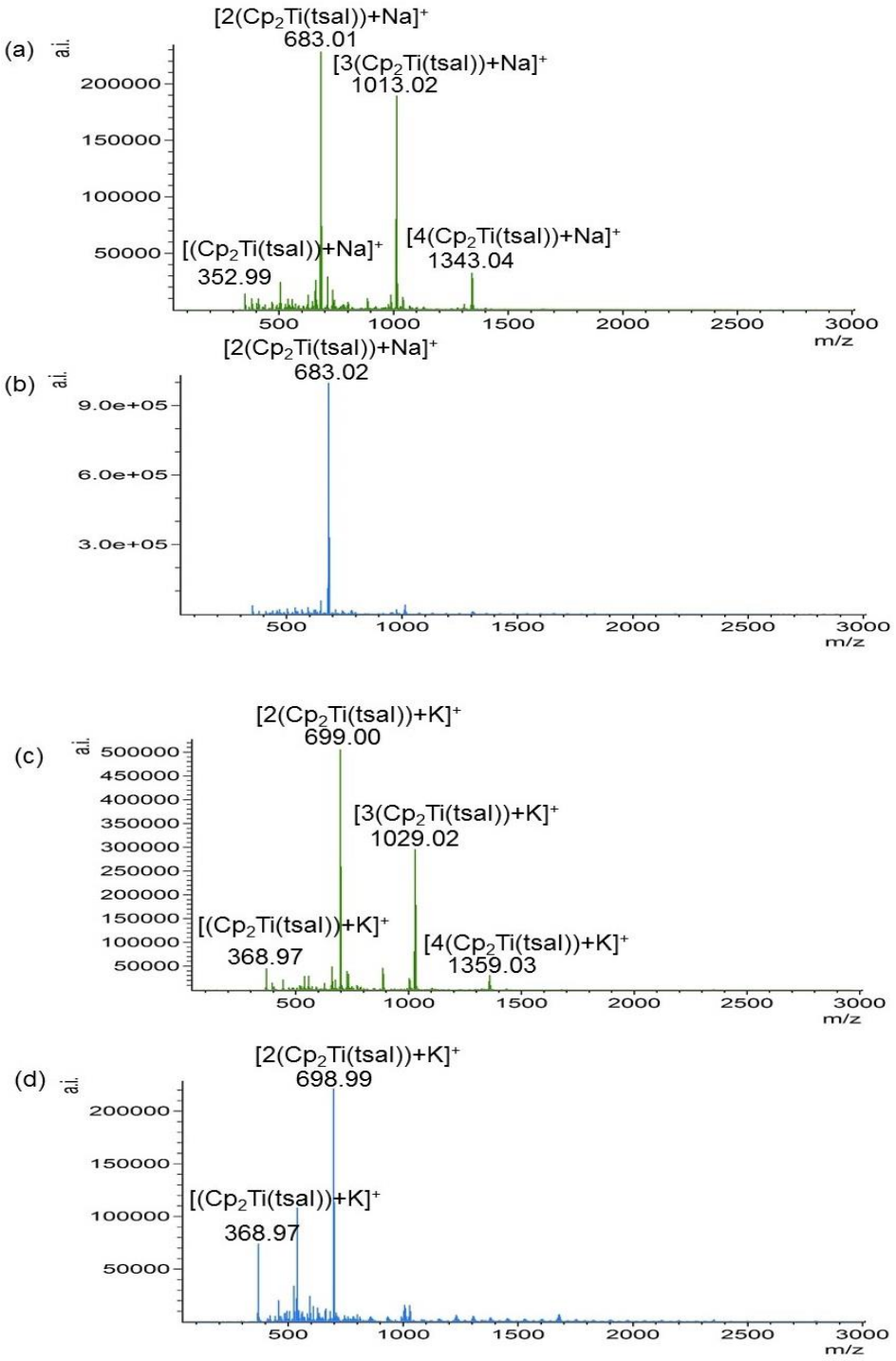

Figure 3.21: Positive-ion ESI mass spectra of a freshly-prepared solution of $Cp_2Ti(tsal)$ with NaCl in methanol with wide range method at capillary exit voltages of (a) 60 V and (b) 180 V. $Cp_2Ti(tsal)$ with KCl in methanol with wide range method at capillary exit voltages of (c) 60 V and (d) 180 V

3.3.4.3 Investigation of $Cp_2Ti(tsal)$ using ESI mass spectrometry in the presence of RbCl and CsCl

Positive-ion ESI-MS spectra for $Cp_2Ti(tsal)$ with RbCl and CsCl in methanol solution using the wide range method, recorded at a capillary exit voltages of 60 V and 180 V, are given in Figure 3.22.

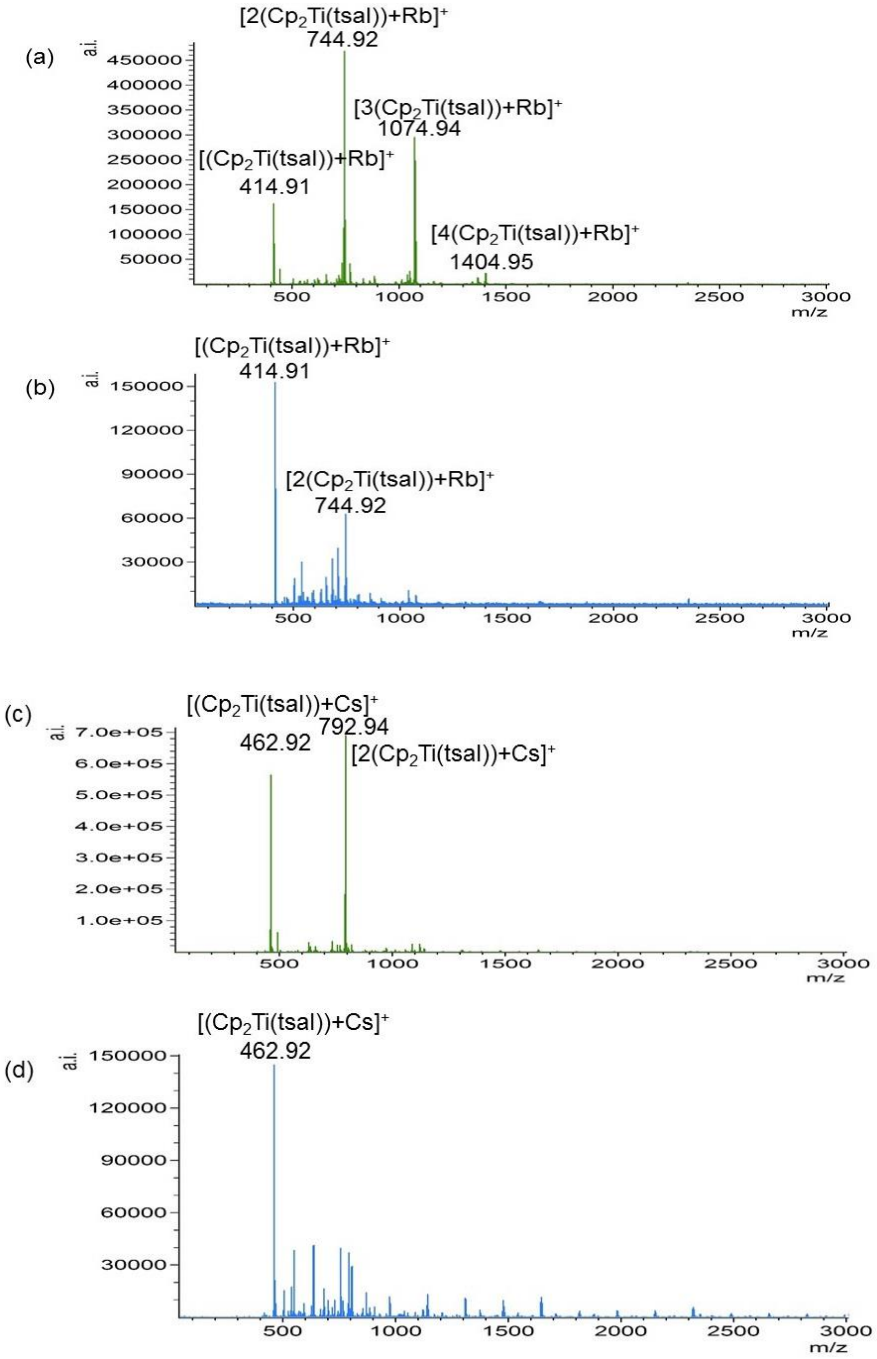

Figure 3.22: Positive-ion ESI mass spectra of a freshly-prepared solution of $Cp_2Ti(tsal)$ with RbCl in methanol with wide range method at capillary exit voltages of (a) 60 V and (b) 180 V. $Cp_2Ti(tsal)$ with CsCl in methanol with wide range method at capillary exit voltages of (c) 60 V and (d) 180 V

The results show that the $[(Cp_2Ti(tsal))+Rb]^+$ ion was observed at various capillary exit voltages and it will become a major ion as the voltage increased. The larger ion $[2(Cp_2Ti(tsal))+Rb]^+$ was the major ion at a capillary exit voltage of 60 V. The largest $[4(Cp_2Ti(tsal))+Rb]^+$ (*m/z* 1404.95) ion can be observed at a capillary exit voltage of 60 V and it will disappear at high capillary exit voltages. As the capillary exit voltage increased to 180 V, only $[(Cp_2Ti(tsal))+Rb]^+$ (*m/z* 414.91) and $[2(Cp_2Ti(tsal))+Rb]^+$ (*m/z* 744.92) ions can be observed.

In the case of CsCl, the results show that the only $[(Cp_2Ti(tsal))+Cs]^+$ and $[2(Cp_2Ti(tsal))+Cs]^+$ ions were observed at various capillary exit voltages. As the capillary exit voltage increased, the larger ion $[2(Cp_2Ti(tsal))+Cs]^+$ intensities decreased and only $[(Cp_2Ti(tsal))+Cs]^+$ (*m/z* 462.92) ion can be observed at a capillary exit voltage of 180 V.

3.3.4.4 Summary of $Cp_2Ti(tsal)$ using ESI mass spectrometry in the presence of added alkali metal salts

The formation of aggregate ions with alkali metal cations was observed during this research. In the case of NaCl, KCl and RbCl, the larger ions $[4(Cp_2Ti(tsal))+Na]^+$ (*m/z* 1343.04), $[4(Cp_2Ti(tsal))+K]^+$ (*m/z* 1359.03) and $[4(Cp_2Ti(tsal))+Rb]^+$ (*m/z* 1404.95) ions were observed at a capillary exit voltage of 60 V with wide range method. $[4(Cp_2Ti(tsal))+Li]^+$ was not observed because it is hard to aggregate around small Li^+ ion. For Cs^+ the charge density is very low therefore there will be less electrostatic attraction for $Cp_2Ti(tsal)$ compared to other alkali metal cations like Na^+, where charge density is higher. The large ions like $[3(Cp_2Ti(tsal))+Cs]^+$ or $[4(Cp_2Ti(tsal))+Cs]^+$ were also not observed in the CsCl case.

3.3.5 Investigation of the reactivity of $Cp_2Ti(tsal)$ towards soft electrophiles

The reactivity of $Cp_2Ti(tsal)$ was investigated towards soft electrophiles E^+ which would be expected to have an affinity for the sulfur [124]. A preliminary investigation in this area used $PhHg^+$ (from readily available PhHgCl) [125]. Reaction products were identified by positive ion ESI-MS. Experimental procedures are described in section 3.2.5.5. Figure 3.23 shows the positive-ion ESI-

MS spectrum for $Cp_2Ti(tsal)$ reacted with one mole equivalent of PhHgCl in methanol solution using the low range method at a capillary exit voltage of 150 V.

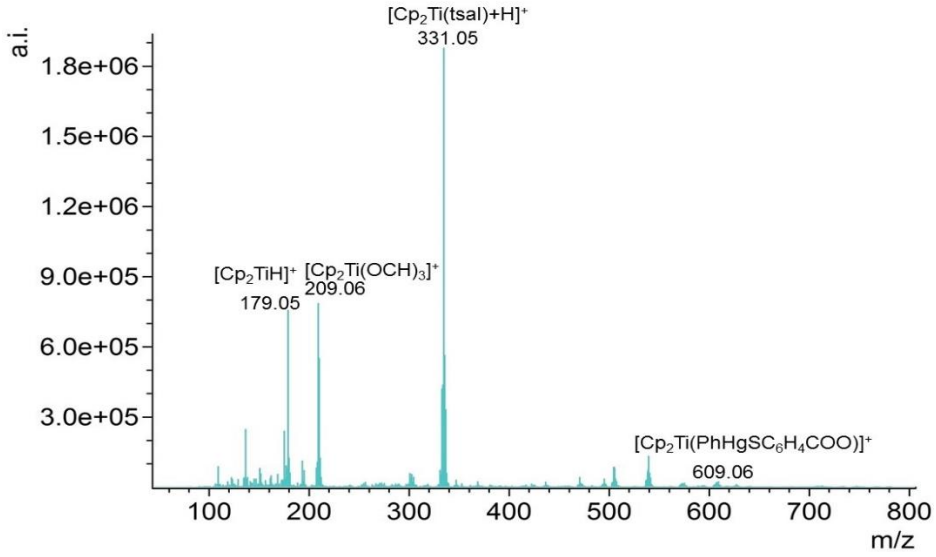

Figure 3.23: Positive-ion ESI mass spectrum of a freshly-prepared solution of $Cp_2Ti(tsal)$ with PhHgCl in methanol with low range method at a capillary exit voltage of 150 V

The $[Cp_2Ti(PhHgSC_6H_4COO)]^+$ ion was observed at a range of capillary exit voltages. At a capillary exit voltage of 150 V, an ion at *m/z* 609.06 was assigned as $[Cp_2Ti(PhHgSC_6H_4COO)]^+$ (calculated *m/z* 609.03) (Figure 3.24).

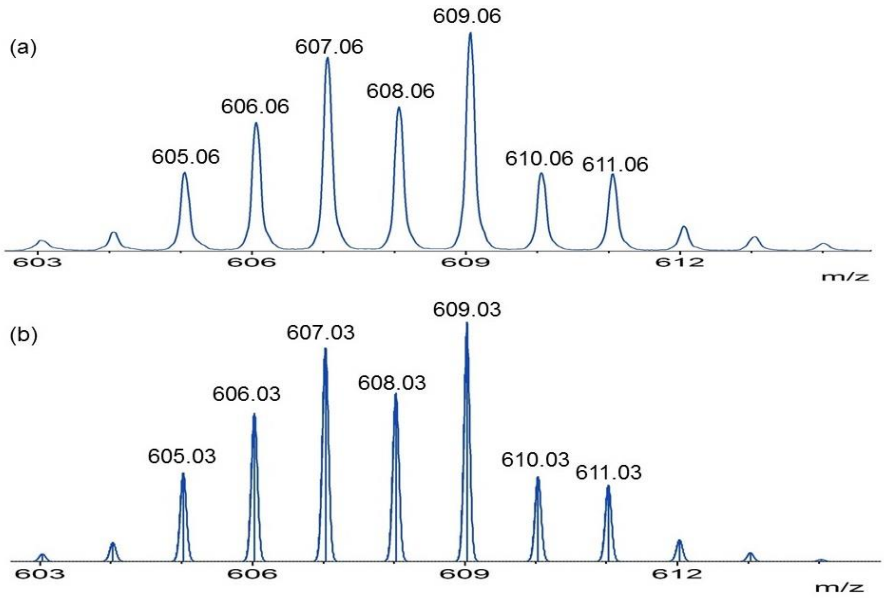

Figure 3.24: An isotope pattern comparison for $[Cp_2Ti(PhHgSC_6H_4COO)]^+$ (a) experimental (*m/z* 609.06) at a capillary exit voltage of 150 V and (b) calculated (*m/z* 609.03)

Two proposed structures of the $[Cp_2Ti(PhHgSC_6H_4COO)]^+$ ion are shown in Figure 3.25.

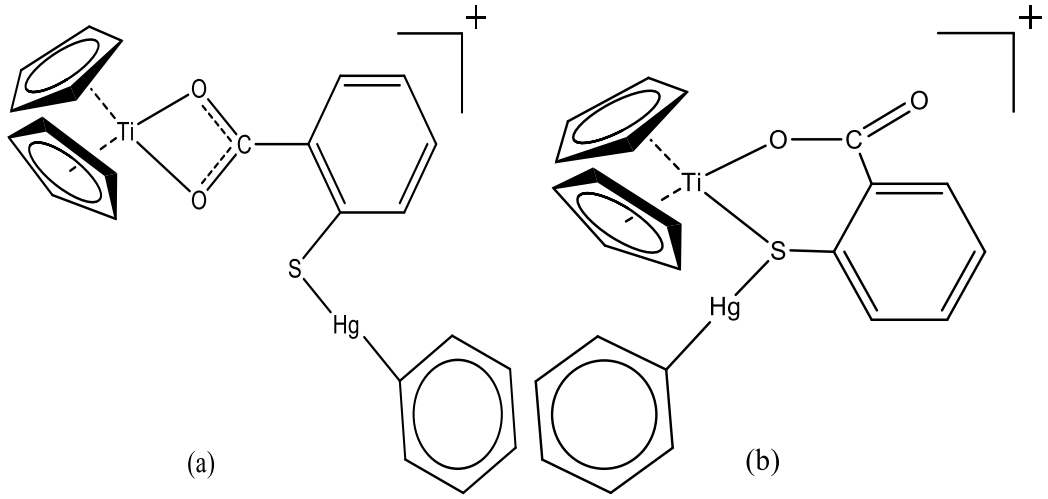

Figure 3.25: The proposed structures of $[Cp_2Ti(PhHgSC_6H_4COO)]^+$ from the reaction of $Cp_2Ti(tsal)$ with one mole equivalent of PhHgCl

In (a) the thiosalicylate ligand is O,O-chelating and the S is uncoordinated but in (b) the $PhHg^+$ cation has coordinated to the chelating tsal ligand, which is S,O chelated to Ti, as in the starting complex.

The intensity of the $[Cp_2Ti(PhHgSC_6H_4COO)]^+$ ion can be affected by the capillary exit voltage; as the capillary exit voltage increases, the intensity ratio of $[Cp_2Ti(PhHgSC_6H_4COO)]^+$ ion peak to the base peak (the highest peak in the spectrum e.g. *m/z* 541.10 $[Cp_3Ti_3O(OCH_3)_6]^+$ at 60 V, *m/z* 209.06 $[Cp_2Ti(OCH_3)]^+$ at 90 V, *m/z* 335.05 $[Cp_2Ti_2O(OCH_3)_3]^+$ at 120 V and 150 V and *m/z* 210.03 $[Cp_2Ti(CH_3OH)]^+$ at 180 V) increases. (The ion at *m/z* 335.05 is proposed to have the formula $[Cp_2Ti_2O(OCH_3)_3]^+$. *m/z* 541.10 $[Cp_3Ti_3O(OCH_3)_6]^+$ ion is equivalent to the $[Cp_3Ti_3O(OCH_3)_6](I_3)$ complex see Section 2.3.2). Figure 3.26 shows the relationship between this relative intensity and capillary exit voltage of $[Cp_2Ti(PhHgSC_6H_4COO)]^+$ ion.

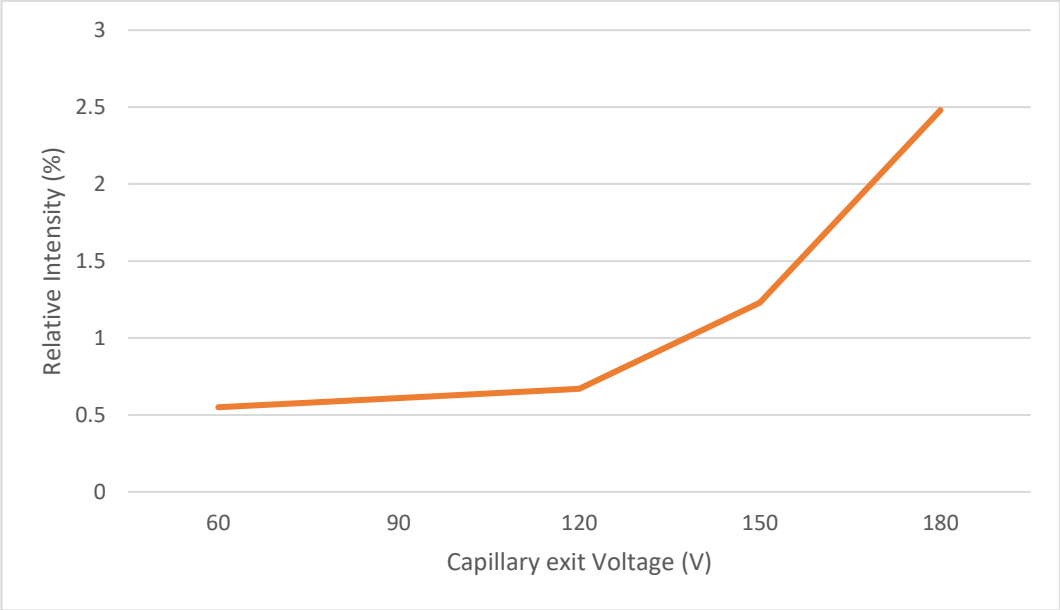

Figure 3.26: Relative Intensity vs capillary exit voltages of $[Cp_2Ti(PhHgSC_6H_4COO)]^+$ species

3.4 Discussion

The positive-ion ESI-MS spectra for $Cp_2Ti(tsal)$ in methanol, recorded at a range of capillary exit voltages, have identified some major species containing one or two Ti centres. Larger Ti clusters which contain three Ti centres like $[2(Cp_2Ti(tsal))+Cp_2Ti(OCH_3)]^+$ was observed using the wide range method.

The positive-ion ESI-MS spectra for $Cp_2Ti(tsal)$ in ethanol and $(EtCp)_2Ti(tsal)$ in methanol have been used to confirm the identity of some species observed in the mass spectra of $Cp_2Ti(tsal)$ in methanol. Most of the corresponding species were observed. The relative intensity of major species can be influenced by the capillary exit voltage.

During this research the possibility of the tsal ligand bridging two Cp_2Ti centres was also investigated. $Cp_2Ti(tsal)Cp_2Ti(OH)^+$ and $Cp_2Ti(tsal)Cp_2Ti(OCH_3)^+$ ions were observed in the $Cp_2Ti(tsal)$ and Cp_2TiCl_2 mixture at a capillary exit voltage of 150 V in methanol solution using the low range method. A very weak ion at *m/z* 543.14 assigned to the $Cp_2Ti(tsal)Cp_2TiCl^+$ ion was observed in this mixture at a capillary exit voltage of 150 V using dichloromethane as solvent and diluted in methanol with the low range method.

The investigation of presence of added alkali metal salts to $Cp_2Ti(tsal)$ in methanol shown the formation of aggregate ions with alkali metal cations. The literature recorded that a higher ions concentration must appear in solution when the alkali metal salt addition increased the system ionic strength [126]. The results are in agreement with these literature results. The larger ions $[4(Cp_2Ti(tsal))+Na]^+$, $[4(Cp_2Ti(tsal))+K]^+$ and $[4(Cp_2Ti(tsal))+Rb]^+$ were observed during this research. The large ions $[4(Cp_2Ti(tsal))+Cs]^+$ and $[4(Cp_2Ti(tsal))+Li]^+$ were not observed due to the low charge density of the Cs^+ ion, and the small size of Li^+.

In an investigation of $Cp_2Ti(tsal)$ towards soft electrophiles E^+ which used $PhHg^+$ (from PhHgCl), the expected species $[Cp_2Ti(PhHgSC_6H_4COO)]^+$ was observed. The intensity of $[Cp_2Ti(PhHgSC_6H_4COO)]^+$ ion can be affected by the capillary exit voltage. As the capillary exit voltage increases, the intensity of $[Cp_2Ti(PhHgSC_6H_4COO)]^+$ species increases.

Chapter 4

An investigation of the ESI-MS behaviour of Cp_2MoCl_2 and $Cp_2Mo(tsal)$

4.1 Introduction

4.1.1 Review of the previous investigation of molybdocene dichloride

Molybdocene dichloride was first reported by Green and Cooper in 1964 [127], it is an organomolybdenum compound, which belongs to the class of metallocene dihalides Cp_2MX_2 (Cp = cyclopentadienyl, M = Ti, Mo, Nb, V and X = halide) [128]. This compound contains two chloride ligands and two η^5-coordinated cyclopentadienyl ligands bound to the central molybdenum(IV) in a pseudo-tetrahedral environment (Figure 4.1) [127].

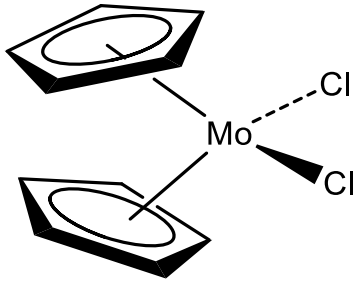

Figure 4.1: Chemical structure of molybdocene dichloride

The hydrolysis chemistry of Cp_2MoCl_2 has been studied and first characterised by Marks and Toney in 1985 [129]. Cp_2MoCl_2 has poor solubility in organic solvents and water [127]. The rate of hydrolysis of both Cl and Cp ligands has been studied. The hydrolysis of the Cp rings is negligible. Dark-red $[Cp_2Mo(OH)(OH_2)]^+$ and $[Cp_2Mo(OH_2)_2]^{2+}$ cations are formed during the hydrolysis [128]. Figure 4.2 shows the halide hydrolysis chemistry of Cp_2MoCl_2.

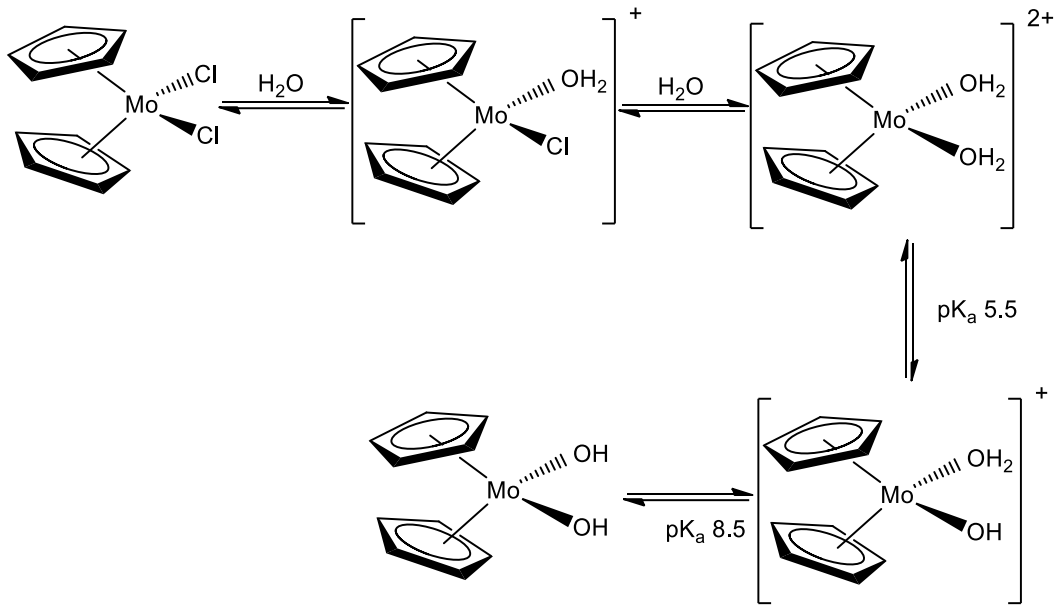

Figure 4.2: Hydrolysis chemistry of Cp_2MoCl_2

Like Cp_2TiCl_2, Cp_2MoCl_2 can act as an antitumor agent against a variety of human tumors and has less toxic effects than *cis*-platin, but its coordination chemistry and mechanism of antitumor actions are significantly different from Cp_2TiCl_2 [130,131]. The studies of Cp_2MoCl_2 have emerged only in the last decade[1]. In contrast to Cp_2TiCl_2, the biochemical and chemical properties of Cp_2MoCl_2 have not been studied in detail [127]. Binding studies between Cp_2MoCl_2 and oligonucleotides and calf-thymus DNA has been initially investigated by Marks' group and later pursued by Harding's and Meléndez's groups [132]. ^{31}P NMR spectroscopy showed that the terminal phosphates of DNA will bind to Cp_2Mo^{2+} [132]. Research has proved that the interactions of Cp_2MoCl_2 with DNA is not directly related to anticancer activity [82]. The mechanism of action of Cp_2MoCl_2 is still unclear and has not been confirmed by any studies [133].

4.1.2 Project outline

This research project carried out a much more in-depth investigation on solutions of Cp_2MoCl_2 in alcohols. An ESI source coupled with a high resolution TOF mass spectrometer was used for investigating the ESI-MS behaviour of the Cp_2MoCl_2 complex. A suitable solvent is very important for the ESI-MS studies; in this study

Cp_2MoCl_2 was dissolved in methanol. At the same time, bis(cyclopentadienyl) thiosalicylatomolybdenum(IV) $Cp_2Mo(tsal)$ (Figure 4.3) was synthesised and also studied by ESI-MS.

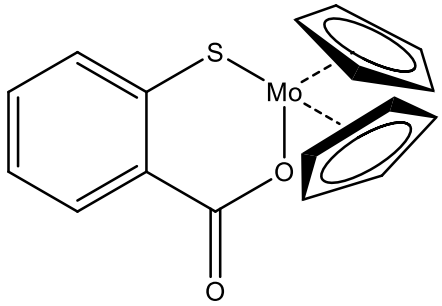

Figure 4.3: Chemical structure of $Cp_2Mo(tsal)$

4.2 Experimental

The chemicals, solvents and instruments used during this research are listed in sections 4.2.1 to 4.2.4.

4.2.1 Chemicals and solvents

Powdered bis(cyclopentadienyl)molybdenum(IV) dichloride and liquid pyridine were obtained from Aldrich Chemical company. Thiosalicylic acid was purchased from Sigma. Univar grade methanol used was distilled. Dichloromethane was obtained from Merck KGaA.

4.2.2 ESI-MS instrumentation

ESI-MS instrumentation was as described for the ESI-MS investigation of Cp_2TiCl_2 (Section 2.2.2).

4.2.3 NMR instrumentation

NMR instrumentation was as described for the ESI-MS investigation of $Cp_2Ti(SC_6H_4CO_2)$ (Section 3.2.3).

4.2.4 Melting point and IR instrumentations

Melting point and IR instrumentations were as described for the ESI-MS investigation of $Cp_2Ti(SC_6H_4CO_2)$ (Section 3.2.4).

4.2.5 Experimental procedures

4.2.5.1 Synthesis of Cp2Mo(tsal)

Cp_2MoCl_2 (50 mg, 0.168 mmol) and thiosalicylic acid (25.9 mg, 0.168 mmol) were suspended in methanol (50 mL) with 3 drops of pyridine and 2 mL of distilled water in a 50 mL round bottom flask with a magnetic stirrer, resulting in a brown suspension. The mixture was stirred for 3 hours, then allowed to evaporate to dryness. The dark green residue was recrystallised by dissolving in CH_2Cl_2 (5 mL) and filtered into a small vial, through a Pasteur pipette containing a small plug of cotton wool. The smaller vial was placed into a larger vial. Ether was added to the outer vial. Which was then capped and stored in the dark for 2 days to give final dark brown solid (yield ca. 46 mg, 72%). Melting point of $Cp_2Mo(tsal)$ 155-158 °C.

4.3 Results and discussion

4.3.1 An investigation of the ESI-MS behaviour of Cp_2MoCl_2

4.3.1.1 Analysis of a freshly-prepared solution of Cp_2MoCl_2 in methanol with low range method

The positive-ion ESI-MS spectrum for Cp_2MoCl_2 in methanol solution using the low range method, recorded at a capillary exit voltage of 90 V, is given in Figure 4.4.

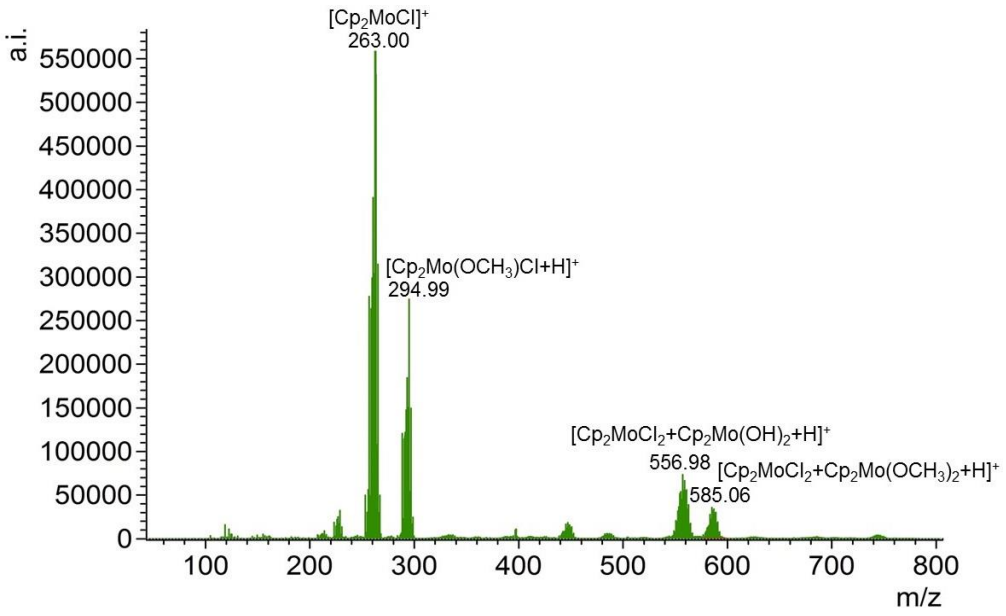

Figure 4.4: Positive-ion ESI mass spectrum of a freshly-prepared solution of Cp_2MoCl_2 in methanol with low range method at a capillary exit voltage of 90 V

The results show that there are two main groups of ions, one group of species at *m/z* 250-300 and the other group of species at *m/z* 550-600. The major species at low *m/z* range containing one molybdenum centre are $[Cp_2MoCl]^+$ (*m/z* 263.00) (Figure 4.5) and $[Cp_2Mo(OCH_3)Cl+H]^+$ (*m/z* 294.99) (Figure 4.6). Ion at *m/z* 294.99 can be also assigned as $[Cp_2MoCl(CH_3OH)]^+$, because protonation will be on oxygen.

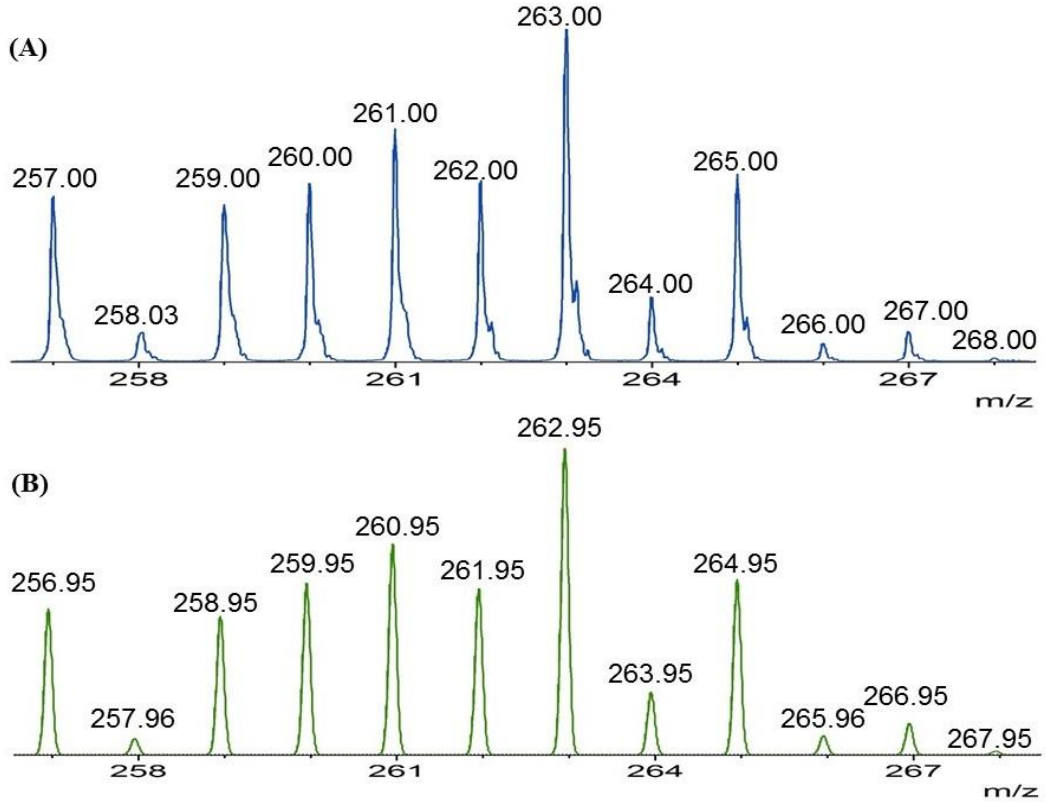

Figure 4.5: An isotope pattern comparison for $[Cp_2MoCl]^+$ (A) experimental (*m/z* 263.00) and (B) calculated (*m/z* 262.95)

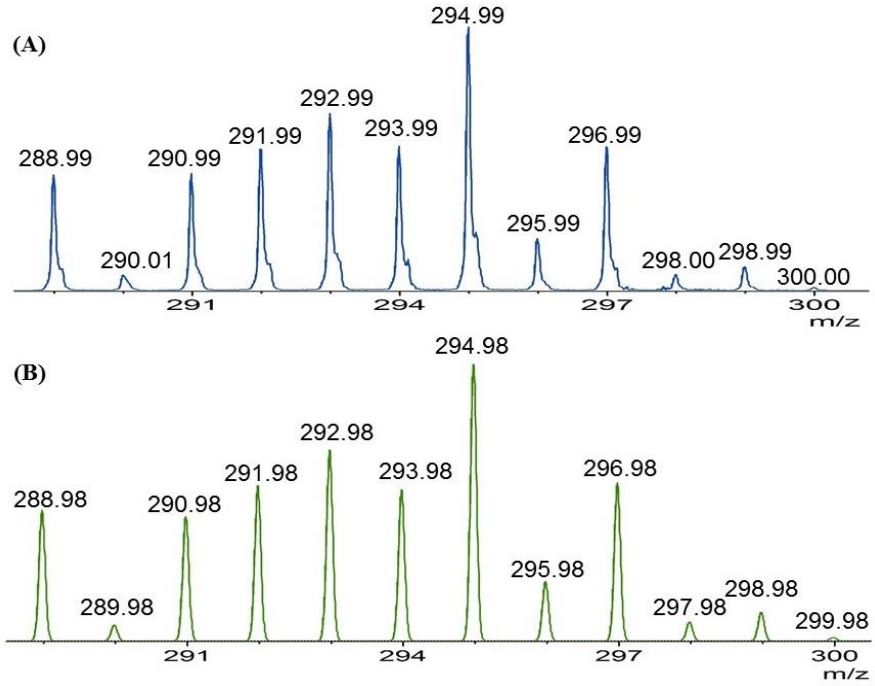

Figure 4.6: An isotope pattern comparison for $[Cp_2Mo(OCH_3)Cl+H]^+$ (A) experimental (*m/z* 294.99) and (B) calculated (*m/z* 294.98)

At high *m/z* region two molybdenum centre species were observed at *m/z* 556.98 and *m/z* 585.06 are assigned as $[Cp_2MoCl_2+Cp_2Mo(OH)_2+H]^+$ (Figure 4.7) and $[Cp_2MoCl_2+Cp_2Mo(OCH_3)_2+H]^+$ (Figure 4.8).

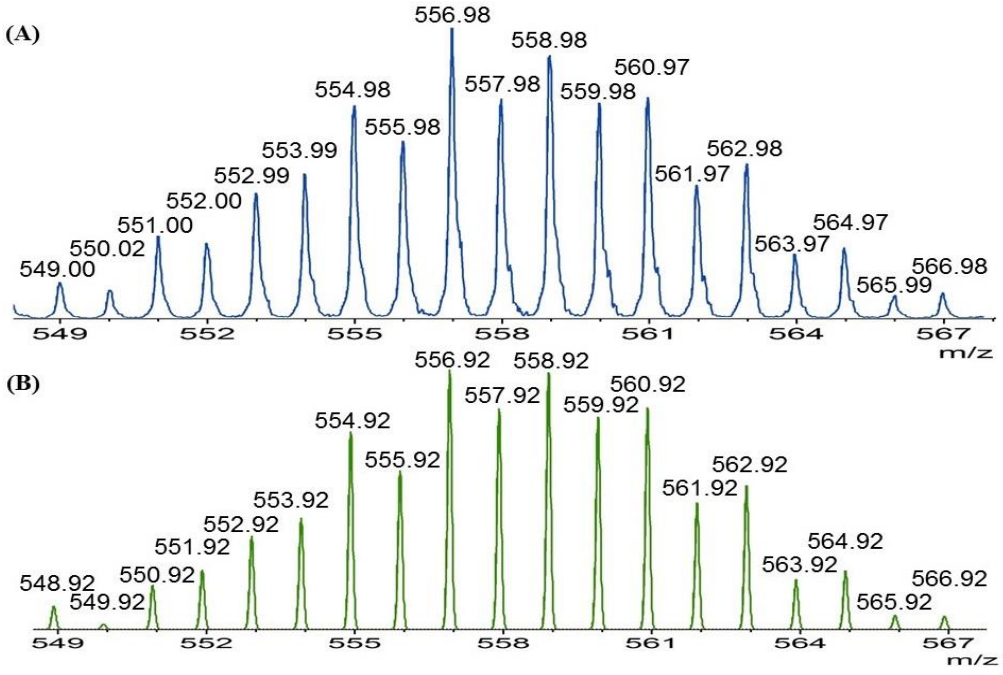

Figure 4.7: An isotope pattern comparison for $[Cp_2MoCl_2+Cp_2Mo(OH)_2+H]^+$ (A) experimental (*m/z* 556.98) and (B) calculated (*m/z* 556.92)

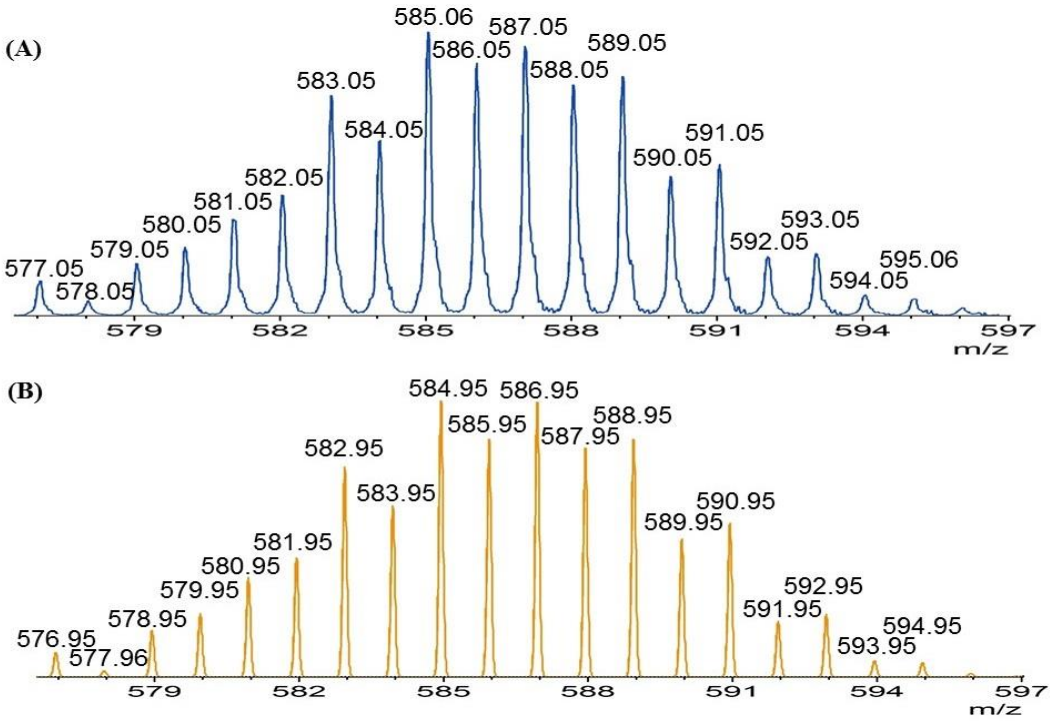

Figure 4.8: An isotope pattern comparison for $[Cp_2MoCl_2+Cp_2Mo(OCH_3)_2+H]^+$ (A) experimental (*m/z* 585.06) and (B) calculated (*m/z* 584.95)

Table 4.1 summarises all the major species which were observed at a capillary exit voltage of 90 V with low method.

Table 4.1: Summary of species observed at a capillary exit voltage of 90 V in a freshly-prepared solution of Cp_2MoCl_2 in methanol with low range method

Species	Experimental (*m/z*)	Calculated (*m/z*)
$[Cp_2MoCl]^+$	263.00	262.95
$[Cp_2Mo(OCH_3)Cl+H]^+$	295.00	294.98
$[Cp_2MoCl_2+Cp_2Mo(OH)_2+H]^+$	556.98	556.92
$[Cp_2MoCl_2+Cp_2Mo(OCH_3)_2+H]^+$	585.06	584.95

The positive-ion ESI-MS spectrum for Cp_2MoCl_2 in methanol solution using the low range method, recorded at a capillary exit voltage of 150 V, is given in Figure 4.9.

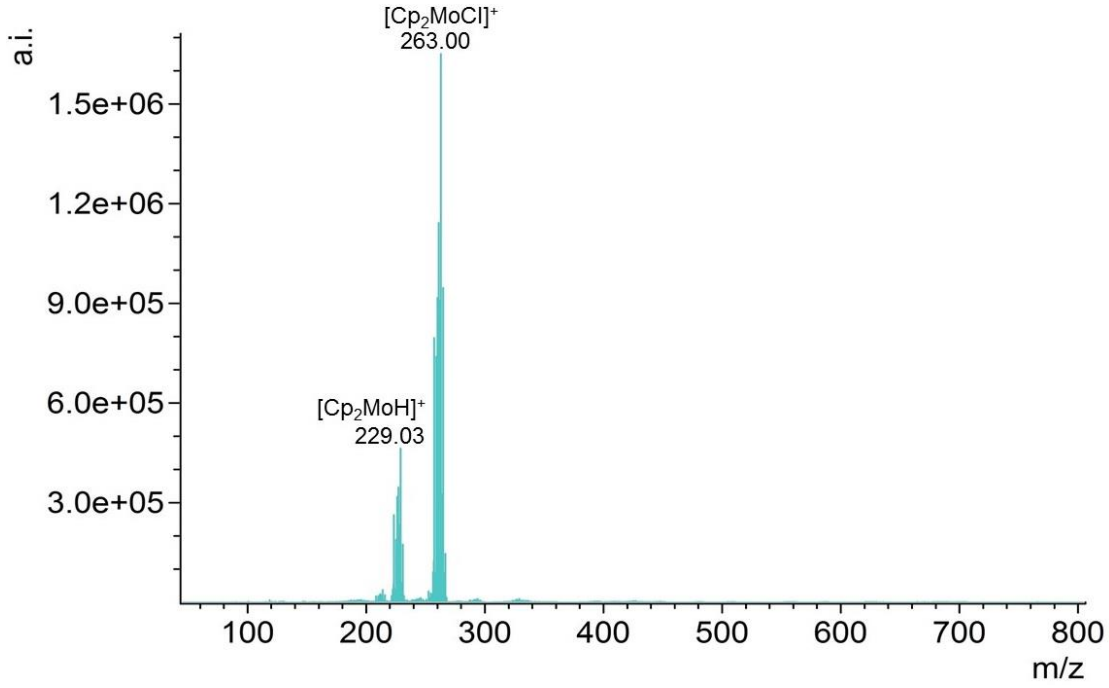

Figure 4.9: Positive-ion ESI mass spectrum of a freshly-prepared solution of Cp_2MoCl_2 in methanol with low range method at a capillary exit voltage of 150 V

The result shows that as the capillary exit voltage increases, the intensity of the low *m/z* range species increases and high *m/z* range species decrease. Two molybdenum centre species also disappeared. The major species at low *m/z* range containing one molybdenum centre are $[Cp_2MoH]^+$ (*m/z* 229.03) (Figure 4.10) and $[Cp_2MoCl]^+$ (*m/z* 263.00).

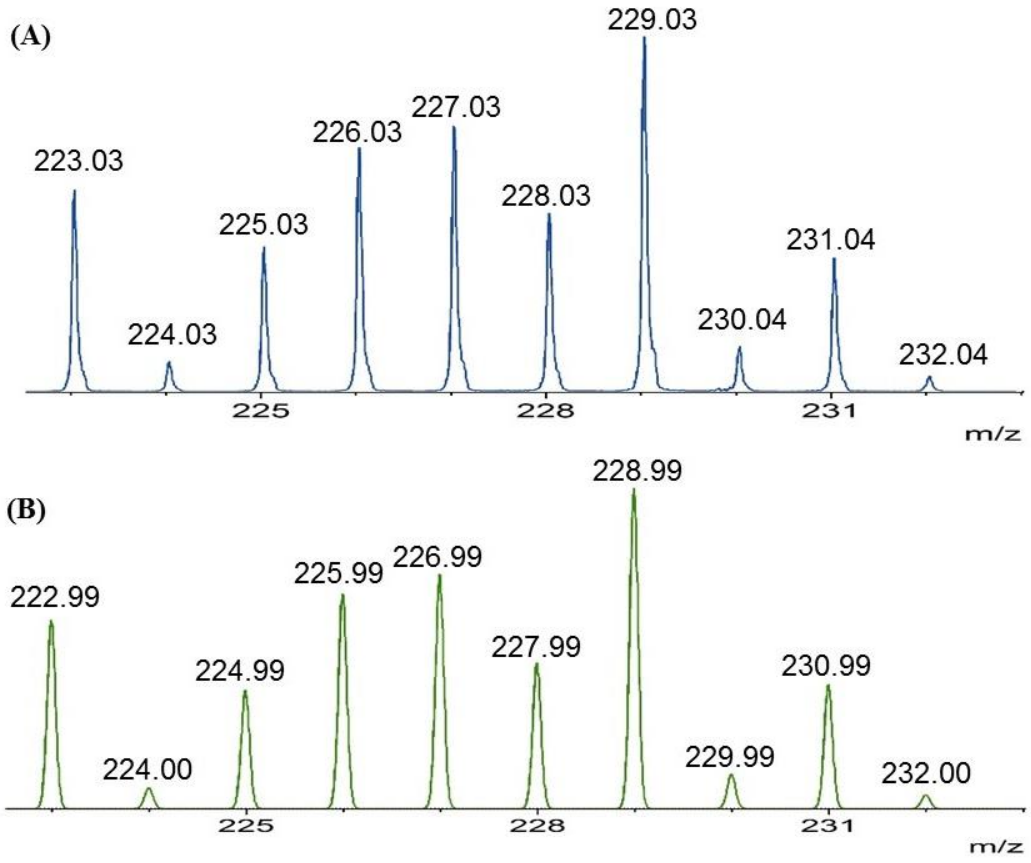

Figure 4.10: An isotope pattern comparison for $[Cp_2MoH]^+$ (A) experimental (*m/z* 229.03) and (B) calculated (*m/z* 228.99)

$[Cp_2MoH]^+$ is one of the major species at low *m/z* range containing one molybdenum centre, this ion is proposed to be formed by β-hydride elimination (Figure 4.11) which is same as the formation of $[Cp_2TiH]^+$.

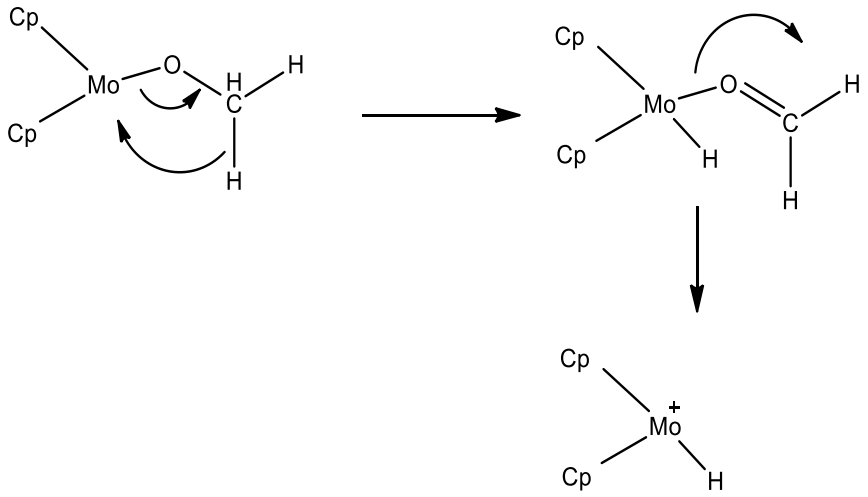

Figure 4.11: Formation of $[Cp_2MoH]^+$ from $[Cp_2Mo(OCH_3)]^+$ species by β -hydride elimination

4.3.1.2 Analysis of a freshly-prepared solution of Cp_2MoCl_2 in methanol with wide range method

To investigate larger Mo clusters which contain three or more Mo required the use of the wide range method. In this research, the wide range method has a maximum at *m/z* 1500. The positive-ion ESI-MS spectrum for Cp_2MoCl_2 in methanol solution using the wide range method, recorded at a capillary exit voltage of 90 V, is given in Figure 4.12.

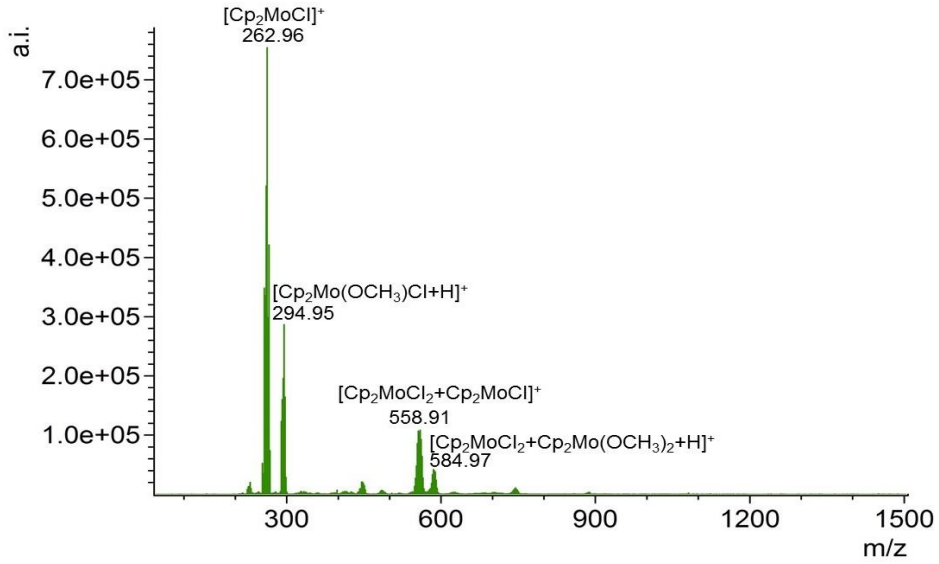

Figure 4.12: Positive-ion ESI mass spectrum of a freshly-prepared solution of Cp_2MoCl_2 in methanol with wide range method at a capillary exit voltage of 90 V

The result shows that some of these species were also observed with the low range method. One new species $[Cp_2MoCl_2+Cp_2MoCl]^+$ (*m/z* 558.91) (Figure 4.13) was observed when using the wide range method.

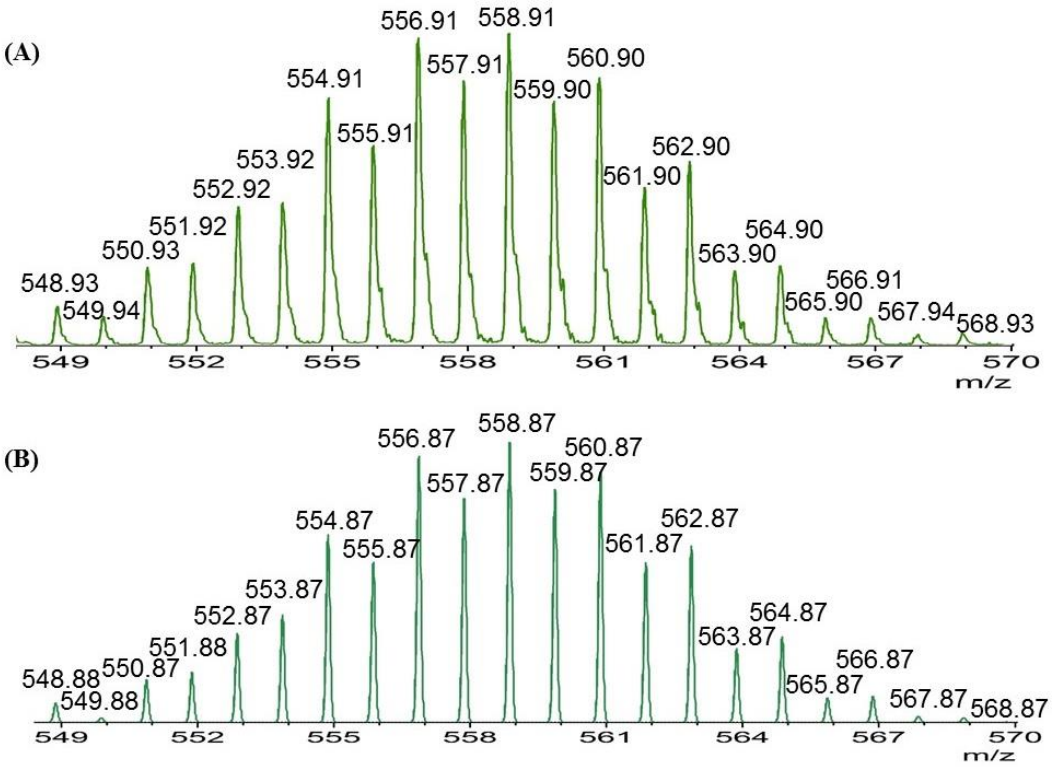

Figure 4.13: An isotope pattern comparison for $[Cp_2MoCl_2+Cp_2MoCl]^+$ (A) experimental (*m/z* 558.91) and (B) calculated (*m/z* 558.87)

Table 4.2 summarises all the major species which were observed at a capillary exit voltage of 90 V with wide method.

Table 4.2: Summary of species observed at a capillary exit voltage of 90 V in a freshly-prepared solution of Cp_2MoCl_2 in methanol with wide range method

Species	Experimental (*m/z*)	Calculated (*m/z*)
$[Cp_2MoCl]^+$	262.96	262.95
$[Cp_2Mo(OCH_3)Cl+H]^+$	294.95	294.98
$[Cp_2MoCl_2+Cp_2MoCl]^+$	558.91	558.87
$[Cp_2MoCl_2+Cp_2Mo(OCH_3)_2+H]^+$	584.97	584.95

The positive-ion ESI-MS spectrum for Cp_2MoCl_2 in methanol solution using the wide range method, recorded at a capillary exit voltage of 150 V, is given in Figure 4.14.

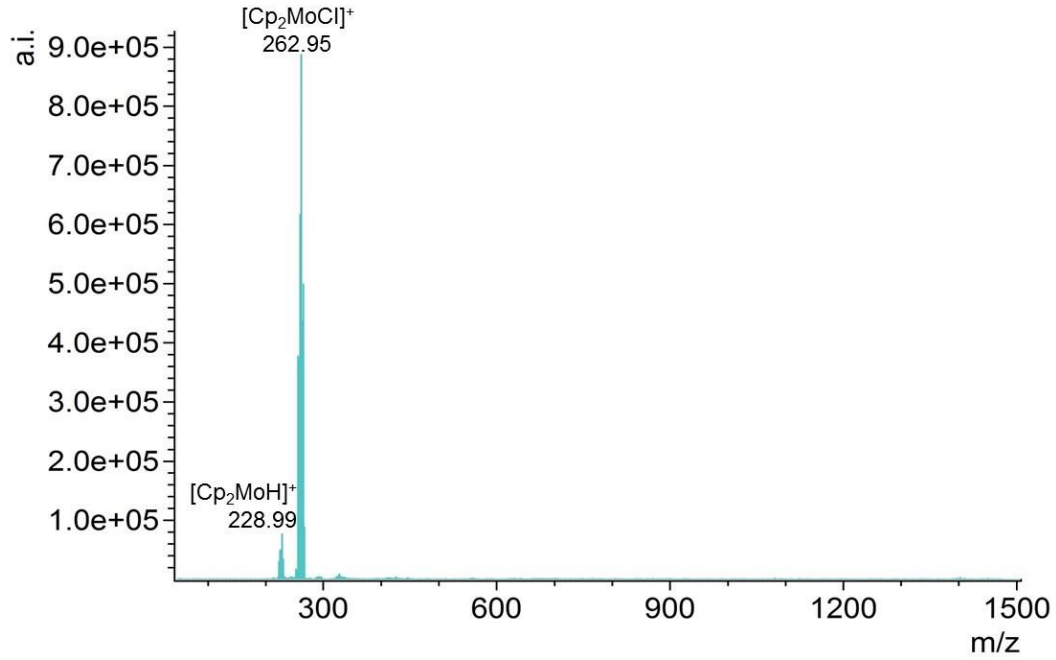

Figure 4.14: Positive-ion ESI mass spectrum of a freshly-prepared solution of Cp_2MoCl_2 in methanol with wide range method at a capillary exit voltage of 150 V

Same as using the low range method, only two species were observed at *m/z* 228.99 and *m/z* 262.95 which are assigned as $[Cp_2MoH]^+$ and $[Cp_2MoCl]^+$. Compare with Figure 4.12, where Mo_2 species were seen, but larger Mo clusters which contain three or more Mo centres were not observed using the wide range method.

4.3.2 An investigation of the ESI-MS behaviour of $Cp_2Mo(tsal)$

4.3.2.1 Introduction

$Cp_2Mo(tsal)$ is a new compound that has never been synthesised before. During this research, $Cp_2Mo(tsal)$ was synthesised by the reaction of Cp_2MoCl_2 with thiosalicylic acid and then recrystallised by the vapour diffusion method. Experimental procedures have been described in section 4.2.5.1. This new complex was characterised by ESI-MS, melting point, ^1H NMR and Infra-red (IR) spectroscopy.

The ^1H NMR spectrum for $Cp_2Mo(tsal)$ is shown in Figure 4.15. The doublet of doublets at 7.90 ppm and 7.33 ppm were assigned to the benzene ring protons close to the S and O. The other two protons on the benzene ring were assigned at 7.11

ppm and 7.06 ppm as the triplets. The protons on the Cp rings were assigned at 5.48 ppm.

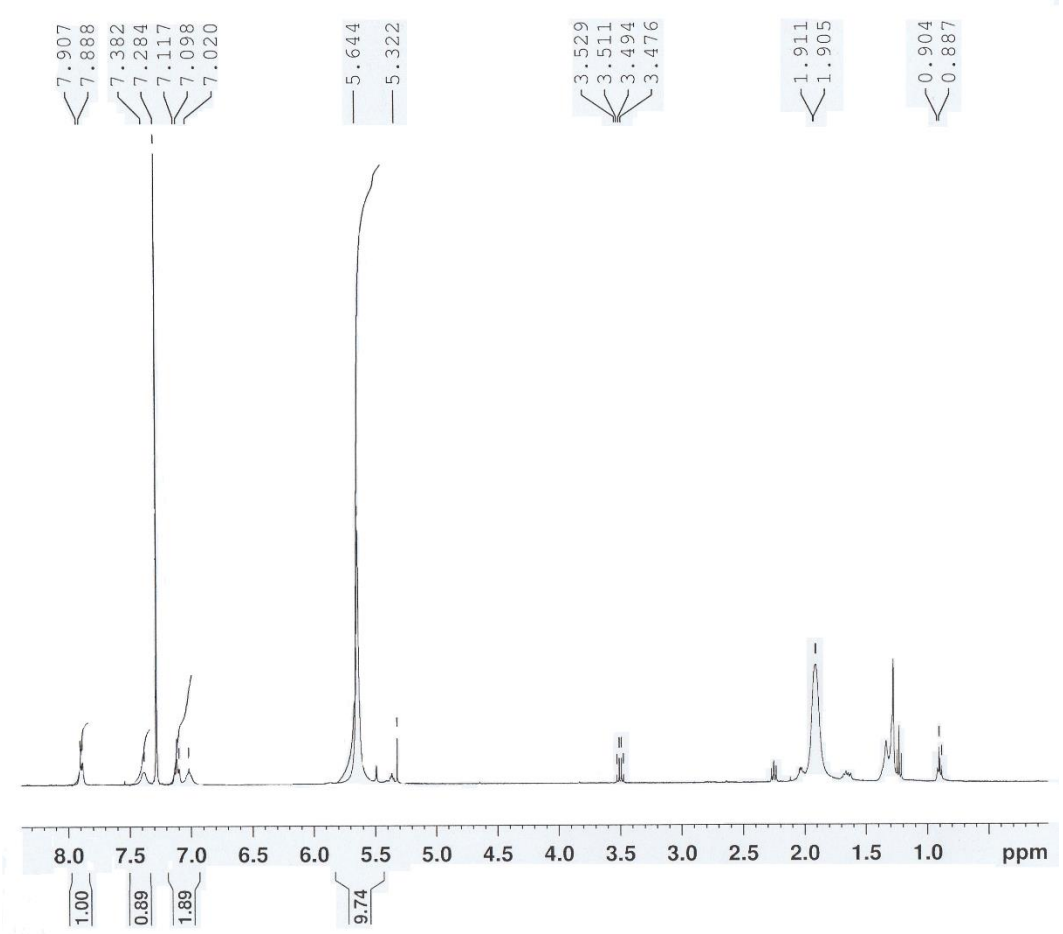

Figure 4.15: ^{1}H NMR spectrum for $Cp_2Mo(tsal)$

Strong bands observed at 1584 and 1377 cm^{-1} are attributed to the C=O and C-O stretching vibrations which are characteristic absorptions of the COO group [119]. The C-H stretching frequency at 3107 cm^{-1} is indicative of the cyclopentadienyl ring and 1428 cm^{-1} due to C-C stretching of π-bond further confirm the presence of the Cp group [119,120].

4.3.2.2 Analysis of a freshly-prepared solution of $Cp_2Mo(tsal)$ in methanol with low range method

The positive-ion ESI-MS spectrum for $Cp_2Mo(tsal)$ in methanol solution using the low range method, recorded at a capillary exit voltage of 90 V, is given in Figure 4.16.

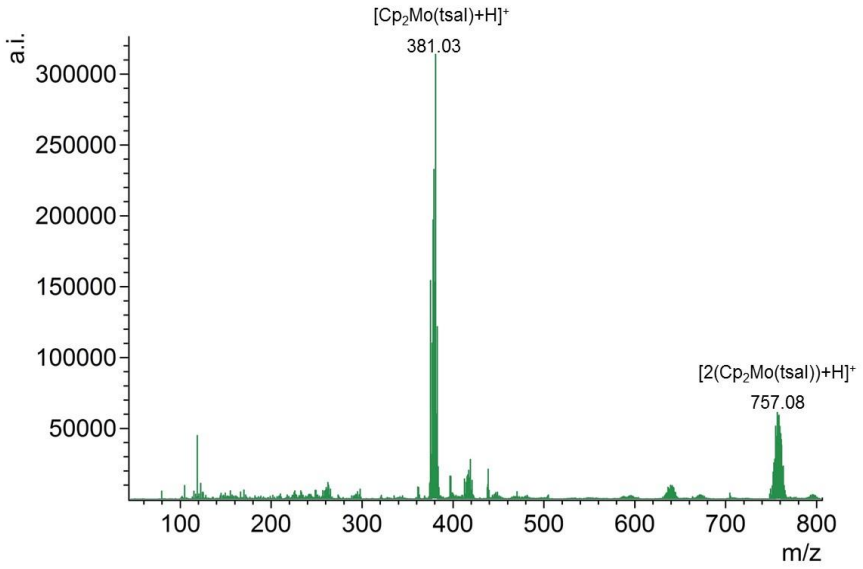

Figure 4.16: Positive-ion ESI mass spectrum of a freshly-prepared solution of $Cp_2Mo(tsal)$ in methanol with low range method at a capillary exit voltage of 90 V

The mass spectrum contains two main peaks, with the base peak of the spectrum at *m/z* 381.03 assigned as $[Cp_2Mo(tsal)+H]^+$ (Figure 4.17). The second peak at *m/z* 757.08 is assigned as $[2(Cp_2Mo(tsal))+H]^+$ (Figure 4.18).

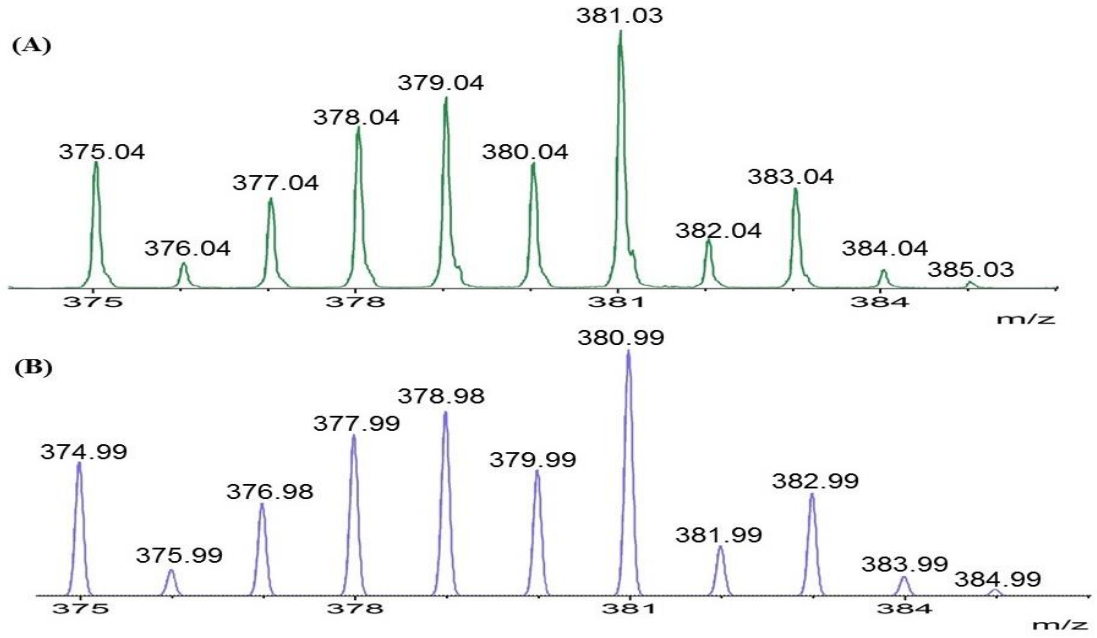

Figure 4.17: An isotope pattern comparison for $[Cp_2Mo(tsal)+H]^+$ (A) experimental (*m/z* 381.03) and (B) calculated (*m/z* 380.99)

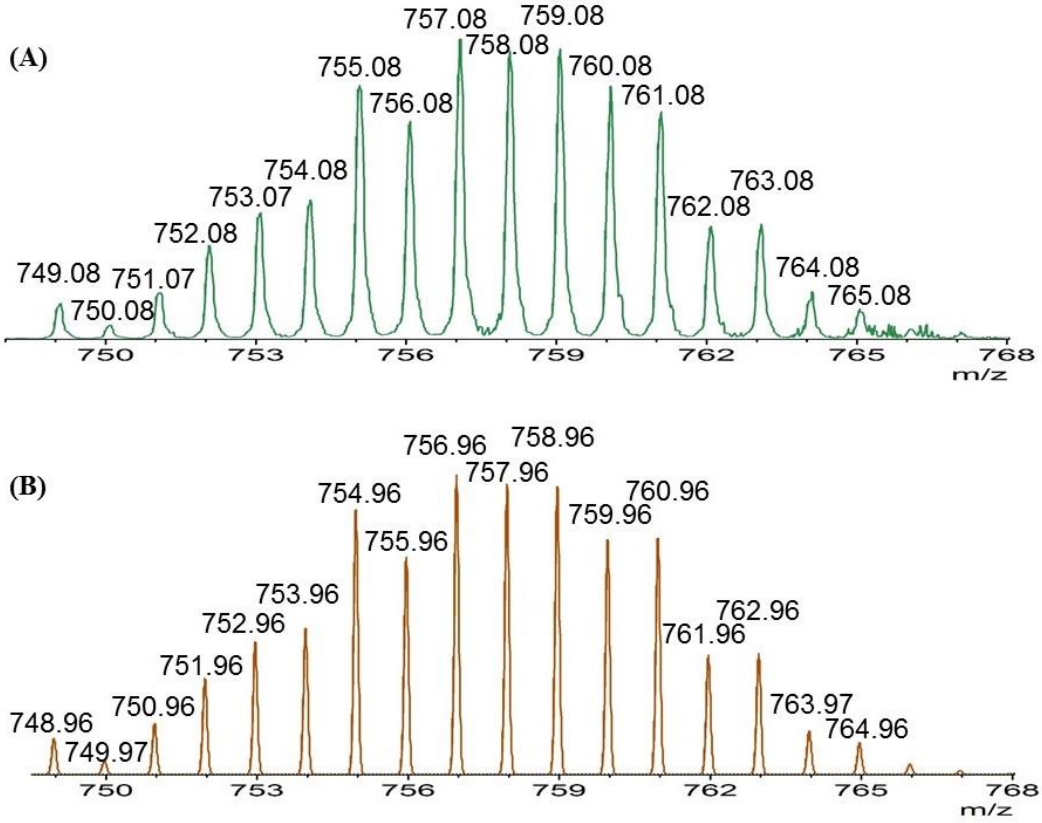

Figure 4.18: An isotope pattern comparison for $[2(Cp_2Mo(tsal))+H]^+$ (A) experimental (*m/z* 757.08) and (B) calculated (*m/z* 756.96)

The positive-ion ESI-MS spectrum for $Cp_2Mo(tsal)$ in methanol solution using the low range method, recorded at a capillary exit voltage of 150 V, is given in Figure 4.19.

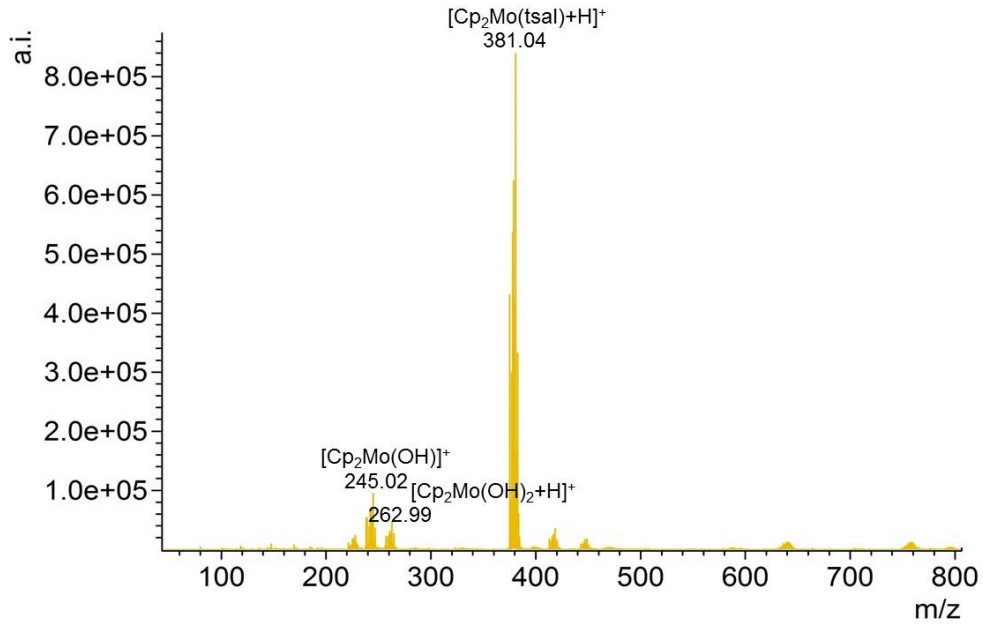

Figure 4.19: Positive-ion ESI mass spectrum of a freshly-prepared solution of $Cp_2Mo(tsal)$ in methanol with low range method at a capillary exit voltage of 150 V

As the capillary exit voltage increased to 150 V, the species in the high *m/z* region disappeared. As for the low capillary exit voltage, the base peak of the spectrum at *m/z* 381.04 is assigned as $[Cp_2Mo(tsal)+H]^+$. A grouping of low intensity species were observed at low *m/z* region. Of the two lower intensity ions, that at *m/z* 245.02 was identified as $[Cp_2Mo(OH)]^+$ (Figure 4.20). The other ion at *m/z* 262.99 was identified as $[Cp_2Mo(OH)_2+H]^+$ (Figure 4.21).

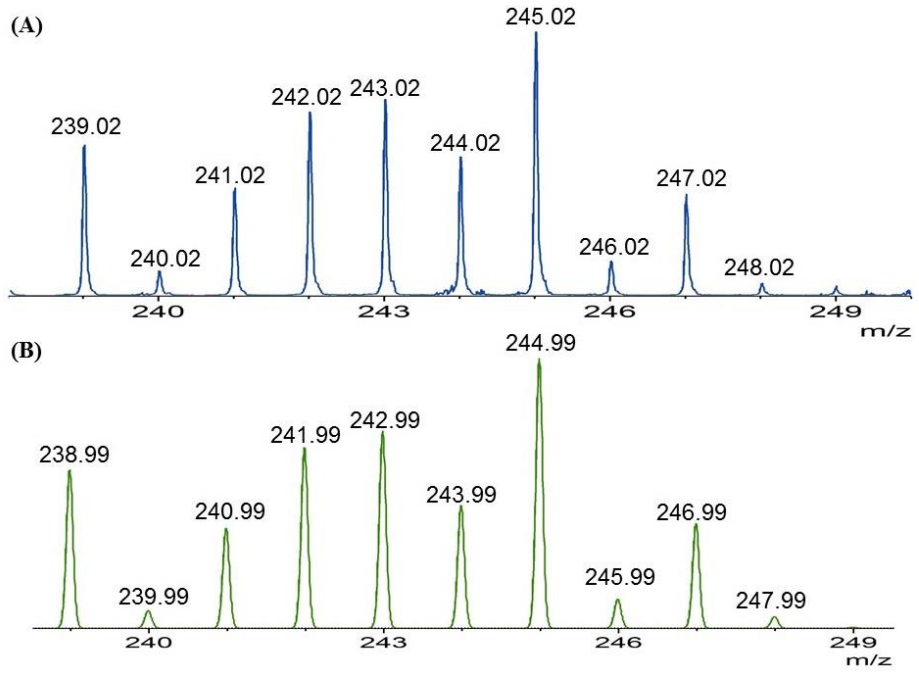

Figure 4.20: An isotope pattern comparison for $[Cp_2Mo(OH)]^+$ (A) experimental (*m/z* 245.02) and (B) calculated (*m/z* 244.99)

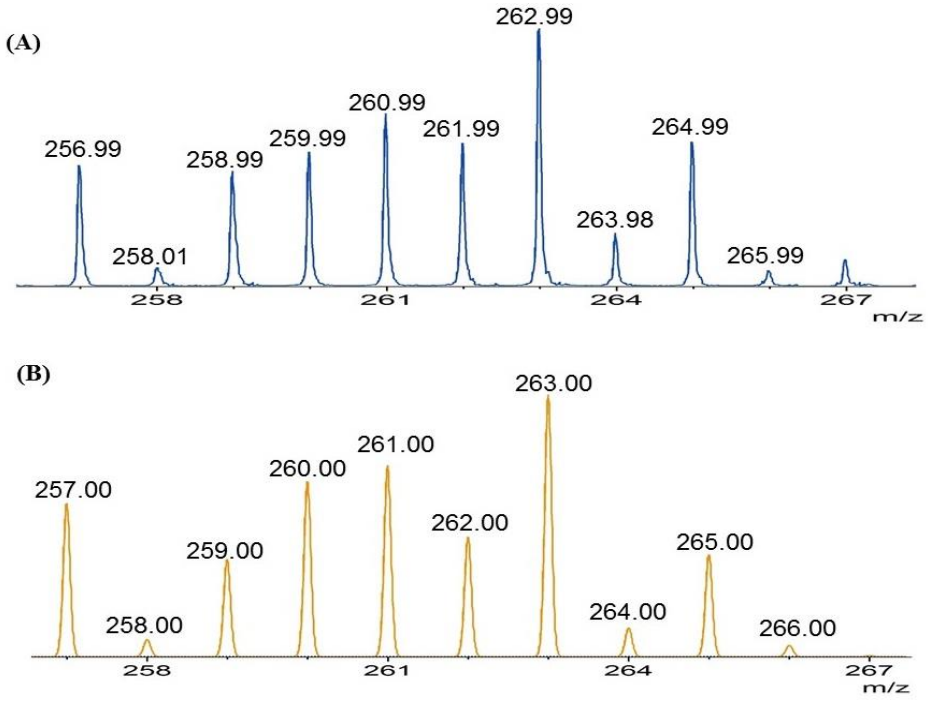

Figure 4.21: An isotope pattern comparison for $[Cp_2Mo(OH)_2+H]^+$ (A) experimental (*m/z* 262.99) and (B) calculated (*m/z* 263.00)

4.3.2.3 Analysis of a freshly-prepared solution of $Cp_2Mo(tsal)$ in methanol with wide range method

The positive-ion ESI-MS spectrum for $Cp_2Mo(tsal)$ in methanol solution using the wide range method, recorded at a capillary exit voltage of 90 V, is given in Figure 4.22.

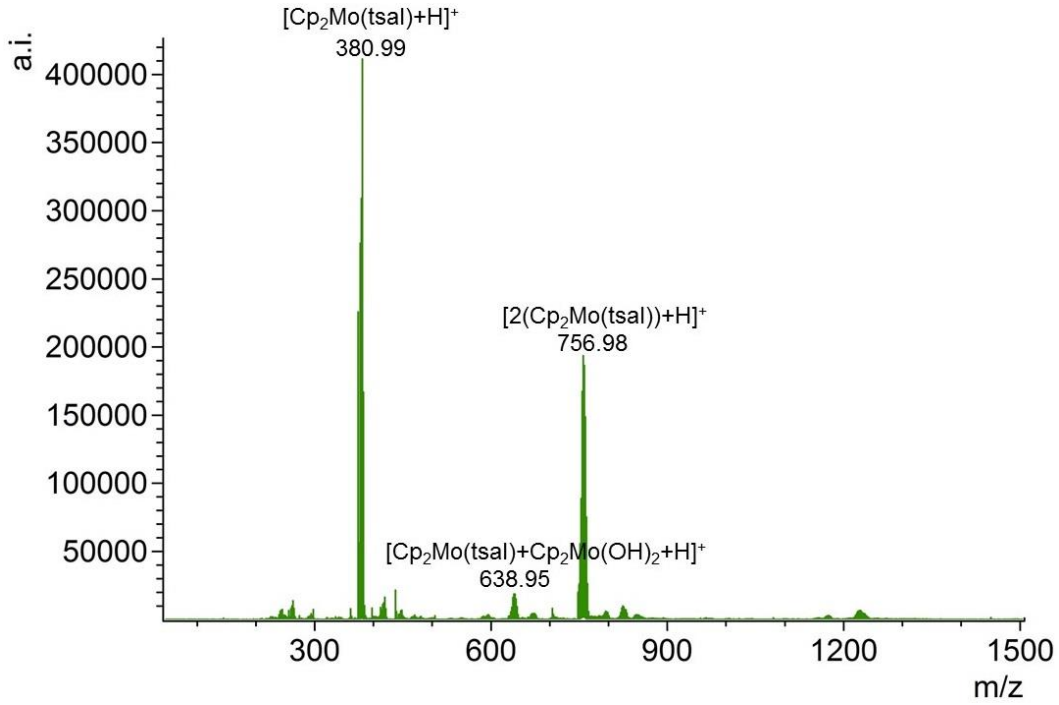

Figure 4.22: Positive-ion ESI mass spectrum of a freshly-prepared solution of $Cp_2Mo(tsal)$ in methanol with wide range method at a capillary exit voltage of 90 V

Same as the low range method, two major ions were observed and assigned as $[Cp_2Mo(tsal)+H]^+$ (*m/z* 380.99) and $[2(Cp_2Mo(tsal))+H]^+$ (*m/z* 756.98). An ion of low intensity at *m/z* 638.95 is assigned as $[Cp_2Mo(tsal)+Cp_2Mo(OH)_2+H]^+$ (calculated *m/z* 638.98) (Figure 4.23).

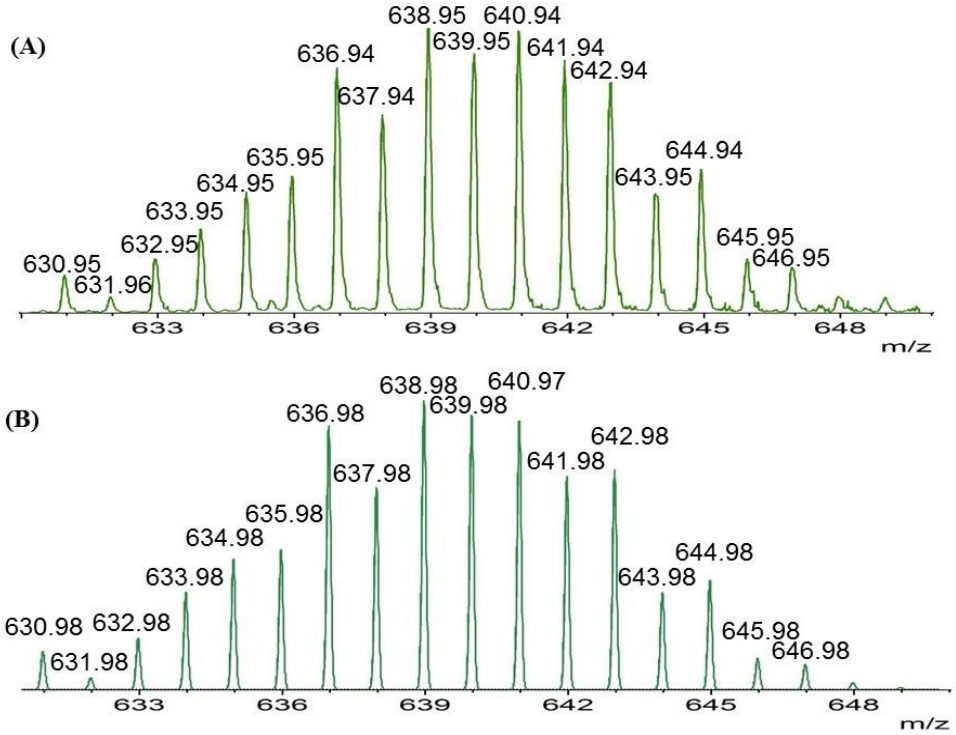

Figure 4.23: An isotope pattern comparison for $[Cp_2Mo(tsal)+Cp_2Mo(OH)_2+H]^+$ (A) experimental (*m/z* 638.95) and (B) calculated (*m/z* 638.98)

The positive-ion ESI-MS spectrum for $Cp_2Mo(tsal)$ in methanol solution using the wide range method, recorded at a capillary exit voltage of 150 V, is given in Figure 4.24.

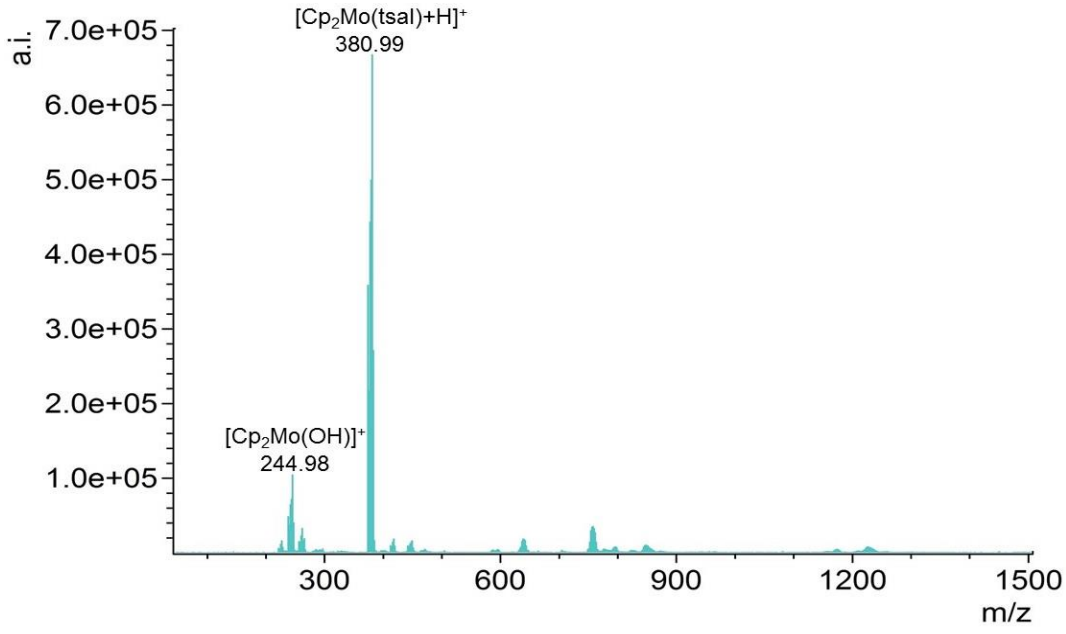

Figure 4.24: Positive-ion ESI mass spectrum of a freshly-prepared solution of $Cp_2Mo(tsal)$ in methanol with wide range method at a capillary exit voltage of 150 V

Same as using the low range method, only two major species were observed at *m/z* 244.98 and *m/z* 380.99 which are assigned as $[Cp_2Mo(OH)]^+$ and $[Cp_2Mo(tsal)+H]^+$. Larger Mo clusters which contain three or more Mo centres were not observed using the wide range method.

4.3.3 Comparison of Cp_2TiCl_2/Cp_2Ti(tsal) systems with Cp_2MoCl_2/Cp_2Mo(tsal) systems

4.3.3.1 Comparison of the ESI-MS spectra of Cp_2TiCl_2 with those of Cp_2MoCl_2

The positive-ion ESI-MS spectra for Cp_2TiCl_2 and Cp_2MoCl_2 in methanol solution using the low range method, recorded at a capillary exit voltage of 90 V are shown in Figure 4.25.

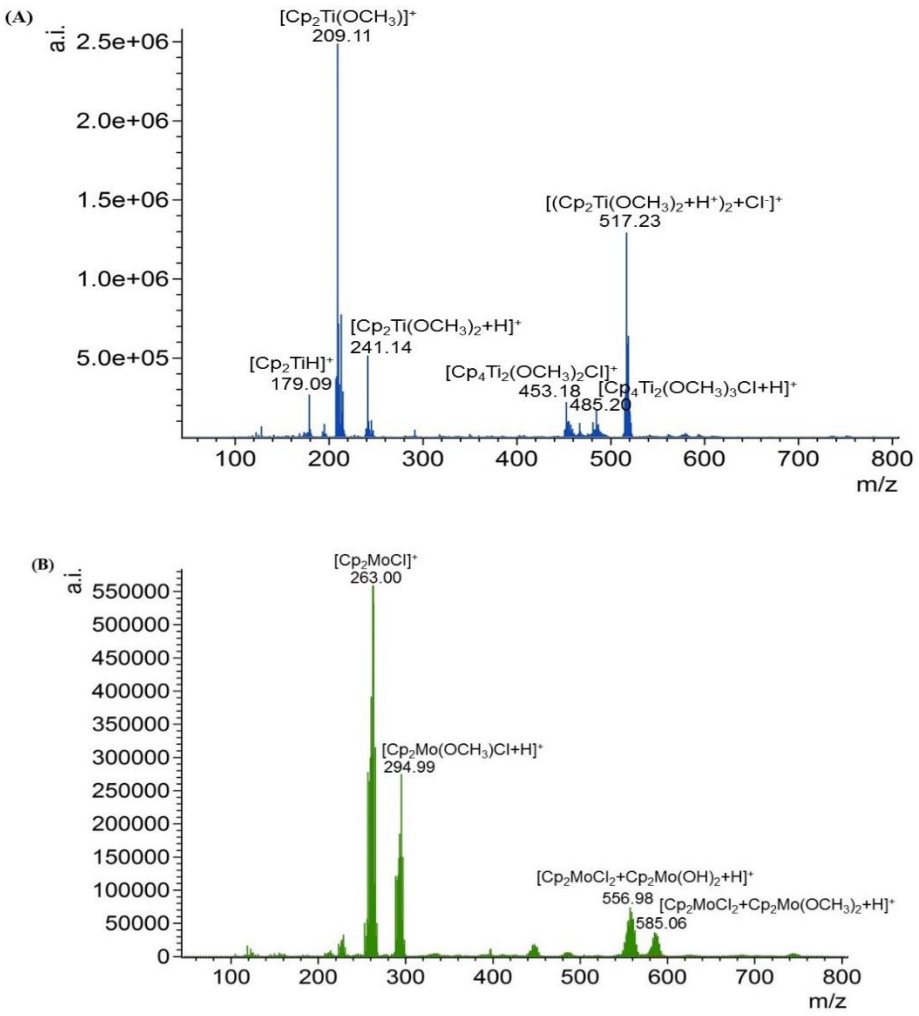

Figure 4.25: Positive-ion ESI mass spectra of a freshly-prepared solution of Cp_2TiCl_2 (A) and Cp_2MoCl_2 (B) in methanol with low range method at a capillary exit voltage of 90 V

The results show that there are two main groups of ions for both mass spectra, one group of species at *m/z* 150-300 and the other group of species were observed at *m/z* 400-600. Interestingly, the major species were observed in reaction of Cp_2TiCl_2 with methanol at low *m/z* range without Cl group, but all the major species in Cp_2MoCl_2 mass spectrum contain a Cl ligand. At high *m/z* range, one Cl ligand observed for each major species in Cp_2TiCl_2 mass spectrum, but in Cp_2MoCl_2 mass spectrum each major species with two Cl ligands. This result indicates alcoholysis of the Cp_2TiCl_2 is easier than alcoholysis of Cp_2MoCl_2. Another reason Mo is softer than Ti, therefore Mo will have more affinity for slightly softer Cl than slightly harder O.

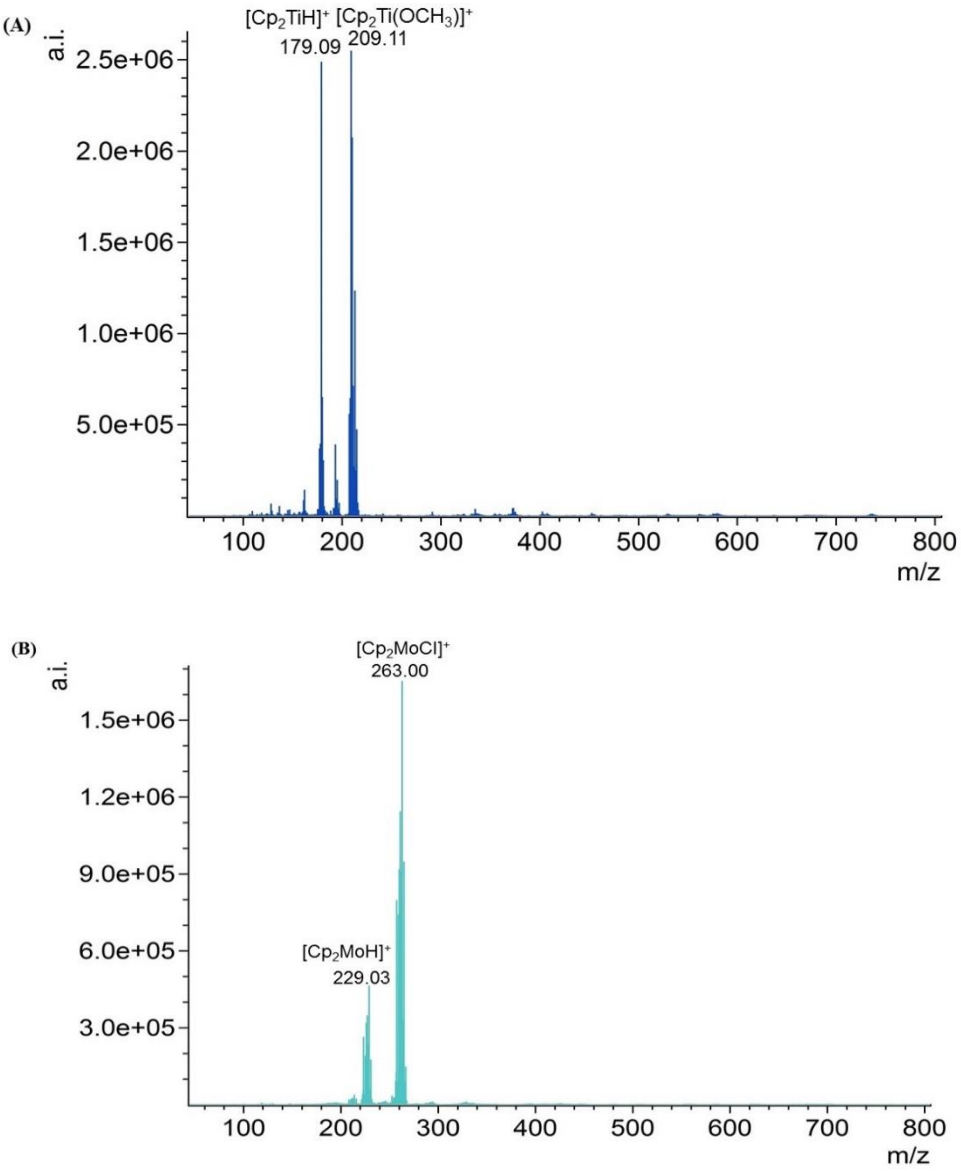

Figure 4.26: Positive-ion ESI mass spectra of a freshly-prepared solution of Cp_2TiCl_2 (A) and Cp_2MoCl_2 (B) in methanol with low range method at a capillary exit voltage of 150 V

As the capillary exit voltage increased to 150 V, both spectra just contain two main peaks and all the species at high *m/z* range disappeared (Figure 4.26). Their base peaks as for the low capillary exit voltage, at *m/z* 209.11 assigned as $Cp_2Ti(OCH_3)^+$ and at *m/z* 263.00 assigned as Cp_2MoCl^+. Also Cp_2TiH^+ ion is more significant at this voltage than Cp_2MoH^+ ion.

4.3.3.2 Comparison of Cp_2Ti(tsal) system with Cp_2Mo(tsal) system

The ^1H NMR and IR spectra of Cp_2Ti(tsal) have been reported in the literature [92,113]. ^1H NMR spectrum of Cp_2Ti(tsal) in $CDCl_3$ shows resonances in the range 7.22 ppm-8.42 ppm for protons on the benzene ring. Ten protons on the Cp rings were assigned at 6.48 ppm [92]. In Cp_2Mo(tsal) case, the chemical shift range is between 7.00 ppm and 7.90 ppm for the protons on the benzene ring and protons on the Cp rings were assigned at 5.48 ppm.

The IR spectrum of Cp_2Ti(tsal) showed absorption bands for Cp rings at 3050 cm^{-1} (C-H stretch), 1455 cm^{-1} (C-C stretch), 1015 cm^{-1} (C-H bending in plane) and 825 cm^{-1} (C-H bending out of plane). The strong carbonyl absorption band of the thiosalicylate ligand is observed at 1600 cm^{-1} [113]. All the corresponding absorption bands also observed for Cp_2Mo(tsal); a strong band at 1584 cm^{-1} is from the carbonyl group of the thiosalicylate ligand. The bands at 3107 cm^{-1} (C-H stretch), 1428 cm^{-1} (C-C stretch), 1035 cm^{-1} (C-H bending in plane) and 833 cm^{-1} (C-H bending out of plane) are attributed to Cp rings.

The positive-ion ESI-MS spectra for Cp_2Ti(tsal) and Cp_2Mo(tsal) in methanol solution using the low range method, recorded at a capillary exit voltage of 90 V are shown in Figure 4.27.

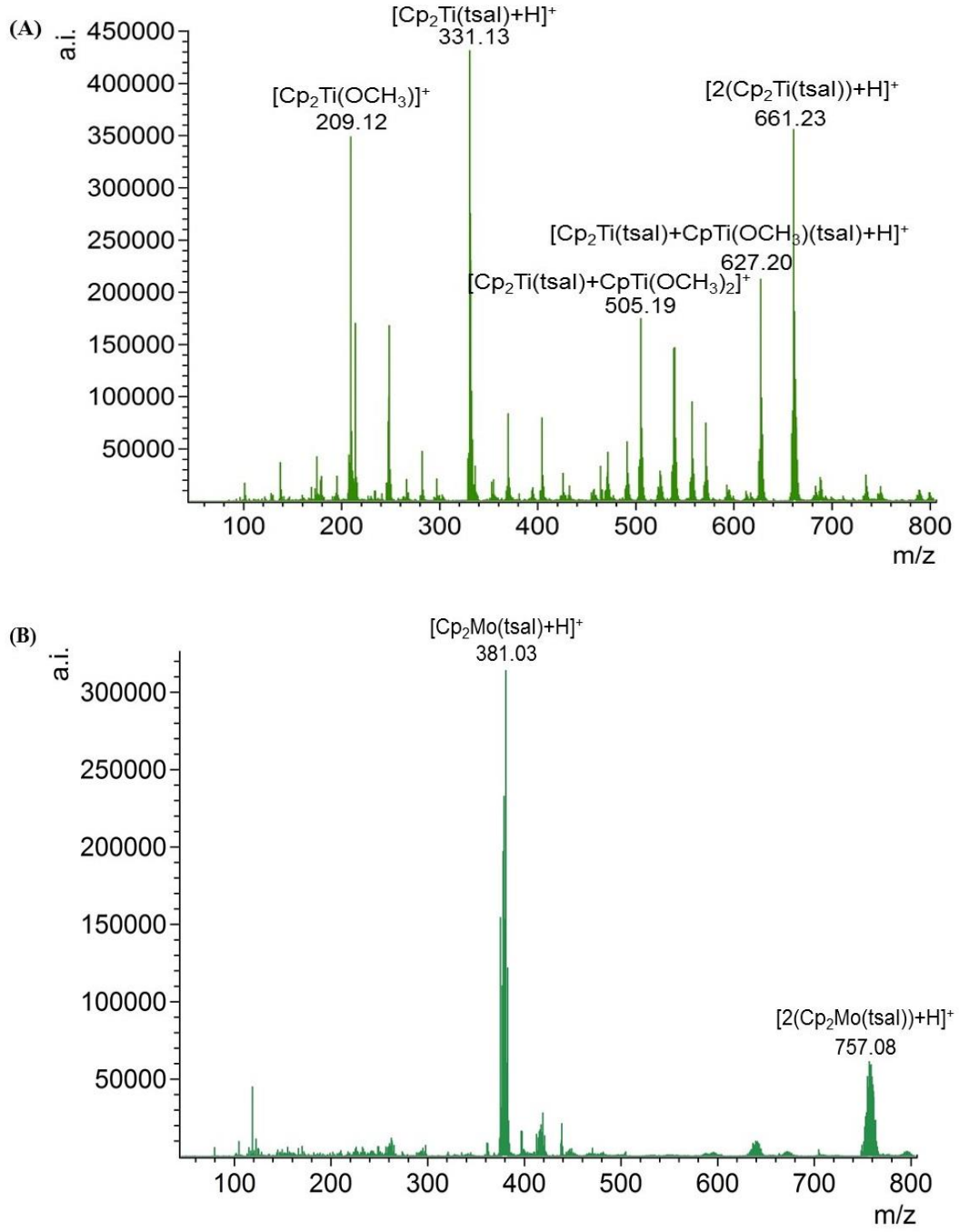

Figure 4.27: Positive-ion ESI mass spectra of a freshly-prepared solution of $Cp_2Ti(tsal)$ (A) and $Cp_2Mo(tsal)$ (B) in methanol with low range method at a capillary exit voltage of 90 V

The results show that $Cp_2Mo(tsal)$ ESI-MS spectrum much simpler than the ESI-MS spectrum of $Cp_2Ti(tsal)$ at capillary exit voltage of 90 V. A lot of species containing two Ti centres can be observed in the ESI mass spectrum of $Cp_2Ti(tsal)$, but in the ESI mass spectrum of $Cp_2Mo(tsal)$ only $[M+H]^+$ and $[2M+H]^+$ ions are observed, with $[M+H]^+$ ion as the base peak for both spectra.

The positive-ion ESI-MS spectra for $Cp_2Ti(tsal)$ and $Cp_2Mo(tsal)$ in methanol solution using the low range method, recorded at a capillary exit voltage of 150 V are shown in Figure 4.28.

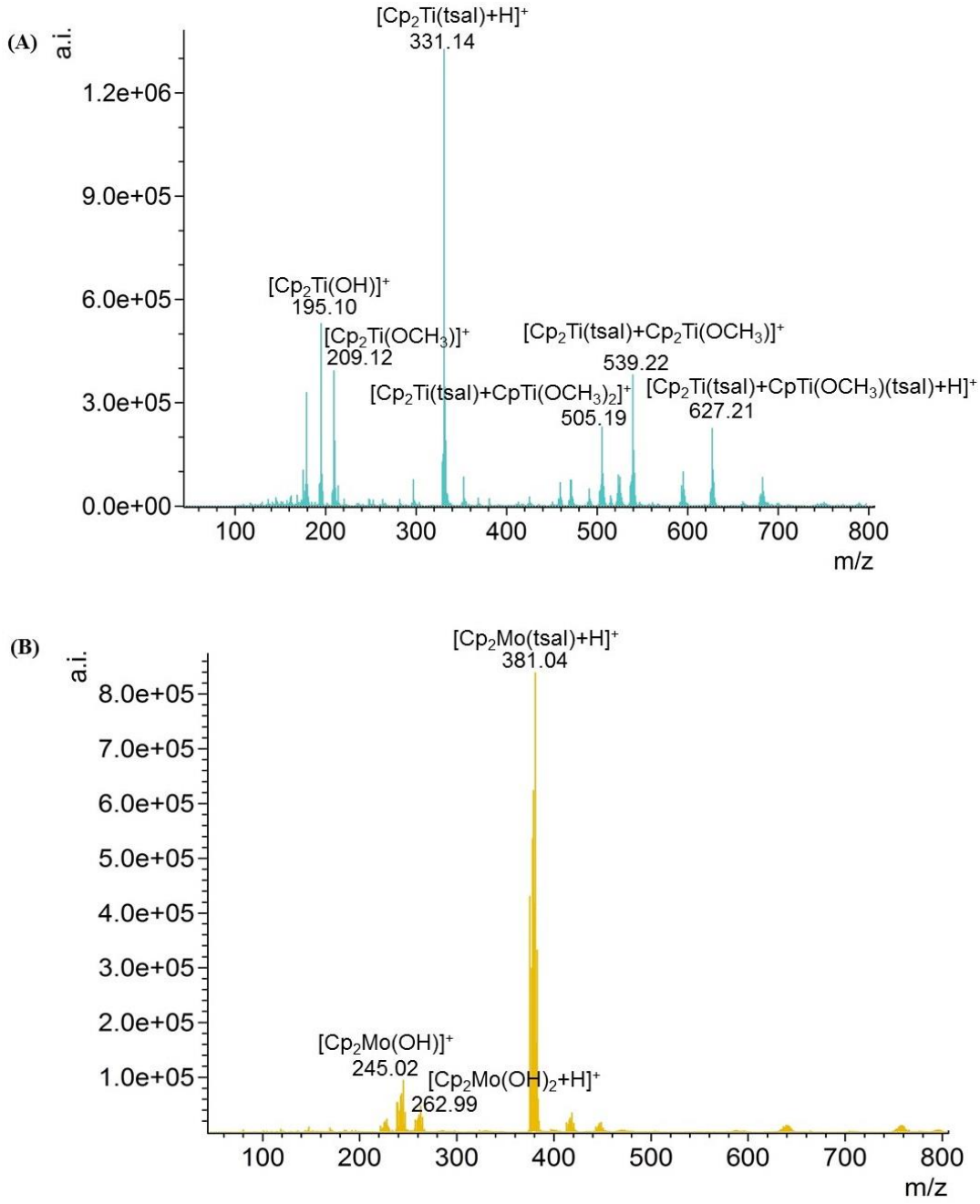

Figure 4.28: Positive-ion ESI mass spectra of a freshly-prepared solution of $Cp_2Ti(tsal)$ (A) and $Cp_2Mo(tsal)$ (B) in methanol with low range method at a capillary exit voltage of 150 V

As for the low capillary exit voltage, more species can be observed on the ESI-MS spectrum for $Cp_2Ti(tsal)$, the base peak is still the $[M+H]^+$ ion. The larger ion

$[2M+H]^+$ was absent from both spectra. The major species at low *m/z* range containing OH groups in both spectra indicated that rapid hydrolysis of the $Cp_2Ti(tsal)$ and $Cp_2Mo(tsal)$ occurred.

4.4 Discussion

During this research a new complex $Cp_2Mo(tsal)$ was synthesised by the reaction of Cp_2MoCl_2 with thiosalicylic acid and then recrystallised by the vapour diffusion method. This complex was characterised by ESI-MS, melting point, ^1H NMR and IR spectroscopy.

The positive-ion ESI-MS spectra for Cp_2MoCl_2 and $Cp_2Mo(tsal)$ in methanol, recorded at a range of capillary exit voltages, have identified some major species containing one or two Mo centres. Larger Mo clusters which contain three or more Mo centres were not observed using the wide range method.

In methanol at various capillary exit voltages, the ESI-MS spectra of Cp_2TiCl_2 were compared to those of Cp_2MoCl_2. This comparison showed that most species observed in Cp_2MoCl_2 ESI-MS spectra contained a Cl ligand. This results indicate that hydrolysis of the Cl ligands in Cp_2MoCl_2 is harder than that in the Cp_2TiCl_2 and the alcoholysis of the Cp_2TiCl_2 is easier than the alcoholysis of Cp_2MoCl_2. Reduction of molybdenum(IV) was not observed when increased capillary exit voltage.

A comparison of the ^1H NMR and IR spectra of $Cp_2Ti(tsal)$ and $Cp_2Mo(tsal)$ showed corresponding chemical shift and absorption bands. Comparing ESI-MS behaviour of those two complexes, the results show that the ESI-MS spectra of $Cp_2Mo(tsal)$ are much simpler than that of $Cp_2Ti(tsal)$. Using the same capillary exit voltage, more species can be observed in the ESI-MS spectra of $Cp_2Ti(tsal)$ which possibly means $Cp_2Ti(tsal)$ undergoes a range of reactions and formation of adducts compared with $Cp_2Mo(tsal)$ or $Cp_2Ti(tsal)$ is less pure.

Chapter 5

Conclusions and recommendations for further work

Some metallocene complexes of titanium and molybdenum were investigated by ESI-MS during this research. Mass spectra of these complexes were collected in positive-ion mode with a range of capillary exit voltages, and low range and wide range methods were used. In this research Ti and Mo systems were investigated. In the future, investigation of some other metallocene complexes like Cp_2ZrCl_2, Cp_2HfCl_2 and Cp_2VCl_2 can be done to more comparisons.

Various alcohols were used as solvents to investigate the ESI-MS behaviour of Cp_2TiCl_2 and $(EtCp)_2TiCl_2$. The results of Cp_2TiCl_2 in methanol showed some major species like Cp_2TiH^+, $[Cp_2Ti(OCH_3)]^+$, $[Cp_2Ti(OCH_3)_2+H]^+$ and $[(Cp_2Ti(OCH_3)_2+H^+)_2+Cl^-]^+$ containing one or two Ti centres. When the capillary exit voltage was greater than 150 V, these species containing two Ti centres like $[(Cp_2Ti(OCH_3)_2+H^+)_2+Cl^-]^+$, $[Cp_4Ti_2(OCH_3)_4H]^+$, $[Cp_4Ti_2(OCH_3)_2Cl]^+$, $[Cp_4Ti_2(OCH_3)_2(OH)]^+$ and $[Cp_4Ti_2(OCH_3)_2(OH)_2H]^+$ disappeared. Larger Ti clusters which contain three or more Ti centres were not observed. During ESI-MS analysis, reduction of titanium(IV) was observed when the capillary exit voltage was greater than 150 V. This was confirmed by the titanocene(III) species $[Cp_2Ti(CH_3OH)]^+$ observed.

In the positive-ion ESI-MS spectra of $Cp_2Ti(tsal)$, larger Ti clusters which contain two Ti centres like $[Cp_2Ti(tsal)+CpTi(OCH_3)_2]^+$, $[Cp_2Ti(tsal)+Cp_2Ti(OCH_3)]^+$ and $[2(Cp_2Ti(tsal))+Na]^+$ were observed using the wide range method. The new complex $(EtCp)_2Ti(tsal)$ was also synthesised and characterised by ESI-MS, elemental analysis, melting point, ^1H NMR and IR. The presence of starting material $(EtCp)_2TiCl_2$ was confirmed in the ^1H NMR and IR spectra. In the future, the synthesis of this complex would need to be repeated with less amount of starting material $(EtCp)_2TiCl_2$, which increases the molar ratio of thiosalicylic acid to $(EtCp)_2TiCl_2$, or by stirring the mixture longer to make sure a pure final product is obtained without the starting material. Some analogues of the major species in

$Cp_2Ti(tsal)$ mass spectra can also be observed in ESI mass spectra of $(EtCp)_2Ti(tsal)$.

$Cp_2Ti(tsal)Cp_2Ti(OH)^+$, $Cp_2Ti(tsal)Cp_2Ti(OCH_3)^+$ and $Cp_2Ti(tsal)Cp_2TiCl^+$ ions were observed during the investigation of the possibility of the tsal ligand bridging two Cp_2Ti centres. The expected species $[Cp_2Ti(PhHgSC_6H_4COO)]^+$ was also observed during the investigation of $Cp_2Ti(tsal)$'s behaviour towards the soft electrophile $PhHg^+$ from PhHgCl. $[Cp_2Ti(PhHgSC_6H_4COO)]^+$ ion should be a promising target for future synthesis investigations and subsequent characterisation by NMR and IR etc.

The formation of aggregate ions with alkali metal cations were observed when investigated of presence of added alkali metal salts to $Cp_2Ti(tsal)$. Large Cs cluster $[4(Cp_2Ti(tsal))+Cs]^+$ was not observed possibly because the Cs^+ ion has a low charge density.

The closely related compounds Cp_2MoCl_2 and $Cp_2Mo(tsal)$ were also characterised by ESI-MS. Comparing ESI-MS behaviour of Ti systems and that of Mo systems, the results showed that less species were observed in Mo spectra and most of them contained a Cl ligand. Reduction was not observed in the Mo system. In the Mo system, the new complex $Cp_2Mo(tsal)$ was synthesised. It is of future interest to determine the crystal structure of complex $Cp_2Mo(tsal)$. Biological testing of complex $Cp_2Mo(tsal)$ has not yet been carried out. Therefore, determination of $Cp_2Mo(tsal)$'s anticancer activity would be of interest in the future.

In this research, all the data were collected using positive ion ESI-MS mode, in the future negative ion ESI-MS mode can be used to investigate the reactivity of $Cp_2Ti(tsal)$ towards added fluoride ions to explore relative binding affinities of the Cp_2Ti centre for tsal versus F donor ligands.

Further investigation could investigate some ligands similar to thiosalicylate ligand and how they react with Cp_2TiCl_2. There are similarities between thiosulfate and thiosalicylate in that both are S/O chelating ligands. The reactivity of Cp_2TiCl_2 towards thiosulfate can be investigated in the future research.

References

[1] Köpf-Maier, P.; Köpf, H. Organometallic titanium, vanadium, niobium, molybdenum and rhenium complexes - Early transition metal antitumor drugs. In *Metal Compounds in Cancer Therapy*; S. P. Fricker, Ed.; Springer Dordrecht, Netherlands, 1995; pp 109-146.

[2] Gao, Z. W.; Hu, D. D.; Gao, L. X.; Zhang, X. l.; Zhang, Z. T.; Liang, Q. Q. Preparation of the substituted salicylato of titanocene derivatives by the liquid-liquid interfacial reaction. *J. Organomet. Chem.* **2001**, *629*, 47-53.

[3] Stamatatos, T. C.; Perlepes, S. P.; Manos, M. J.; Tasiopoulos, A. J.; Klouras, N. Unexpected formation, X-ray structure, and characterization of the triangular $[Ti_3O(OMe)_6(\eta^5\text{-}C_5H_5)_3](I_3)$ complex from hydrolysis and methanolysis of $[Ti(\eta^5\text{-}C_5H_5)_2I_2]$. *J. Coord. Chem.* **2011**, *64*, 2377-2387.

[4] Castro Rodríguez, M.; Rodríguez García, I.; Rodríguez Maecker, R. N.; Pozo Morales, L.; Oltra, J. E.; Rosales Martínez, A. Cp_2TiCl: An ideal reagent for green chemistry? *Org. Process Res. Dev.* **2017**, *21*, 911-923.

[5] Clearfield, A.; Warner, D. K.; Saldarriaga-Molina, C. H.; Ropal, R.; Bernal, I. Structural studies of $(\pi\text{-}C_5H_5)_2MX_2$ complexes and their derivatives. Structure of bis(π-cyclopentadienyl)titanium dichloride. *Can. J. Chem.* **1975**, *53*, 1622-1629.

[6] Valadares, M. C.; Klein, S. I.; Queiroz, M. L. S. Titanocene modulation of cytokine imbalance induced by Ehrlich ascites tumour progression. *Eur. J. Pharmacol.* **2004**, *503*, 203-208.

[7] O'Connor, K.; Gill, C.; Tacke, M.; Rehmann, F. J. K.; Strohfeldt, K.; Sweeney, N.; Fitzpatrick, J. M.; Watson, R. W. G. Novel titanocene anti-cancer drugs and their effect on apoptosis and the apoptotic pathway in prostate cancer cells. *Apoptosis* **2006**, *11*, 1205-1214.

[8] Bannon, J. H.; Fichtner, I.; O'Neill, A.; Pampillón, C.; Sweeney, N. J.; Strohfeldt, K.; Watson, R. W.; Tacke, M.; Mc Gee, M. M. Substituted titanocenes induce caspase-dependent apoptosis in human epidermoid carcinoma cells in vitro and exhibit antitumour activity in vivo. *Br. J. Cancer* **2007**, *97*, 1234-1241.

[9] Chimento, A.; Saturnino, C.; Iacopetta, D.; Mazzotta, R.; Caruso, A.; Plutino, M. R.; Mariconda, A.; Ramunno, A.; Sinicropi, M. S.; Pezzi, V.; Longo, P. Inhibition of human topoisomerase I and II and anti-proliferative effects on MCF-7 cells by new titanocene complexes. *Bioorg. Med. Chem.* **2015**, *23*, 7302-7312.

[10] Köpf-Maier, P.; Köpf, H. Non-platinum group metal antitumor agents. History, current status, and perspectives. *Chem. Rev.* **1987**, *87*, 1137-1152.

[11] Tinoco, A. D.; Thomas, H. R.; Incarvito, C. D.; Saghatelian, A.; Valentine, A. M. Cytotoxicity of a Ti(IV) compound is independent of serum proteins.

Proc. Natl. Acad. Sci. U. S. A. **2012**, *109*, 5016-5021, S5016/5011-S5016/5016.

[12] Tiekink, E. R. T.; Henderson, W. Coordination chemistry of 3- and 4-mercaptobenzoate ligands: Versatile hydrogen-bonding isomers of the thiosalicylate (2-mercaptobenzoate) ligand. *Coord. Chem. Rev.* **2017**, *341*, 19-52.

[13] Wehr-Candler, T.; Henderson, W. Coordination chemistry of the thiosalicylate ligand. *Coord. Chem. Rev.* **2016**, *313*, 111-155.

[14] Duran, N.; Clegg, W.; Cucurull-Sánchez, L.; Coxall, R. A.; Jiménez, H. R.; Moratal, J. M.; Lloret, F.; González-Duarte, P. Unprecedented stabilization of cobalt(II) in a tetrahedral S_2O_2 environment: The use of a redox-noninnocent ligand. *Inorganic Chemistry* **2000**, *39*, 4821-4832.

[15] Srinivasan, B. R.; Sawant, J. V.; Sawant, S. C.; Raghavaiah, P. *catena*-Poly[[(pentaaqua)(4-nitrobenzoato-O,O')barium(II)] (μ-4-nitrobenzoato-O,O')]: A barium(II) coordination polymer showing O-H...O and C-H...O interactions. *Journal of Chemical Sciences* **2007**, *119*, 593-601.

[16] Hasan, M.; Sankhla, B.; Kapoor, R. Thiosalicylates of aluminium, titanium, and zirconium. *Australian Journal of Chemistry* **1968**, *21*, 1651-1652.

[17] Tóth, I.; Brücher, E.; Zékány, L. Equilibrium studies of the systems of aluminum(III), gallium(III), and indium(III) mercaptoacetate, 3-mercaptopropionate and 2-mercaptobenzoate. *Magy. Kem. Foly.* **1984**, *90*, 149-154.

[18] Hughes, M. N.; Man, W.-K. Thallium(I) derivatives of some aminoacids and other acidic ligands. Studies in solution and the solid state. *Inorganica Chimica Acta* **1976**, *20*, 237-242.

[19] Ramakrishna, R. S.; Fernandopulle, M. E. Complexes of thallium(I) and thallium(III) with thiosalicylic acid (o-mercaptobenzoic acid) and salicylic acid. *Journal of Inorganic and Nuclear Chemistry* **1971**, *33*, 1940-1942.

[20] Cragg, R. H.; Lane, R. D. Contributions to group IV organometallic chemistry: IV. Preparation and properties of some organosilicon derivatives of salicylic and related acids. *Journal of Organometallic Chemistry* **1981**, *212*, 301-310.

[21] Kita, Y.; Yasuda, H.; Sugiyama, Y.; Fukata, F.; Haruta, J.-i.; Tamura, Y. O-silylated ketene acetal chemistry: divinyloxysilane derivatives as novel and useful bifunctional protecting agents for proton-acidic materials. *Tetrahedron Letters* **1983**, *24*, 1273-1276.

[22] Mazières, S.; Lavayssière, H.; Dousse, G.; Satgé, J. Physical-chemical studies and reactivity of new divalent germanium species. *Inorganica Chimica Acta* **1996**, *252*, 25-32.

[23] Knighton, R.; Song, X.; Pike, R.; de Dios, A. C.; Casabianca, L.; Eng, G. Synthesis and structural determination of two triphenyltin thiosalicylates. *Journal of Coordination Chemistry* **2009**, *62*, 3110-3116.

[24] Xanthopoulou, M. N.; Kourkoumelis, N.; Hadjikakou, S. K.; Hadjiliadis, N.; Kubicki, M.; Karkabounas, S.; Bakas, T. Structural and biological studies of organotin(IV) derivatives with 2-mercapto-benzoic acid and 2-mercapto-4-methyl-pyrimidine. *Polyhedron* **2008**, *27*, 3318-3324.

[25] Al-Niaimi, N. S.; Al-Saadi, B. M. Thiosalicylic acid complexes of divalent zinc, cadmium, mercury and lead. *Journal of Inorganic and Nuclear Chemistry* **1974**, *36*, 1617-1622.

[26] Cohen, A.; King, H.; Strangeways, W. I. Trypanocidal action and chemical constitution. Part X. Arylthioarsinites. *Journal of the Chemical Society* **1931**, 3043-3057.

[27] Sagatys, D. S.; Smith, G.; Bott, R. C.; Healy, P. C. The preparation and crystal structure of ammonium bismuth(III) thiosalicylate dihydrate. *Australian Journal of Chemistry* **2003**, *56*, 941-943.

[28] Saito, Y.; Chikuma, M.; Iwado, A.; Saito, Y. Isolation and characterization of thiosalicylic acid selenotrisulfide. *Fresenius' Journal of Analytical Chemistry* **1994**, *348*, 776-777.

[29] Gardner, S. A. Mercapto acid compounds of tellurium(II): stabilization of tellurium sulfur bonded compounds via intramolecular chelation. *Journal of Organometallic Chemistry* **1980**, *190*, 363-369.

[30] Sen, D. N.; Kantak, U. N. Cyclopentadienyltitanium. IV. chelates. *J. Indian Chem. Soc.* **1969**, *46*, 358-362.

[31] Ramakrishna, R. S.; Fernandopulle, M. E.; Nalliah, B. Spectrophotometric and electrometric studies on the composition and stability of the vanadyl complex of o-mercaptobenzoic acid (thiosalicylic acid). *Journal of Inorganic and Nuclear Chemistry* **1971**, *33*, 2071-2075.

[32] Karet, G. B.; Castro, S. L.; Folting, K.; Bollinger, J. C.; Heintz, R. A.; Christou, G. Dinuclear, trinuclear and mixed-metal hexanuclear aggregates of vanadium: crystal structures and properties of $[NEt_4]_3[V_2Cl_9]$, $[PPh_4]_2[V_3OCl_4(O_2CC_6H_4SH)_5]$ and $[NEt_4]_4[V_2Li_4O_2Cl_4(O_2CC_6H_4S)_4]$. *J. Chem. Soc., Dalton Trans.* **1998**, 67-72.

[33] Weschler, C. J.; Deutsch, E. Thiolato sulfur as an electron-transfer bridge. Chromium(II)-catalyzed aquation of thiolatobis(ethylenediamine)chromium(III) complexes in aqueous perchloric acid media. *Inorg. Chem.* **1976**, *15*, 139-145.

[34] Li-Kao, J.; González, O.; Baggio, R. F.; Garland, M. T.; Carrillo, D. Bis(triethylammonium) bis(2-mercaptobenzoato-O,S)dioxomolybdate(VI). *Acta Crystallogr., Sect. C: Cryst. Struct. Commun.* **1995**, *C51*, 575-578.

[35] Li-Kao, J.; González, O.; Mariezcurrena, R.; Baggio, R.; Garland, M. T.; Carrillo, D. A cis-oxo[diphenylhydrazido(2-)]molybdenum complex: $(Et_3NH)_2[MoO(NNPh_2)(SC_6H_4CO_2)_2]$. *Acta Crystallogr., Sect. C: Cryst. Struct. Commun.* **1995**, *C51*, 2486-2489.

[36] Majumdar, A.; Pal, K.; Sarkar, S. Necessity of fine tuning in Mo(IV) bis(dithiolene) complexes to warrant nitrate reduction. *Dalton Trans.* **2009**, 1927-1938.

[37] Hegetschweiler, K.; Keller, T.; Amrein, W.; Schneider, W. Identification and characterization of trinuclear molybdenum-sulfur clusters by fast atom bombardment (FAB) mass spectrometry. *Inorg. Chem.* **1991**, *30*, 873-876.

[38] Bodini, M. E.; Del Valle, M. A. Redox chemistry and spectroscopy of 2-mercaptobenzoic acid and its manganese(II) and (III) complexes in dimethylsulphoxide. *Polyhedron* **1990**, *9*, 1181-1186.

[39] Depree, C. V.; Main, L.; Nicholson, B. K.; Roberts, K. Preparation and structures of tetrameric and dimeric manganese carbonyl complexes incorporating thiosalicylato ligands. *Journal of Organometallic Chemistry* **1996**, *517*, 201-207.

[40] Bolzati, C.; Boschi, A.; Duatti, A.; Prakash, S.; Uccelli, L.; Refosco, F.; Tisato, F.; Bandoli, G. Geometrically controlled selective formation of nitrido technetium(V) asymmetrical heterocomplexes with bidentate ligands. *Journal of the American Chemical Society* **2000**, *122*, 4510-4511.

[41] Jiang, C.; Hor, T. S. A.; Yan, Y. K.; Henderson, W.; McCaffrey, L. J. Ligand exchange reactions of $[Re_2(\mu\text{-}OR)_3(CO)_6]^-$ (R = H, Me) with sulfur, selenium, phosphorus and nitrogen donor ligands, investigated by electrospray mass spectrometry. *Dalton* **2000**, 3204-3211.

[42] Sokolov, M.; Fyodorova, N.; Pervukhina, N.; Fedorov, V. Re(V) thiosalicylate complexes. Crystal structure of $(Ph_4As)[ReO(SC_6H_4CO_2)_2py]\cdot H_2O$. *Inorganic Chemistry Communications* **2001**, *4*, 261-263.

[43] Hieber, W.; Kaiser, K. Über Metall-Stickoxid-Komplexe, XXIII. Über das Verhalten zweizähliger schwefel- und stickstoffhaltiger Liganden gegenüber Dinitrosyleisenbromid. *Zeitschrift für anorganische und allgemeine Chemie* **1968**, *358*, 271-281.

[44] Tsai, M.-L.; Hsieh, C.-H.; Liaw, W.-F. Dinitrosyl iron complexes (DNICs) containing S/N/O ligation: Transformation of Roussin's red ester into the neutral $\{Fe(NO)_2\}^{10}$ DNICs. *Inorg. Chem.* **2007**, *46*, 5110-5117.

[45] Saouma, C. T.; Kaminsky, W.; Mayer, J. M. Decomposition of a mixed-valence [2Fe-2S] cluster gives linear tetra-ferric and ferrous clusters. *Polyhedron* **2013**, *58*, 60-64.

[46] Chan, S. L.-F.; Sun, R. W.-Y.; Choi, M.-Y.; Zeng, Y.; Shek, L.; Chui, S. S.-Y.; Che, C.-M. An anti-cancer trinuclear ruthenium(III) complex with 2-

thiosalicylate ligands attenuates Wnt-β-catenin signaling. *Chem. Sci.* **2011**, *2*, 1788-1792.

[47] Chan, S. L.-F.; Gao, S.; Chui, S. S.-Y.; Shek, L.; Huang, J.-S.; Che, C.-M. Supramolecular self-assembly of 1D and 3D heterometallic coordination polymers with triruthenium building blocks. *Chemistry - A European Journal* **2012**, *18*, 11228-11237, S11228/11221-S11228/11216.

[48] Ainscough, E. W.; Brodie, A. M.; Coll, R. K.; Mair, A. J. A.; Waters, J. M. Linked triosmium cluster complexes containing thiolato-carboxylato ligands: The crystal and molecular structures of $[\{Os_3H(CO)_{10}\}_2(\mu\text{-}SC_6H_4CO_2)]$ and $[\{Os_3H(CO)_{10}\}_2(\mu\text{-}SCH_2CH_2CO_2)]$. *journal of Organometallic Chemistry* **1996**, *509*, 259-264.

[49] Cave, D.; Gascon, J.-M.; Bond, A. D.; Teat, S. J.; Wood, P. T. Layered metal organosulfides: hydrothermal synthesis, structure and magnetic behaviour of the spin-canted magnet $Co(1,2\text{-}(O_2C)(S)C_6H_4)$. *chemical Communications (Cambridge, United Kingdom)* **2002**, 1050-1051.

[50] Henderson, W.; Nicholson, B. K.; Oliver, A. G.; Rickard, C. E. F. Dimeric rhodium(III), iridium(III) and ruthenium(II) thiosalicylate complexes. *J. Organomet. Chem.* **2001**, *625*, 40-46.

[51] McCaffrey, L. J.; Henderson, W.; Nicholson, B. K.; Mackay, J. E.; Dinger, M. B. Platinum(II), palladium(II), and nickel(II) thiosalicylate complexes. *J. Chem. Soc., Dalton Trans.* **1997**, 2577-2586.

[52] Kumar, L.; Puthraya, K. H.; Srivastava, T. S. Neutral mixed-ligand complexes of 2,2'-bipyridinedichloroplatinum(II) with dianionic aromatic chelating ligands as potential photosensitizers. *Inorg. Chim. Acta* **1984**, *86*, 173-178.

[53] Henderson, W.; McCaffrey, L. J.; Nicholson, B. K. Synthesis and biological activity of platinum(II) and palladium(II) thiosalicylate complexes with mixed ancillary donor ligands. *Dalton* **2000**, 2753-2760.

[54] Al Radadi, N. S.; Al Ashqar, S. M. A.; Mostafa, M. M. Synthesis and Characterization of Some New Binary and Ternary Cu(II) Complexes. *Synthesis and Reactivity in Inorganic and Metal-Organic Chemistry* **2011**, *41*, 203-210.

[55] Bott, R. C.; Healy, P. C.; Sagatys, D. S. Electrochemical synthesis and structural characterization of the trinuclear copper(I)-copper(II) complex: bis[bis(triphenylphosphine)copper(I)] [bis(thiosalicylate)copper(II)]. *Chemical Communications (Cambridge, United Kingdom)* **1998**, 2403-2404.

[56] Nomiya, K.; Kasuga, N. C.; Takamori, I.; Tsuda, K. Synthesis, characterization and X-ray crystal structure of $[Ag(Htsa)(PPh_3)_3]$ (H_2tsa=o-$HS(C_6H_4)CO_2H$). Comparison with $[Au(Htsa)(PPh_3)]$. *Polyhedron* **1998**, *17*, 3519-3530.

[57] Sun, D.; Yan, Z.-H. A novel one-dimensional silver cylinder stabilized by mixed 2-mercaptobenzoic acid and ethylenediamine ligands. *Acta Crystallogr., Sect. C: Cryst. Struct. Commun.* **2012**, *68*, m229-m232.

[58] Bult, A.; Bajema, B. L.; Klasen, H. B.; Metting, H. J.; Fox, C. L., Jr. Remarks on the structure-activity relationship of some antibacterial silver nonsulfanilamide compounds. *Pharm. Weekbl., Sci. Ed.* **1981**, *3*, 79-81.

[59] Nomiya, K.; Yamamoto, S.; Noguchi, R.; Yokoyama, H.; Kasuga, N. C.; Ohyama, K.; Kato, C. Ligand-exchangeability of 2-coordinate phosphinegold(I) complexes with AuSP and AuNP cores showing selective antimicrobial activities against Gram-positive bacteria. Crystal structures of [Au(2-Hmpa)(PPh_3)] and [Au(6-Hmna)(PPh_3)] (2-H_2mpa = 2-mercaptopropionic acid, 6-H_2mna = 6-mercaptonicotinic acid). *J. Inorg. Biochem.* **2003**, *95*, 208-220.

[60] Domínguez, C.; Heinrich, B.; Donnio, B.; Coco, S.; Espinet, P. Room-temperature columnar mesophases in triazine-gold thiolate metal-organic supramolecular aggregates. *Chem. - Eur. J.* **2013**, *19*, 5988-5995.

[61] Henderson, W. The chemistry of cyclometallated gold(III) complexes with C,N-donor ligands. In *Advances in Organometallic Chemistry*; R. West and A. F. Hill, Eds.; Academic Press, 2006; pp 207-265.

[62] Parish, R. V. Biologically-active gold(III) complexes. *Met.-Based Drugs* **1999**, *6*, 271-276.

[63] Kilpin, K. J.; Henderson, W.; Nicholson, B. K. Cycloaurated triphenylphosphine-sulfide and -selenide. *Dalton Trans.* **2010**, *39*, 1855-1864.

[64] Zhu, Y.; Cameron, B. R.; Mosi, R.; Anastassov, V.; Cox, J.; Qin, L.; Santucci, Z.; Metz, M.; Skerlj, R. T.; Fricker, S. P. Inhibition of the cathepsin cysteine proteases B and K by square-planar cycloaurated gold(III) compounds and investigation of their anti-cancer activity. *J. Inorg. Biochem.* **2011**, *105*, 754-762.

[65] Humphrey, S. M.; Mole, R. A.; Rawson, J. M.; Wood, P. T. Hydrothermal synthesis and magnetic properties of novel Mn(II) and Zn(II) materials with thiolato-carboxylate donor ligand frameworks. *Dalton Trans.* **2004**, 1670-1678.

[66] Jacobsen, F. E.; Cohen, S. M. Using model complexes to augment and advance metalloproteinase inhibitor design. *Inorg. Chem.* **2004**, *43*, 3038-3047.

[67] Ge, S.-Z.; Liu, Q.; Deng, S.; Sun, Y.-Q.; Chen, Y.-P. Two new luminescent cadmium thiolato-carboxylates with 2,2'-bipyridine. *J. Inorg. Organomet. Polym. Mater.* **2013**, *23*, 571-578.

[68] Waldo, J. H. Some new water-soluble organomercury compounds. *J. Am. Chem. Soc.* **1931**, *53*, 992-996.

[69] Wilm, M. Principles of electrospray ionization. *Mol. Cell. Proteomics* **2011**, *10*, doi: M111.009407.

[70] Banerjee, S.; Mazumdar, S. Electrospray Ionization mass spectrometry: a technique to access the information beyond the molecular weight of the analyte. *Int. J. Anal. Chem.* **2012**, Article no. 282574.

[71] Ho, C. S.; Lam, C. W. K.; Chan, M. H. M.; Cheung, R. C. K.; Law, L. K.; Lit, L. C. W.; Ng, K. F.; Suen, M. W. M.; Tai, H. L. Electrospray ionisation mass spectrometry: principles and clinical applications. *Clin Biochem Rev* **2003**, *24*, 3-12.

[72] Henderson, W.; McIndoe, J. S. *Mass Spectrometry of Inorganic and Organometallic Compounds*; Wiley: Chichester, England, 2005.

[73] Arakawa, R. Application of mass spectrometry to coordination chemistry. *J. Mass Spectrom. Soc. Jpn.* **2008**, *56*, 247-262.

[74] Henderson, W.; Nicholson, B. K.; McCaffrey, L. J. Applications of electrospray mass spectrometry in organometallic chemistry. *Polyhedron* **1998**, *17*, 4291-4313.

[75] Di Marco, V. B.; Bombi, G. G. Electrospray mass spectrometry (ESI-MS) in the study of metal-ligand solution equilibria. *Mass Spectrom. Rev.* **2006**, *25*, 347-379.

[76] Schalley, C. A.; Castellano, R. K.; Brody, M. S.; Rudkevich, D. M.; Siuzdak, G.; Rebek, J., Jr. Investigating molecular recognition by mass spectrometry: Characterization of calixarene-based self-assembling capsule hosts with charged guests. *J. Am. Chem. Soc.* **1999**, *121*, 4568-4579.

[77] Colton, R.; Traeger, J. C. The application of electrospray mass spectrometry to ionic inorganic and organometallic systems. *Inorganica Chimica Acta* **1992**, *201*, 153-155.

[78] Henderson, W.; Oliver, A. G.; Downard, A. J. Synthesis and X-ray structure of diphenyl ferrocenylmethylphosphonate, $FeCH_2P(O)(OPh)_2$, and a study of some ferrocenylmethyl compounds by electrospray mass spectrometry. *Polyhedron* **1996**, *15*, 1165-1173.

[79] Goodwin, N. J.; Henderson, W.; Nicholson, B. K.; Sarfo, J. K.; Fawcett, J.; Russell, D. R. Synthesis and reactivity of the ferrocene-derived phosphine $[Fe(\eta\text{-}C_5H_5)\{\eta\text{-}C_5H_4CH_2P(CH_2OH)_2\}]$. *J. Chem. Soc., Dalton Trans.* **1997**, 4377-4384.

[80] Goodwin, N. J.; Henderson, W.; Nicholson, B. K. An air-stable, primary alkylphosphine: $FcCH_2PH_2$ [Fc = $(\eta^5\text{-}C_5H_5)Fe(\eta^5\text{-}C_5H_4)$]. *chemical Communications (Cambridge, United Kingdom)* **1997**, 31-32.

[81] Xu, X.; Nolan, S. P.; Cole, R. B. Electrochemical oxidation and nucleophilic addition reactions of metallocenes in electrospray mass spectrometry. *Analytical Chemistry* **1994**, *66*, 119-125.

[82] Waern, J. B.; Harding, M. M. Coordination chemistry of the antitumor metallocene molybdocene dichloride with biological ligands. *Inorg. Chem.* **2004**, *43*, 206-213.

[83] Collins, S.; Linnolahti, M.; Zamora, M. G.; Zijlstra, H. S.; Rodríguez Hernández, M. T.; Perez-Camacho, O. Activation of Cp_2ZrX_2 (X = Me, Cl) by methylaluminoxane as studied by electrospray ionization mass spectrometry: relationship to polymerization catalysis. *macromolecules (Washington, DC, United States)* **2017**, *50*, 8871-8884.

[84] Ryumae, I.; Tanaka, M. Identification of titanium species in solutions and characterization of oxidation behavior using ESI-MS. *Bunseki Kagaku* **2014**, *63*, 581-592.

[85] Ravera, M.; Cassino, C.; Monti, E.; Gariboldi, M.; Osella, D. Enhancement of the cytotoxicity of titanocene dichloride by aging in organic co-solvent. *J. Inorg. Biochem.* **2005**, *99*, 2264-2269.

[86] Bond, A. M.; Colton, R.; Englert, U.; Hüegel, H.; Marken, F. Characterization of titanocene(III) complexes of β-diketonates by electrochemical, spectroscopic and crystallographic methods: stabilization of oxidized and reduced β-diketonate radicals by acetyl and titanocene derivatization, respectively. *Inorg. Chim. Acta* **1995**, *235*, 117-126.

[87] Simonsen, M. E.; Søgaard, E. G. Identification of Ti clusters during nucleation and growth of sol-gel-derived TiO_2 nanoparticles. *Eur. J. Mass Spectrom.* **2013**, *19*, 265-273.

[88] Berkessel, A.; Brandenburg, M.; Schäfer, M. Mass-spectrometric and kinetic studies on the mechanism and degradation pathways of titanium salalen catalysts for asymmetric epoxidation with aqueous hydrogen peroxide. *Adv. Synth. Catal.* **2008**, *350*, 1287-1294.

[89] Løver, T.; Henderson, W.; Bowmaker, G. A.; Seakins, J. M.; Cooney, R. P. Electroscopy mass spectrometry of highly moisture-sensitive metal alkoxides. *J. Mater. Chem.* **1997**, *7*, 1553-1558.

[90] Kemmitt, T.; Al-Salim, N. I.; Gainsford, G. J.; Henderson, W. Titanium amino alcohol complexes from: α-titanic acid: x-ray crystal structure of titanium bis[2,2'-(methylimino)diethanolate]. *Aust. J. Chem.* **1999**, *52*, 915-919.

[91] Eberle, R. P.; Schürch, S. Titanocene binding to oligonucleotides. *J. Inorg. Biochem.* **2018**, *184*, 1-7.

[92] Li, J.; Gao, Z.; Zhang, C.; Gao, L. Synthesis and structural characterization of substituted salicylate titanocene complexes: Three supramolecular frameworks determined by weak interactions. *J. Chem. Crystallogr.* **2009**, *39*, 623-631.

[93] Guo, M.; Guo, Z.; Sadler, P. J. Titanium(IV) targets phosphoesters on nucleotides: implications for the mechanism of action of the anticancer drug titanocene dichloride. *JBIC, J. Biol. Inorg. Chem.* **2001**, *6*, 698-707.

[94] Potter, G. D. A novel series of titanocene dichloride derivatives: Synthesis, characterization and assessment of their cytotoxic properties. PhD Thesis, Queen's University, Kingston, Ontario, Canada, 2008.

[95] Abeysinghe, P. M.; Harding, M. M. Antitumour bis(cyclopentadienyl) metal complexes: titanocene and molybdocene dichloride and derivatives. *Dalton Transactions* **2007**, 3474-3482.

[96] Wu, Y.; Wang, X.; Luo, Y.; Wang, J.; Jian, Y.; Sun, H.; Zhang, G.; Zhang, W.; Gao, Z. Solvent strategy for unleashing the Lewis acidity of titanocene dichloride for rapid Mannich reactions. *RSC Adv.* **2016**, *6*, 15298-15303.

[97] Tang, S.-Y.; Rijs, N. J.; Li, J.; Schlangen, M.; Schwarz, H. Ligand-controlled CO_2 activation mediated by cationic titanium hydride complexes, $[LTiH]^+$ (L=Cp_2, O). *Chem. - Eur. J.* **2015**, *21*, 8483-8490.

[98] Luo, Y.; Wu, Y.; Wang, Y.; Sun, H.; Xie, Z.; Zhang, W.; Gao, Z. Ethanol promoted titanocene Lewis acid catalyzed synthesis of quinazoline derivatives. *RSC Adv.* **2016**, *6*, 66074-66077.

[99] Strohalm, M.; Hassman, M.; Kosata, B.; Kodicek, M. mMass data miner: an open source alternative for mass spectrometric data analysis. *Rapid Commun Mass Spectrom* **2008**, *22*, 905-908.

[100] Elschenbroich, C. *Organometallics*; Weinheim, 2006.

[101] Morcillo, S. P.; Miguel, D.; Campana, A. G.; Alvarez de Cienfuegos, L.; Justicia, J.; Cuerva, J. M. Recent applications of Cp_2TiCl in natural product synthesis. *Org. Chem. Front.* **2014**, *1*, 15-33.

[102] Stewart, I. I.; Horlick, G. Electrospray mass spectra of lanthanides. *Anal. Chem.* **1994**, *66*, 3983-3993.

[103] Mountford, P. Reactions of $[Cp_2Ti(N^tBu)(py)]$ with S-H bonds and synthesis of $[Cp_2Ti(\mu\text{-}S)_2TiCp_2]$. *J. Organomet. Chem.* **1997**, *528*, 15-18.

[104] Nadasdi, T. T.; Stephan, D. W. Bimetallic titanium alkoxides: synthesis and structure of $Cp_2Ti(Ph)(\mu\text{-}OCH_2C(CH_3)_2CH_2O)(Ph)TiCp_2$; a precursor to macrocyclic metallocene derivatives. *Can. J. Chem.* **1991**, *69*, 167-171.

[105] Honold, B.; Thewalt, U.; Herberhold, M.; Alt, H. G.; Kool, L. B.; Rausch, M. D. Zweikernige dicyclopentadienyltitan-komplexe mit sauerstoff-brücke. die struktur von $[Cp_2Ti]_2(\mu\text{-}O)$. *Journal of Organometallic Chemistry* **1986**, *314*, 105-111.

[106] Yu, H.; Jia, G.; Lin, Z. O-Abstraction reactions of nitrous oxide with $Cp_2Ti(II)$ and other middle transition metal complexes. *Organometallics* **2009**, *28*, 1158-1164.

[107] Fouad, E. A.; Feng, X. Use of pervaporation to separate butanol from dilute aqueous solutions: effects of operating conditions and concentration polarization. *J. Membr. Sci.* **2008**, *323*, 428-435.

[108] Duke, R.; Cassady, C. J. Electron transfer dissociation and collision-induced dissociation mass spectrometry of trivalent metal adducted oligosaccharides. Presented at 255th ACS National Meeting & Exposition, New Orleans, LA, United States, March 18-22, 2018.

[109] Thewalt, U.; Berhalter, K.; Neuse, E. W. The crystal and molecular structure of acetonitrilechlorodicyclopentadienyltitanium tetrachloroferrate(III). Some Moessbauer and x-ray photoelectron spectroscopic data. *Transition Met. Chem. (Weinheim, Ger.)* **1985**, *10*, 393-395.

[110] Seewald, P. A.; White, G. S.; Stephan, D. W. Cationic complexes of titanium(III); phosphine substitution reactions. *Can. J. Chem.* **1988**, *66*, 1147-1152.

[111] Borkowsky, S. L.; Baenziger, N. C.; Jordan, R. F. Generation and reactivity of titanocene benzyl $Cp_2Ti(CH_2Ph)(L)^+$ complexes. Oxidation and protonolysis chemistry of $Cp_2Ti(CH_2Ph)_2$. *Organometallics* **1993**, *12*, 486-495.

[112] Hanna, T. E.; Lobkovsky, E.; Chirik, P. J. Dihydrogen and Silane Addition to Base-Free, Monomeric Bis(cyclopentadienyl)titanium Oxides. *Inorg. Chem.* **2007**, *46*, 2359-2361.

[113] Sen, D. N.; Kantak, U. N. *Proceedings of the chemistry symposium, 1969: Chandigarh, September 23-26, 1969*; Symposium Organising Sub-committee, Dept. of Atomic Energy, Govt. of India: Delhi, 1969.

[114] Burlakov, V. V.; Arndt, P.; Baumann, W.; Spannenberg, A.; Rosenthal, U.; Letov, A. V.; Lyssenko, K. A.; Korlyukov, A. A.; Strunkina, L. I.; Minacheva, M. K.; Shur, V. B. Synthesis and X-ray crystal structure determination of new zwitterionic complexes of titanocene. *Organometallics* **2001**, *20*, 4072-4079.

[115] Bakač, A.; Orhanovič, M. The kinetics and mechanism of the oxidation of titanium(III) by thiocyanatopentaamminecobalt(III) and azidopentaamminecobalt(III) ions. *Inorganica Chimica Acta* **1977**, *21*, 173-178.

[116] Monti, B.; Santi, C.; Bagnoli, L.; Marini, F.; Sancineto, L. Zinc chalcogenolates as green reagents. *Curr. Green Chem.* **2016**, *3*, 68-75.

[117] Umebayashi, T.; Yamaki, T.; Tanaka, S.; Asai, K. Visible light-induced degradation of methylene blue on S-doped TiO_2. *Chem. Lett.* **2003**, *32*, 330-331.

[118] Fish, R. W.; Rosenblum, M. A convenient synthesis of some haloferrocenes. *J. Organomet. Chem.* **1965**, *30*, 1253-1254.

[119] Dang, Y.; Zhang, Y.; Shi, S. Bis-substituted benzoato complexes of bis(cyclopentadienyl)titanium(IV). *Synth. React. Inorg. Met.-Org. Chem.* **1987**, *17*, 347-360.

[120] Reid, A. F.; Scaife, D. E.; Wailes, P. C. The characterization of solid cyclopentadienyl metal compounds by their near-infrared reflection spectra. *Spectrochim. Acta* **1964**, *20*, 1257-1268.

[121] Djebara, M.; Stoquert, J. P.; Abdesselam, M.; Muller, D.; Chami, A. C. FTIR analysis of polyethylene terephthalate irradiated by MeV He^{+}. *Nucl. Instrum. Methods Phys. Res., Sect. B* **2012**, *274*, 70-77.

[122] Koch, K. J.; Aggerholm, T.; Nanita, S. C.; Cooks, R. G. Clustering of nucleobases with alkali metals studied by electrospray ionization tandem mass spectrometry: implications for mechanisms of multistrand DNA stabilization. *J. Mass Spectrom.* **2002**, *37*, 676-686.

[123] Aggerholm, T.; Nanita, S. C.; Koch, K. J.; Cooks, R. G. Clustering of nucleosides in the presence of alkali metals: Biologically relevant quartets of guanosine, deoxyguanosine and uridine observed by ESI-MS/MS. *J. Mass Spectrom.* **2003**, *38*, 87-97.

[124] Wagh, Y. B.; Kuwar, A.; Sahoo, S. K.; Gallucci, J.; Dalal, D. S. Highly selective fluorimetric sensor for Cu^{2+} and Hg^{2+} using a benzothiazole-based receptor in semi-aqueous media and molecular docking studies. *RSC Adv.* **2015**, *5*, 45528-45534.

[125] Roof, L. C.; Smith, D. M.; Drake, G. W.; Pennington, W. T.; Kolis, J. W. Synthesis and reactivity of $[Fe_3(CO)_9Te]^{2-}$. *Inorg. Chem.* **1995**, *34*, 337-345.

[126] Qin, K.; Yan, Y.; Zhang, Y.; Tang, Y. Direct production of levulinic acid in high yield from cellulose: joint effect of high ion strength and microwave field. *RSC Adv.* **2016**, *6*, 39131-39136.

[127] Waern, J. B.; Harding, M. M. Bioorganometallic chemistry of molybdocene dichloride. *J. Organomet. Chem.* **2004**, *689*, 4655-4668.

[128] Vujevic, G.; Janiak, C. Structural studies of bis(cyclopentadienyl)molybdenum-amino acid complexes. *Z. Anorg. Allg. Chem.* **2003**, *629*, 2585-2590.

[129] Abeysinghe, P. M.; Harding, M. M. Antitumour bis(cyclopentadienyl) metal complexes: titanocene and molybdocene dichloride and derivatives. *Dalton Trans* **2007**, 3474-3482.

[130] Rodríguez, M. I.; Chávez-Gil, T.; Colón, Y.; Díaz, N.; Meléndez, E. Molybdenocene-DNA interaction studies using electrochemical analysis. *J. Electroanal. Chem.* **2005**, *576*, 315-322.

[131] Waern, J. B.; Turner, P.; Harding, M. M. Synthesis and hydrolysis of thiol derivatives of molybdocene dichloride incorporating electron-withdrawing substituents. *Organometallics* **2006**, *25*, 3417-3421.

[132] Melendez, E. Bioorganometallic chemistry of molybdenocene dichloride and its derivatives. *J. Organomet. Chem.* **2012**, *706-707*, 4-12.

[133] Braga, S. S.; Marques, M. P. M.; Sousa, J. B.; Pillinger, M.; Teixeira-Dias, J. J. C.; Goncalves, I. S. Inclusion of molybdenocene dichloride (Cp_2MoCl_2) in 2-hydroxypropyl- and trimethyl-β-cyclodextrin: Structural and biological properties. *J. Organomet. Chem.* **2005**, *690*, 2905-2912.